A model-reduction approach in micromechanics of materials preserving the variational structure of constitutive relations

Jean-Claude Michel, Pierre Suquet

A model-reduction approach in micromechanics of materials preserving the variational structure of constitutive relations.

Jean-Claude Michel[a], Pierre Suquet[a,*]

[a]*Laboratoire de Mécanique et d'Acoustique, CNRS, UPR 7051, Aix-Marseille Univ, Centrale Marseille, 4, impasse Nikola Tesla, CS 40006, 13453 Marseille Cedex 13, France, {michel,suquet}@lma.cnrs-mrs.fr*

Abstract

In 2003 the authors proposed a model-reduction technique, called the Nonuniform Transformation Field Analysis (NTFA), based on a decomposition of the local fields of internal variables on a reduced basis of modes, to analyze the effective response of composite materials. The present study extends and improves on this approach in different directions. It is first shown that when the constitutive relations of the constituents derive from two potentials, this structure is passed to the NTFA model. Another structure-preserving model, the hybrid NTFA model of Fritzen and Leuschner, is analyzed and found to differ (slightly) from the primal NTFA model (it does not exhibit the same variational upper bound character). To avoid the "on-line" computation of local fields required by the hybrid model, new reduced evolution equations for the reduced variables are proposed, based on an expansion to second order (TSO) of the potential of the hybrid model. The coarse dynamics can then be entirely expressed in terms of quantities which can be pre-computed once for all. Roughly speaking, these pre-computed quantities depend only on the average and fluctuations per phase of the modes and of the associated stress fields. The accuracy of the new NTFA-TSO model is assessed by comparison with full-field simulations. The acceleration provided by the new coarse dynamics over the full-field computations (and over the hybrid model) is then spectacular, larger by three orders of magnitude than the acceleration due to the sole reduction of unknowns.

Keywords: Composite materials, model reduction, variational methods.

1. Introduction

A common engineering practice in the analysis of composite structures is to use *effective* or *homogenized* material properties instead of taking into account all details of the individual phase properties and geometrical arrangement.

The homogenization of *linear* properties of composites is now a rather well documented subject, supported by significant theoretical advances. The reader is referred to Milton (2002)

*Corresponding author. Tel: +33 491164208 ; fax: +33 491164481

for a state-of-the art of the subject. Provided that the length scales are well separated (*i.e.* when the typical length scale of the heterogeneities is small compared to the typical length scale of the structure), the linear effective properties of a composite can be completely determined by solving once for all a finite number of unit-cell problems (six in general). Then the analysis of a structure comprised of such a composite material can be performed using these pre-computed effective linear properties. In summary, the analysis of a linear composite structure consists of two totally independent steps, first an homogenization step at the unit-cell level only, and second a standard structural analysis performed at the structure level only.

The situation is more complicated when the composite is made of individual constituents governed by two potentials, free-energy and dissipation potential, accounting for reversible and irreversible processes respectively and even worse when one of these potentials (or both) is non quadratic. The most common examples of such materials are viscoelastic or elasto-viscoplastic materials. The overall response of the composite is history-dependent and this includes the history of local fields. It has long been recognized by Rice (1970), Mandel (1972) or Suquet (1985), that the exact description of the effective constitutive relations of such composites requires the determination of all microscopic plastic strains *at the unit-cell level*. For structural computations, the consequence of this theoretical result is that the two levels of computation, the level of the structure and the level of the unit-cell, remain intimately coupled. With the increase in computational power, numerical FEM^2 strategies for solving these coupled problems have been proposed (see Feyel and Chaboche, 2000; Terada and Kikuchi, 2001, for instance) but are so far limited by the formidable size of the corresponding problems.

A common practice to avoid these coupled computations is to investigate the response of representative volume elements by full-field methods and to use the response of these simulations to calibrate postulated phenomenological macroscopic models. There is however a considerable arbitrariness in the choice of the macroscopic model and most of the huge information generated by the full-field simulations is lost, or discarded.

An alternative line of thought consists in viewing the equations for the local plastic field as a system of ordinary differential equations (an infinite number of them, or a large number after discretization) at each integration point of the structure. It is therefore quite natural to resort to *model-reduction techniques* to reduce the complexity of the local plastic strain fields. Reduced-order models aim at achieving a compromise between analytical approaches, which are costless but often very limited by nonlinearity, and full-field simulations which resolve all complex details of the exact solutions, even though they are not always essential to the understanding of the problem, but come at a very high cost. Model-reduction has a long history in Fluid Mechanics (see Sirovich, 1987; Holmes et al., 1996, for instance) and in many other fields of computational physics (Lucia et al., 2004). Its use in Solid Mechanics is more recent (see Ryckelynck and Benziane, 2010; Chinesta and Cueto, 2014, and the references herein).

One of the earliest, and pioneering, attempt to reduce the complexity of the plastic strain fields in micromechanics of materials is the Transformation Field Analysis (TFA) of Dvorak (1992) which assumes uniformity of the plastic strain in the phases or in subdomains. It has been further developed in Dvorak et al. (1994), extended to periodic composites by Fish et al. (1997) and has been incorporated successfully in structural computations (Dvorak et al., 1994;

Fish and Yu, 2002; Kattan and Voyiadjis, 1993). However, the assumption of uniform plastic strain fields is far from reality and in order to reproduce accurately the actual effective behavior of the composite, it is essential to capture correctly the heterogeneity of the plastic strain field which requires a large number of subdomains.

This last observation has motivated the introduction in Michel et al. (2000), Michel and Suquet (2003) of the Nonuniform Transformation Field Analysis (NTFA) where the (visco)plastic strain field within each phase is decomposed on a finite set of plastic modes which can present large deviations from uniformity. The reduced variables are the components of the (visco)plastic strain field on the (visco)plastic modes. Approximate evolution laws for these variables have been proposed (Michel and Suquet, 2003, 2009). A significant advantage of the NTFA is that it provides localization rules allowing for the reconstruction of local fields which are used to predict local phenomena such as the distribution of stresses or the plastic dissipation at the microscopic scale (Michel and Suquet, 2009). This model, which will be called the *original* NTFA model, was first applied to two-dimensional situations by Michel and Suquet (2003, 2004, 2009). It has subsequently been applied to three-dimensional problems by Fritzen and Böhlke (2010) and extended to phases with transformation strains by Largenton et al. (2014). A step towards a more rational derivation of the evolution equation for the reduced variables has been achieved by Fritzen and Leuschner (2013), who proposed a hybrid form of the incremental variational principles for materials governed by two potentials. Their extension of the original NTFA model is discussed in the present paper (section 5) and has motivated some of the developments here, as will be explained.

The NTFA model consists of two main steps:

1. In a first step, common to all reduced-order models, a *reduced basis* has to be selected (the element of this basis are called modes). However, by contrast with most other model-reduction techniques (see Radermacher and Reese, 2014, for instance), the natural variables for the decomposition are the internal variables and not the displacement (or velocity) field. Several methods are available to construct this basis, in which the modes are either identified once for all, or are enriched "on-the-fly". The selection of modes is not our main purpose here and it will be assumed that these modes have been identified separately, in a preliminary step of the reduced-order model. The snapshot Proper Orthogonal Decomposition (POD) will be used in the present study. The reduced variables are the components of the fine variables, which are the fields of internal variables, on these modes.
2. In a second step, *reduced evolution equations* (evolution equations for the reduced variables) have to be derived, a problem which can be alternatively described as defining the "coarse dynamics" from the "fine dynamics". Actually in several reduced-order models this step is omitted (and not even mentioned) and the coarse dynamics is simply obtained by computing the fine variables and applying the fine dynamics to them. This requires the "on-line" evaluation of the fine variables (in the course of the computation of the coarse variables) and can be very costly, at least in the micromechanical problems that we have in mind. The hybrid model of Fritzen and Leuschner (2013) belongs to this category and requires the evaluation of local fields which implies constant back-and-forth

exchanges between the fine and the coarse scales resulting in a significant slowing down of the method, as will be seen in section 7.

By contrast, the aim of the present study, as well as that of the original NTFA model (Michel and Suquet, 2003), is to arrive at a coarse dynamics *involving no "on-line" computation of local fields* but only quantities which can be pre-computed "off-line". To this aim, an additional modeling step is required. This additional modeling was done in a rather heuristic way in the original model (Michel and Suquet, 2003). It is done here in a more rigorous and more systematic way using the so-called Tangent Second-Order (TSO) approach. The derivation of the coarse dynamics is based on two ingredients. First it is noted that the variational structure of the equations is preserved for the reduced variables, and second the reduced potentials are simplified by making use of linearization techniques which have proven their usefulness in nonlinear homogenization (Ponte Castañeda and Suquet, 1998). Another key ingredient in the derivation of this new "coarse dynamics" is the hybrid formulation of the NTFA model due to Fritzen and Leuschner (2013) (in a slightly different form). We prove here that their hybrid model is not fully equivalent to the primal NTFA model (and does not exhibit the same variational upper bound character), but is close to it when the modes are rich enough. Then a linearization technique allows to replace the "on-line" computations of local fields required by the hybrid model, by "off-line" computations. The coarse dynamics can then be entirely expressed in terms of quantities which can be pre-computed once for all. Roughly speaking, these pre-computed quantities depend only on the average and fluctuations per phase of the modes and of stress fields associated with them. The acceleration provided by the new coarse dynamics is then spectacular. Although the derivation of the "coarse dynamics" is the main contribution of the present study, it is worth noting that the notion of global modes proposed by Largenton et al. (2014) for linearly viscoelastic phases, is generalized here to nonlinear constituents. These global modes extend over several different phases instead of the local modes defined per phase as in the original approach (Michel and Suquet, 2003).

The paper is organized as follows. Two classes of constitutive relations for the individual phases, standard and non-standard, are recalled in section 2. Then the incremental variational principle for composites with standard phases (Ortiz and Stainier, 1999; Miehe et al., 2002; Lahellec and Suquet, 2007a), combining the free-energy and the dissipation potential of the phases, is presented in section 3. It is shown in section 4 that this variational principle is preserved when the NTFA decomposition is assumed so that the NTFA model can be said to be "structure-preserving" in the sense of Lall et al. (2003). The hybrid formulation of Fritzen and Leuschner (2013) (under a form adapted to the present notations) is discussed in section 5. The tangent-second-order expansion of the relevant potential is developed in section 6 where it is in particular found that this expansion depends only on pre-computed quantities. All the previous developments are made for standard constituents but can be extended heuristically to non-standard constituents. Finally, two study cases of metal-matrix composites reinforced with short fibers are considered in section 7. The phases follow either a linear kinematic hardening rule (the model is then standard) or a nonlinear kinematic hardening rule (in which case the

model is non-standard). The capability of the NTFA-TSO model to reproduce the full-field simulations at a much lower cost is shown. The computational time is reduced by a factor of at least 10^4 with respect to full-field simulations and by a factor of at least $4\ 10^3$ with respect to the hybrid NTFA model.

2. Constitutive relations

2.1. Individual constituents

The composite materials considered in this study are comprised of individual constituents undergoing partly reversible and partly irreversible transformations. These transformations can be modelled by a finite number of *internal variables* $\boldsymbol{\alpha}$ which entail the irreversible phenomena taking place in the material. The state variables of the material are the observable strain $\boldsymbol{\varepsilon}$ and the internal variables $\boldsymbol{\alpha}$. Attention is limited here to infinitesimal transformations so that the strain is measured by the linearized strain tensor $\boldsymbol{\varepsilon}$. It is further assumed that the stress derives from a *free-energy* function $w(\boldsymbol{\varepsilon}, \boldsymbol{\alpha})$ function of the state variables of the material,

$$\boldsymbol{\sigma} = \frac{\partial w}{\partial \boldsymbol{\varepsilon}}(\boldsymbol{\varepsilon}, \boldsymbol{\alpha}). \tag{1}$$

In addition, the evolution of the internal variables $\boldsymbol{\alpha}$ is governed by a differential equation and it is assumed here that this evolution is triggered by the driving forces $\boldsymbol{\mathcal{A}}$ associated with $\boldsymbol{\alpha}$ by derivation of the free-energy w,

$$\dot{\boldsymbol{\alpha}} = \boldsymbol{\mathcal{F}}(\boldsymbol{\mathcal{A}}), \quad \text{where } \boldsymbol{\mathcal{A}} = -\frac{\partial w}{\partial \boldsymbol{\alpha}}(\boldsymbol{\varepsilon}, \boldsymbol{\alpha}). \tag{2}$$

Most associated and non-associated models for elasto-plastic or elasto-visco-plastic materials, with or without damage, can be formulated in the framework of (1) and (2).

The variational structure underlying the present study requires an additional restriction on the form of the functions $\boldsymbol{\mathcal{F}}$ in (2), namely the satisfaction of generalized Onsager's reciprocity relations,

$$\frac{\partial \dot{\alpha}_i}{\partial \mathcal{A}_j} = \frac{\partial \dot{\alpha}_j}{\partial \mathcal{A}_i}, \quad i.e. \quad \frac{\partial \mathcal{F}_i}{\partial \mathcal{A}_j}(\boldsymbol{\mathcal{A}}) = \frac{\partial \mathcal{F}_j}{\partial \mathcal{A}_i}(\boldsymbol{\mathcal{A}}). \tag{3}$$

These symmetry relations imply the existence of a potential $\psi(\boldsymbol{\mathcal{A}})$ (called the *force potential*), such that

$$\boldsymbol{\mathcal{F}}(\boldsymbol{\mathcal{A}}) = \frac{\partial \psi}{\partial \boldsymbol{\mathcal{A}}}(\boldsymbol{\mathcal{A}}), \quad i.e. \quad \dot{\boldsymbol{\alpha}} = \frac{\partial \psi}{\partial \boldsymbol{\mathcal{A}}}(\boldsymbol{\mathcal{A}}). \tag{4}$$

When both w and ψ are convex functions of their arguments, the corresponding materials are called generalized standard materials (Halphen and Nguyen, 1975; Germain et al., 1983). Introducing the convex dual φ of ψ (φ is the *dissipation potential*), the relation (2) can be inverted into

$$\boldsymbol{\mathcal{A}} = \frac{\partial \varphi}{\partial \dot{\boldsymbol{\alpha}}}(\dot{\boldsymbol{\alpha}}). \tag{5}$$

Upon elimination of $\mathcal{A}$ between (2) and (5), the constitutive relations for a generalized standard material (GSM) take the compact form:

$$\boldsymbol{\sigma} = \frac{\partial w}{\partial \boldsymbol{\varepsilon}}(\boldsymbol{\varepsilon}, \boldsymbol{\alpha}), \quad \frac{\partial w}{\partial \boldsymbol{\alpha}}(\boldsymbol{\varepsilon}, \boldsymbol{\alpha}) + \frac{\partial \varphi}{\partial \dot{\boldsymbol{\alpha}}}(\dot{\boldsymbol{\alpha}}) = 0. \tag{6}$$

When the Onsager symmetry relations (3) are not satisfied, and assuming that the function $\mathcal{F}$ is invertible, with inverse $\mathcal{G}$, the material is said to be *non-standard* and its constitutive equations are

$$\boldsymbol{\sigma} = \frac{\partial w}{\partial \boldsymbol{\varepsilon}}(\boldsymbol{\varepsilon}, \boldsymbol{\alpha}), \quad \frac{\partial w}{\partial \boldsymbol{\alpha}}(\boldsymbol{\varepsilon}, \boldsymbol{\alpha}) + \mathcal{G}(\dot{\boldsymbol{\alpha}}) = 0. \tag{7}$$

Most of the subsequent arguments are developed rigorously for generalized standard materials and extended heuristically to non-standard materials.

Remark 1: As one of the reviewers pointed out, it would be interesting to consider a more general class of constitutive relations where the rate of the internal variables depends not only on the driving force $\mathcal{A}$ but also on the strain-rate $\dot{\boldsymbol{\varepsilon}}$ and on the internal variables themselves $\boldsymbol{\alpha}$

$$\dot{\boldsymbol{\alpha}} = \mathcal{F}(\mathcal{A}, \dot{\boldsymbol{\varepsilon}}, \boldsymbol{\alpha}), \quad \text{where } \mathcal{A} = -\frac{\partial w}{\partial \boldsymbol{\alpha}}(\boldsymbol{\varepsilon}, \boldsymbol{\alpha}). \tag{8}$$

This would cover for instance the case of Kelvin-Voigt materials or damage. This wider class of constitutive relations is not considered in the present study, but it is anticipated that it can be handled in the same way as the constitutive relations (2) (see remark 2 in section 6.3).

2.2. Incremental variational principle

Following Mialon (1986), Ortiz and Stainier (1999), Miehe (2002), Lahellec and Suquet (2007a) among others, the time derivative $\dot{\boldsymbol{\alpha}}$ in (6) can be approximated by a difference quotient after use of an implicit backward time-integration scheme. More specifically, upon discretization of the time interval of study, the time-derivative of a function f at time t_{n+1} is replaced by the difference quotient $(f(t_{n+1}) - f(t_n))/(t_{n+1} - t_n)$ and the constitutive relations (6) for a GSM are written at the end of the time step. This time-discretization procedure applied to (6) leads to the discretized system

$$\boldsymbol{\sigma} = \frac{\partial w}{\partial \boldsymbol{\varepsilon}}(\boldsymbol{\varepsilon}, \boldsymbol{\alpha}), \quad \frac{\partial w}{\partial \boldsymbol{\alpha}}(\boldsymbol{\varepsilon}, \boldsymbol{\alpha}) + \frac{\partial \varphi}{\partial \dot{\boldsymbol{\alpha}}}\left(\frac{\boldsymbol{\alpha} - \boldsymbol{\alpha}_n}{\Delta t}\right) = 0, \quad \Delta t = t_{n+1} - t_n, \tag{9}$$

where the internal variables $\boldsymbol{\alpha}_n$ at time t_n are known, and the unknowns at time t_{n+1} are $\boldsymbol{\sigma}$, $\boldsymbol{\varepsilon}$ and $\boldsymbol{\alpha}$. It is readily seen that the second relations in (9) are the Euler-Lagrange equations for the following variational problem

$$\inf_{\boldsymbol{\alpha}} \quad J(\boldsymbol{\varepsilon}, \boldsymbol{\alpha}), \qquad J(\boldsymbol{\varepsilon}, \boldsymbol{\alpha}) = w(\boldsymbol{\varepsilon}, \boldsymbol{\alpha}) \; + \; \Delta t \; \varphi\left(\frac{\boldsymbol{\alpha} - \boldsymbol{\alpha}_n}{\Delta t}\right).$$

Then, defining the potential

$$w_\Delta(\boldsymbol{\varepsilon}) = \inf_{\boldsymbol{\alpha}} \quad J(\boldsymbol{\varepsilon}, \boldsymbol{\alpha}),$$

the following remarkable result is obtained, where the stress is expressed as the derivative of a single potential with respect to the strain:

$$\boldsymbol{\sigma} = \frac{\partial w_\Delta}{\partial \boldsymbol{\varepsilon}}(\boldsymbol{\varepsilon}). \tag{10}$$

2.3. A simple example of a generalized standard material

The behavior of elasto-viscoplastic materials is commonly described by a generalized standard model accounting for isotropic and kinematic hardening,

$$\left.\begin{array}{rcl} \boldsymbol{\sigma} &=& \boldsymbol{L} : (\boldsymbol{\varepsilon} - \boldsymbol{\varepsilon}_{\mathsf{v}}), \\ \dot{\boldsymbol{\varepsilon}}_{\mathsf{v}} &=& \dfrac{3}{2}\dot{p}\dfrac{\boldsymbol{s} - \boldsymbol{X}}{(\sigma - X)_{\mathsf{eq}}}, \quad \dot{p} = \dot{\varepsilon}_0 \left[\dfrac{((\sigma - X)_{\mathsf{eq}} - R(p))^+}{\sigma_0}\right]^n, \\ \dot{\boldsymbol{X}} &=& \boldsymbol{H} : \dot{\boldsymbol{\varepsilon}}_{\mathsf{v}}, \end{array}\right\} \tag{11}$$

where $\boldsymbol{s}$ is the stress deviator, $\sigma_{\mathsf{eq}} = \sqrt{\frac{3}{2}\boldsymbol{s} : \boldsymbol{s}}$ denotes the usual von Mises stress, $(.)^+$ is the Mc Cauley bracket ($A^+ = A$ if $A \geq 0, \quad A^+ = 0$ if $A \leq 0$), and the yield stress R associated with isotropic hardening is a function of the cumulated plastic strain $p(t) = \int_0^t \dot{p}(s)\, ds$. The internal variables are

$$\boldsymbol{\alpha} = (\boldsymbol{\varepsilon}_{\mathsf{v}}, p).$$

The free-energy consists of three terms, the recoverable elastic energy, the energy stored in the back-stress $\boldsymbol{X}$ associated with kinematic hardening and the energy stored in the isotropic hardening of the material,

$$w(\boldsymbol{\varepsilon}, \boldsymbol{\varepsilon}_{\mathsf{v}}, p) = \frac{1}{2}(\boldsymbol{\varepsilon} - \boldsymbol{\varepsilon}_{\mathsf{v}}) : \boldsymbol{L} : (\boldsymbol{\varepsilon} - \boldsymbol{\varepsilon}_{\mathsf{v}}) + \frac{1}{2}\boldsymbol{\varepsilon}_{\mathsf{v}} : \boldsymbol{H} : \boldsymbol{\varepsilon}_{\mathsf{v}} + w_{st}(p), \quad w_{st}(p) = \int_0^p R(q)dq. \tag{12}$$

The thermodynamic forces corresponding to $\boldsymbol{\varepsilon}_{\mathsf{v}}$ and p are denoted by $\boldsymbol{\mathcal{A}}_{\mathsf{v}}$ and $\mathcal{A}_{\mathsf{p}}$ respectively,

$$\boldsymbol{\mathcal{A}}_{\mathsf{v}} = \boldsymbol{\sigma} - \boldsymbol{X}, \quad \mathcal{A}_{\mathsf{p}} = -R(p).$$

The force potential ψ is

$$\psi(\boldsymbol{\mathcal{A}}_{\mathsf{v}}, \mathcal{A}_{\mathsf{p}}) = \frac{\sigma_0 \dot{\varepsilon}_0}{n+1}\left[\frac{((\mathcal{A}_{\mathsf{v}})_{\mathsf{eq}} + \mathcal{A}_{\mathsf{p}})^+}{\sigma_0}\right]^{n+1}, \tag{13}$$

and the equations (11) can be retrieved from the above potentials (12) and (13) by means of the relations (1), (2) and (4).

2.4. A non-standard material

The kinematic hardening modeled by the 3rd equation in (11) is linear since the back-stress $\boldsymbol{X}$ is a linear function of the viscoplastic strain $\boldsymbol{\varepsilon}_{\mathsf{v}}$. It has been observed by several authors (Chaboche, 2008) that the Bauschinger effect is better captured by a model with *nonlinear* kinematic hardening, where the evolution of the back-stress $\boldsymbol{X}$ is governed by a differential equation with spring-back introduced by Armstrong and Frederick (1966),

$$\dot{\boldsymbol{X}} = \boldsymbol{H} : \dot{\boldsymbol{\varepsilon}}_{\mathsf{v}} - \eta\, \boldsymbol{X}\, \dot{p}. \tag{14}$$

The model (14) (and subsequent refinements which will not be considered here) is commonly used to predict the lifetime of metallic or polymeric structures under repeated thermomechanical loadings (see Samrout et al., 1997; Amiable et al., 2006, among others).

The model (14) is non-standard because of the evolution equation for the back-stress $\boldsymbol{X}$. It is not even in the non-standard form (2) since the back-stress $\boldsymbol{X}$ is not defined directly from the plastic strain, but is deduced from the integration of the differential equation (14). Besson et al. (2010) have written (14) in a more convenient form by introducing another tensorial variable $\boldsymbol{\beta}$ associated with kinematic hardening but separate from the plastic strain. The internal variables are therefore

$$\boldsymbol{\alpha} = (\boldsymbol{\varepsilon}_{\mathsf{v}}, \boldsymbol{\beta}, p).$$

The free-energy is taken in the form

$$w(\boldsymbol{\varepsilon}, \boldsymbol{\varepsilon}_{\mathsf{v}}, \boldsymbol{\beta}, p) = \frac{1}{2}(\boldsymbol{\varepsilon} - \boldsymbol{\varepsilon}_{\mathsf{v}}) : \boldsymbol{L} : (\boldsymbol{\varepsilon} - \boldsymbol{\varepsilon}_{\mathsf{v}}) + \frac{1}{2}\boldsymbol{\beta} : \boldsymbol{H} : \boldsymbol{\beta} + w_{st}(p). \tag{15}$$

The thermodynamic forces are

$$\boldsymbol{\sigma} = \boldsymbol{L} : (\boldsymbol{\varepsilon} - \boldsymbol{\varepsilon}_{\mathsf{v}}), \quad \boldsymbol{\mathcal{A}}_{\mathsf{v}} = \boldsymbol{\sigma}, \quad \boldsymbol{\mathcal{A}}_{\beta} = -\boldsymbol{H} : \boldsymbol{\beta}, \quad \mathcal{A}_{\mathsf{p}} = -R(p). \tag{16}$$

The force potential ψ is defined as

$$\psi(\boldsymbol{\mathcal{A}}_{\mathsf{v}}, \boldsymbol{\mathcal{A}}_{\beta}, \mathcal{A}_{\mathsf{p}}) = \frac{\sigma_0 \dot{\varepsilon}_0}{n+1} \left[\frac{((\mathcal{A}_{\mathsf{v}} + \mathcal{A}_{\beta})_{\mathsf{eq}} + \mathcal{A}_{\mathsf{p}})^+}{\sigma_0} \right]^{n+1}, \tag{17}$$

and the evolution equations for the internal variables are written in the form $\dot{\boldsymbol{\alpha}} = \boldsymbol{\mathcal{F}}(\boldsymbol{\mathcal{A}})$,

$$\left.\begin{aligned}
\dot{\boldsymbol{\varepsilon}}_{\mathsf{v}} = \quad \boldsymbol{\mathcal{F}}_{\mathsf{v}}(\boldsymbol{\mathcal{A}}) = \quad & \frac{\partial \psi}{\partial \boldsymbol{\mathcal{A}}_{\mathsf{v}}}(\boldsymbol{\mathcal{A}}_{\mathsf{v}}, \boldsymbol{\mathcal{A}}_{\beta}, \mathcal{A}_{\mathsf{p}}) = \frac{3}{2}\dot{p}\frac{(\boldsymbol{\mathcal{A}}_{\mathsf{v}} + \boldsymbol{\mathcal{A}}_{\beta})^{\mathsf{dev}}}{(\mathcal{A}_{\mathsf{v}} + \mathcal{A}_{\beta})_{\mathsf{eq}}}, \\
\dot{\boldsymbol{\beta}} = \quad \boldsymbol{\mathcal{F}}_{\beta}(\boldsymbol{\mathcal{A}}) = \quad & \frac{\partial \psi}{\partial \boldsymbol{\mathcal{A}}_{\beta}}(\boldsymbol{\mathcal{A}}_{\mathsf{v}}, \boldsymbol{\mathcal{A}}_{\beta}, \mathcal{A}_{\mathsf{p}}) + \eta \boldsymbol{H}^{-1} : \boldsymbol{\mathcal{A}}_{\beta} \, \frac{\partial \psi}{\partial \mathcal{A}_{\mathsf{p}}}(\boldsymbol{\mathcal{A}}_{\mathsf{v}}, \boldsymbol{\mathcal{A}}_{\beta}, \mathcal{A}_{\mathsf{p}}) \\
= \quad & \dot{\boldsymbol{\varepsilon}}_{\mathsf{v}} - \eta \boldsymbol{\beta} \, \dot{p}, \\
\dot{p} = \quad \boldsymbol{\mathcal{F}}_{\mathsf{p}}(\boldsymbol{\mathcal{A}}) = \quad & \frac{\partial \psi}{\partial \mathcal{A}_{\mathsf{p}}}(\boldsymbol{\mathcal{A}}_{\mathsf{v}}, \boldsymbol{\mathcal{A}}_{\beta}, \mathcal{A}_{\mathsf{p}}) = \dot{\varepsilon}_0 \, \left[\frac{((\mathcal{A}_{\mathsf{v}} + \mathcal{A}_{\beta})_{\mathsf{eq}} + \mathcal{A}_{\mathsf{p}})^+}{\sigma_0} \right]^n,
\end{aligned}\right\} \tag{18}$$

where $\boldsymbol{\mathcal{A}}^{\mathsf{dev}}$ denotes the deviator of a tensor $\boldsymbol{\mathcal{A}}$. Setting $\boldsymbol{X} = -\boldsymbol{\mathcal{A}}_{\beta}$ and multiplying the evolution equation for $\boldsymbol{\beta}$ by $\boldsymbol{H}$ yields

$$\dot{\boldsymbol{X}} = \boldsymbol{H} : \dot{\boldsymbol{\varepsilon}}_{\mathsf{v}} - \eta \, \boldsymbol{X} \, \dot{p},$$

which coincides with the initial evolution equation for $\boldsymbol{X}$. The non-standard character comes from the last term in $\boldsymbol{\mathcal{F}}_{\beta}$.

3. Composite materials

3.1. Exact local problem

A representative volume element (r.v.e.) V of the composite is comprised of P phases occupying domains $V^{(r)}$ with characteristic functions $\chi^{(r)}$ and volume fraction $c^{(r)}$. The spatial averaging over V and $V^{(r)}$ are denoted by $\langle . \rangle$ and $\langle . \rangle^{(r)}$ respectively. Each individual phase is

governed by the differential equations (6) with potentials $w^{(r)}$ and $\varphi^{(r)}$. The free-energy w and the dissipation potential φ at position $\boldsymbol{x}$ are given by

$$w(\boldsymbol{x},\boldsymbol{\varepsilon},\boldsymbol{\alpha}) = \sum_{r=1}^{P} \chi^{(r)}(\boldsymbol{x}) w^{(r)}(\boldsymbol{\varepsilon},\boldsymbol{\alpha}), \quad \varphi(\boldsymbol{x},\dot{\boldsymbol{\alpha}}) = \sum_{r=1}^{P} \chi^{(r)}(\boldsymbol{x}) \varphi^{(r)}(\dot{\boldsymbol{\alpha}}).$$

The r.v.e. V is subjected to a path of macroscopic strain $\overline{\boldsymbol{\varepsilon}}(t)$ and periodicity conditions[1] are assumed on ∂V. The local problem to be solved to determine the local fields $\boldsymbol{\sigma}(\boldsymbol{x},t)$, $\boldsymbol{\varepsilon}(\boldsymbol{x},t)$ and $\boldsymbol{\alpha}(\boldsymbol{x},t)$ consists of the generalized thermoelastic problem (19), in which the field of internal variables $\boldsymbol{\alpha}(\boldsymbol{x})$ is fixed, coupled with the differential equation (20) at every point $\boldsymbol{x}$ in the volume element,

$$\left.\begin{aligned} &\boldsymbol{\sigma}(\boldsymbol{x},t) = \frac{\partial w}{\partial \boldsymbol{\varepsilon}}(\boldsymbol{x},\boldsymbol{\varepsilon}(\boldsymbol{x},t),\boldsymbol{\alpha}(\boldsymbol{x},t)), \quad \text{div } \boldsymbol{\sigma}(\boldsymbol{x},t) = 0 \quad \text{in } V\times[0,T], \\ &\boldsymbol{\varepsilon}(\boldsymbol{x},t) = \overline{\boldsymbol{\varepsilon}}(t) + \tfrac{1}{2}(\boldsymbol{\nabla}\boldsymbol{u}^*(\boldsymbol{x},t) + \boldsymbol{\nabla}\boldsymbol{u}^{*T}(\boldsymbol{x},t)), \quad \boldsymbol{u}^* \text{ periodic on } \partial V, \end{aligned}\right\} \tag{19}$$

and

$$\frac{\partial w}{\partial \boldsymbol{\alpha}}(\boldsymbol{x},\boldsymbol{\varepsilon}(\boldsymbol{x},t),\boldsymbol{\alpha}(\boldsymbol{x},t)) + \frac{\partial \varphi}{\partial \dot{\boldsymbol{\alpha}}}(\boldsymbol{x},\dot{\boldsymbol{\alpha}}(\boldsymbol{x},t)) = 0 \quad \text{in } V\times[0,T]. \tag{20}$$

It is assumed that, the field $\boldsymbol{\alpha}$ being fixed, the periodic boundary value problem (19) has a unique solution, the local strain field $\boldsymbol{\varepsilon}$. The second line in (19) imply in particular that $\langle \boldsymbol{\varepsilon}(\boldsymbol{x},t)\rangle = \overline{\boldsymbol{\varepsilon}}(t)$.

The *homogenized* (or effective) response of the composite along the path of prescribed strain $\{\overline{\boldsymbol{\varepsilon}}(t), t\in[0,T]\}$ is the history of average stress $\{\overline{\boldsymbol{\sigma}}(t), t\in[0,T]\}$ where

$$\overline{\boldsymbol{\sigma}}(t) = \langle \boldsymbol{\sigma}(\boldsymbol{x},t)\rangle .$$

3.2. Effective incremental principle

The effective response of the composite can be derived from an *effective incremental potential*. After time-discretization, the overall stress $\overline{\boldsymbol{\sigma}}$ at time t_{n+1} derives from the effective potential $\widetilde{w}_\Delta$ (Lahellec and Suquet, 2007a,b) (deduced from the local variational principle (10)),

$$\overline{\boldsymbol{\sigma}} = \frac{\partial \widetilde{w}_\Delta}{\partial \overline{\boldsymbol{\varepsilon}}}(\overline{\boldsymbol{\varepsilon}}), \quad \widetilde{w}_\Delta(\overline{\boldsymbol{\varepsilon}}) = \inf_{\boldsymbol{\varepsilon}\in\mathcal{K}(\overline{\boldsymbol{\varepsilon}})} \left\langle \inf_{\boldsymbol{\alpha}} \quad J(\boldsymbol{\varepsilon},\boldsymbol{\alpha}) \right\rangle , \tag{21}$$

where $\overline{\boldsymbol{\varepsilon}}$ is the prescribed macroscopic strain at time t_{n+1} and J is the incremental potential defined as

$$J(\boldsymbol{x},\boldsymbol{\varepsilon},\boldsymbol{\alpha}) = \sum_{r=1}^{P} \left(w^{(r)}(\boldsymbol{\varepsilon},\boldsymbol{\alpha}) + \Delta t\ \varphi^{(r)}\left(\frac{\boldsymbol{\alpha}-\boldsymbol{\alpha}_n(\boldsymbol{x})}{\Delta t}\right)\right) \chi^{(r)}(\boldsymbol{x}),$$

and

$$\mathcal{K}(\overline{\boldsymbol{\varepsilon}}) = \{\boldsymbol{\varepsilon} = \overline{\boldsymbol{\varepsilon}} + \frac{1}{2}(\boldsymbol{\nabla}\boldsymbol{u}^* + \boldsymbol{\nabla}\boldsymbol{u}^{*T}), \quad \boldsymbol{u}^* \text{ periodic on } \partial V\}.$$

The solution $\boldsymbol{\varepsilon}$ of the variational problem (21) is precisely the solution of the local problem (19)(20).

[1] Other boundary conditions can be considered provided the Hill-Mandel condition is satisfied (Suquet, 1987).

4. The primal NTFA model

4.1. Reduced variables and effective potentials

A rather common feature of plastic strain fields in elasto-plastic heterogeneous systems under monotonic loadings, is that these fields quickly adopt a specific pattern which remains fixed in time, with an amplitude which varies with time. This striking feature is observed both experimentally (Latourte et al., 2014) or numerically (Idiart et al., 2006). It has led Michel and Suquet (2003) to generalize the Transformation Field Analysis (TFA) of Dvorak (1992) by assuming a decomposition of the local plastic strain field on a basis of a few shape functions (the observed nonuniform patterns), called *plastic modes*. The corresponding decomposition in the present context consists in assuming the following decomposition for each field of internal variables

$$\boldsymbol{\alpha}(\boldsymbol{x},t) = \sum_{k=1}^{M} \xi^{(k)}(t)\ \boldsymbol{\mu}^{(k)}(\boldsymbol{x}), \tag{22}$$

where the fields $\boldsymbol{\mu}^{(k)}(\boldsymbol{x})$ are called *modes*. The modes have the same tensorial character as the internal variables $\boldsymbol{\alpha}$. To avoid a possible indeterminacy in the definition of the reduced variables $\xi^{(k)}$, it is further assumed that

$$\textit{the modes } \boldsymbol{\mu}^{(k)} \text{ are linearly independent fields.}$$

How the modes are chosen or generated is not the objective of this study and the reader is referred to Michel and Suquet (2003, 2004, 2009) for a discussion of this point. It suffices to say that several techniques, such as the Proper Orthogonal Decomposition (POD) (also known under different names, Singular Value Decomposition, or Karhunen-Loève decomposition), are available in the literature to select the modes (Berkooz et al., 1993; Chatterjee, 2000; Chinesta and Cueto, 2014, and the references herein). Therefore the modes are assumed to be known in the remainder of this study.

An upper bound for the incremental potential is obtained, upon inversion of the order of the infima in (21)

$$\inf_{\boldsymbol{\varepsilon}\in\mathcal{K}(\overline{\boldsymbol{\varepsilon}})} \left\langle \inf_{\boldsymbol{\alpha}} \quad J(\boldsymbol{\varepsilon},\boldsymbol{\alpha}) \right\rangle \leq \inf_{\boldsymbol{\xi}} \quad \widetilde{J}(\overline{\boldsymbol{\varepsilon}},\boldsymbol{\xi}), \tag{23}$$

where

$$\widetilde{J}(\overline{\boldsymbol{\varepsilon}},\boldsymbol{\xi}) = \widetilde{w}(\overline{\boldsymbol{\varepsilon}},\boldsymbol{\xi}) + \Delta t\ \widetilde{\varphi}\left(\frac{\boldsymbol{\xi}-\boldsymbol{\xi}_n}{\Delta t}\right),$$

with

$$\widetilde{w}(\overline{\boldsymbol{\varepsilon}},\boldsymbol{\xi}) = \inf_{\boldsymbol{\varepsilon}\in\mathcal{K}(\overline{\boldsymbol{\varepsilon}})} \left\langle w(\boldsymbol{\varepsilon},\boldsymbol{\alpha}(\boldsymbol{\xi}))\right\rangle, \quad \widetilde{\varphi}(\dot{\boldsymbol{\xi}}) = \langle \varphi(\dot{\boldsymbol{\alpha}}(\dot{\boldsymbol{\xi}}))\rangle. \tag{24}$$

The NTFA model is obtained by replacing the reduced incremental potential $\widetilde{w}_\Delta$ by the right-hand-side of (23)

$$\widetilde{w}^+_\Delta(\overline{\boldsymbol{\varepsilon}}) = \inf_{\boldsymbol{\xi}} \widetilde{J}(\overline{\boldsymbol{\varepsilon}},\boldsymbol{\xi}). \tag{25}$$

In this approximation the overall stress is given, according to (21), by

$$\overline{\boldsymbol{\sigma}} \simeq \frac{\partial \widetilde{w}^+_\Delta}{\partial \overline{\boldsymbol{\varepsilon}}}(\overline{\boldsymbol{\varepsilon}}) = \frac{\partial \widetilde{w}}{\partial \overline{\boldsymbol{\varepsilon}}}(\overline{\boldsymbol{\varepsilon}},\boldsymbol{\xi}). \tag{26}$$

$\boldsymbol{\xi}$ satisfies the Euler-Lagrange equation corresponding to the minimization problem in (25)

$$\frac{\partial \widetilde{w}}{\partial \boldsymbol{\xi}}(\overline{\boldsymbol{\varepsilon}}, \boldsymbol{\xi}) + \frac{\partial \widetilde{\varphi}}{\partial \dot{\boldsymbol{\xi}}}\left(\frac{\boldsymbol{\xi} - \boldsymbol{\xi}_n}{\Delta t}\right) = 0,$$

and in the limit as $\Delta t \to 0$

$$\frac{\partial \widetilde{w}}{\partial \boldsymbol{\xi}}(\overline{\boldsymbol{\varepsilon}}, \boldsymbol{\xi}) + \frac{\partial \widetilde{\varphi}}{\partial \dot{\boldsymbol{\xi}}}\left(\dot{\boldsymbol{\xi}}\right) = 0. \tag{27}$$

The structure of these equations is better recognized by introducing the force $\mathfrak{a}$ associated with $\boldsymbol{\xi}$,

$$\mathfrak{a} = -\frac{\partial \widetilde{w}}{\partial \boldsymbol{\xi}}(\overline{\boldsymbol{\varepsilon}}, \boldsymbol{\xi}). \tag{28}$$

According to (27), $\mathfrak{a}$ is related to the evolution of the variables $\boldsymbol{\xi}$ by

$$\mathfrak{a} = \frac{\partial \widetilde{\varphi}}{\partial \dot{\boldsymbol{\xi}}}\left(\dot{\boldsymbol{\xi}}\right). \tag{29}$$

The comparison of (26), (28) and (29) with (1), (2) and (5) shows that the above NTFA model, for the composite is a generalized standard model, called in the sequel the *primal* NTFA model, with state variables $(\overline{\boldsymbol{\varepsilon}}, \boldsymbol{\xi})$, free-energy $\widetilde{w}$ and dissipation potential $\widetilde{\varphi}$. In this respect the NTFA approach is said to be *structure-preserving* in the sense that it preserves the structure of the constitutive relations derived from two potentials.

4.2. Local problem associated with the primal NTFA model

The minimization with respect to $\boldsymbol{\varepsilon}$ in the definition (24) of the effective free-energy $\widetilde{w}$ shows that the field $\boldsymbol{\sigma} = \dfrac{\partial w}{\partial \boldsymbol{\varepsilon}}(\boldsymbol{\varepsilon}, \boldsymbol{\alpha})$ is, for fixed $\boldsymbol{\alpha}$, solution of the generalized thermoelastic problem (19). The minimization with respect to $\boldsymbol{\xi}$ leads to the differential equations (27).

To interpret (27) we note that:

$$-\frac{\partial \widetilde{w}}{\partial \xi^{(k)}}(\overline{\boldsymbol{\varepsilon}}, \boldsymbol{\xi}) = -\langle \frac{\partial w}{\partial \boldsymbol{\alpha}}(\boldsymbol{\varepsilon}, \boldsymbol{\alpha}) : \boldsymbol{\mu}^{(k)} \rangle, \quad \frac{\partial \widetilde{\varphi}}{\partial \dot{\xi}^{(k)}}(\dot{\boldsymbol{\xi}}) = \langle \frac{\partial \varphi}{\partial \dot{\boldsymbol{\alpha}}}(\dot{\boldsymbol{\alpha}}) : \boldsymbol{\mu}^{(k)} \rangle. \tag{30}$$

Therefore the local problem associated with the primal NTFA model obtained under the decomposition (22) consists of the thermoelastic problem (19) where the NTFA decomposition (22) is enforced, coupled with M differential equations for the $\xi^{(k)}$,

$$\langle \frac{\partial w}{\partial \boldsymbol{\alpha}}(\boldsymbol{\varepsilon}, \boldsymbol{\alpha}) : \boldsymbol{\mu}^{(k)} \rangle + \langle \frac{\partial \varphi}{\partial \dot{\boldsymbol{\alpha}}}(\dot{\boldsymbol{\alpha}}) : \boldsymbol{\mu}^{(k)} \rangle = 0, \quad k = 1, ..., M. \tag{31}$$

The differential equations (20) are no more satisfied pointwisely at every material point $\boldsymbol{x}$, but only in projection on each mode $\boldsymbol{\mu}^{(k)}$. The number of differential equations has been reduced from an infinite number (the differential equations (20) at every point $\boldsymbol{x}$ in V) to the M differential equations (31).

Remark: In Michel and Suquet (2003, 2004, 2009), the differential equation (31) was obtained formally by multiplying the constitutive relations of the individual phases by $\boldsymbol{\mu}^{(k)}$ and averaging over V. The incremental variational principle is a rigorous way of deriving these equations, but is equivalent to the procedure used in Michel and Suquet (2003) where (31) corresponds to eq (44).

4.3. On the integration in time of the NTFA constitutive equations

By comparison with the full-field simulations, the advantage of the NTFA method is to reduce the number of ordinary differential equations (ODEs) from a large number (the number of discretization points in the full-field simulations) to M ODEs (M being the number of modes). This provides a significant gain in CPU-time (more details will be given in section 7). However it should be noted that part of the gain which could be expected from this reduction is lost because the ODE (27) still involves a strong coupling between the microscopic scale and the macroscopic scale to compute $\widetilde{w}$ and $\widetilde{\varphi}$. In the examples considered here, the problem does not reside in the effective energy $\widetilde{w}$ which can be expressed explicitly in terms of quantities computed once for all. By contrast, except in the specific situation of linearly viscous constituents discussed in section 4.4, the evaluation of the effective potential $\widetilde{\varphi}$ or of its derivative in (27), requires according to (30),

(a) the storage of the modes $\boldsymbol{\mu}^{(\ell)}(\boldsymbol{x})$,

(b) the computation of the local field of plastic strain $\dot{\boldsymbol{\alpha}}(\boldsymbol{x}) = \sum_{\ell=1}^{M} \dot{\xi}^{(\ell)} \boldsymbol{\mu}^{(\ell)}(\boldsymbol{x})$ and the associated field of forces $\boldsymbol{\mathcal{A}}(\boldsymbol{x}) = \dfrac{\partial \varphi}{\partial \dot{\boldsymbol{\alpha}}} \left(\sum_{\ell=1}^{M} \dot{\xi}^{(\ell)} \boldsymbol{\mu}^{(\ell)}(\boldsymbol{x}) \right)$,

(c) the scalar product of this local field with the mode $\boldsymbol{\mu}^{(\ell)}$.

All these steps are resource-consuming, not only in terms of CPU time (mostly step (b)) but also in terms of memory storage (step (a)). If the effective constitutive relations have to be evaluated a large number of times, for instance at every time-step and at every integration point of a macroscopic structure subjected to a time dependent loading (a simple example of such a situation is considered in Michel and Suquet, 2009), the cost of this evaluation remains high, and even though it is less than the cost of a full-field calculation on the volume element that is required by a nested FEM^2 approach, both costs are of the same order of magnitude.

The aim of the original NTFA model (Michel and Suquet, 2003) was precisely to make approximations to express the constitutive relations with constitutive parameters which can be *pre-computed* once for all, therefore avoiding the on-line computation of local fields. The objective of the present study is the same, namely to arrive to an ODE for $\boldsymbol{\xi}$ where all parameters can be pre-computed, but where the *coarse dynamics* (*i.e.* the ODE for the reduced variables $\boldsymbol{\xi}$) is deduced from the variational principles, rather that found heuristically, as was the case in our initial approach (Michel and Suquet, 2003). Such an approximation is discussed in section 6 and it is shown in section 7 that the acceleration provided by this NTFA-TSO model is by several orders of magnitude larger than that resulting from the sole NTFA decomposition (22).

4.4. Linear viscoelastic constituents

When the constituents of the composite are linearly viscoelastic, the effective potential $\widetilde{\varphi}$ can be expressed explicitly in terms of quantities which can be computed once for all, by contrast with more general constituents where such explicit expressions do not exist. The linear

viscoelastic constituents under consideration here are Maxwellian and the constitutive relations for phase r read as

$$\boldsymbol{\sigma} = \boldsymbol{L}^{(r)} : (\boldsymbol{\varepsilon} - \boldsymbol{\varepsilon}_{\mathsf{v}}), \quad \dot{\boldsymbol{\varepsilon}}_{\mathsf{v}} = \boldsymbol{M}_{\mathsf{v}}^{(r)} : \boldsymbol{\sigma}.$$

This constitutive relation is a particular case of (11), with no isotropic or kinematic hardening ($\boldsymbol{H} = \boldsymbol{0},\ R(p) = 0$) and with a rate-sensitivity exponent $n = 1$. The internal variable of the system is $\boldsymbol{\alpha} = \boldsymbol{\varepsilon}_{\mathsf{v}}$, the free-energy and the dissipation potential in phase r are

$$w^{(r)}(\boldsymbol{\varepsilon}, \boldsymbol{\alpha}) = \frac{1}{2}(\boldsymbol{\varepsilon} - \boldsymbol{\alpha}) : \boldsymbol{L}^{(r)} : (\boldsymbol{\varepsilon} - \boldsymbol{\alpha}), \quad \varphi^{(r)}(\dot{\boldsymbol{\alpha}}) = \frac{1}{2}\dot{\boldsymbol{\alpha}} : \boldsymbol{L}_{\mathsf{v}}^{(r)} : \dot{\boldsymbol{\alpha}},$$

where $\boldsymbol{L}_{\mathsf{v}}^{(r)} = \left(\boldsymbol{M}_{\mathsf{v}}^{(r)}\right)^{-1}$. The thermodynamic force $\boldsymbol{\mathcal{A}}$ coincides with the stress $\boldsymbol{\sigma}$ and the local problem to be solved for fixed $\boldsymbol{\alpha} = \boldsymbol{\varepsilon}_{\mathsf{v}}$ is the linear thermoelastic problem

$$\boldsymbol{\sigma} = \boldsymbol{L}(\boldsymbol{x}) : (\boldsymbol{\varepsilon} - \boldsymbol{\varepsilon}_{\mathsf{v}}), \quad \text{div}\, \boldsymbol{\sigma} = 0, \quad \langle \boldsymbol{\varepsilon}(t) \rangle = \overline{\boldsymbol{\varepsilon}}(t), \quad \text{boundary conditions on } \partial V. \tag{32}$$

After due account of the NTFA decomposition (22), the solution of this problem can be expressed by the superposition theorem as

$$\boldsymbol{\varepsilon}(\boldsymbol{x}) = \boldsymbol{A}(\boldsymbol{x}) : \overline{\boldsymbol{\varepsilon}} + \sum_{\ell=1}^{M} (\boldsymbol{D} * \boldsymbol{\mu}^{(\ell)})(\boldsymbol{x}) \xi^{(\ell)}, \tag{33}$$

where $\boldsymbol{A}(\boldsymbol{x})$ is the strain concentration tensor, expressing the local strain field caused by an average strain $\overline{\boldsymbol{\varepsilon}}$ when the eigenstrain $\boldsymbol{\alpha}$ vanishes, $\boldsymbol{D}(\boldsymbol{x}, \boldsymbol{x}')$ is the nonlocal Green operator expressing the strain at point $\boldsymbol{x}$ resulting from a unit eigenstrain at point $\boldsymbol{x}'$, when the average strain vanishes and $*$ denotes the convolution in space. The stress field corresponding to (33) can be expressed as

$$\boldsymbol{\sigma}(\boldsymbol{x}) = \boldsymbol{L}(\boldsymbol{x}) : \boldsymbol{A}(\boldsymbol{x}) : \overline{\boldsymbol{\varepsilon}} + \sum_{\ell=1}^{M} \boldsymbol{\rho}^{(\ell)}(\boldsymbol{x}) \xi^{(\ell)}, \quad \boldsymbol{\rho}^{(\ell)}(\boldsymbol{x}) = \boldsymbol{L}(\boldsymbol{x}) : \left((\boldsymbol{D} * \boldsymbol{\mu}^{(\ell)}) - \boldsymbol{\mu}^{(\ell)} \right)(\boldsymbol{x}), \tag{34}$$

and the effective thermoelastic energy is

$$\widetilde{w}(\overline{\boldsymbol{\varepsilon}}, \boldsymbol{\xi}) = \frac{1}{2}\overline{\boldsymbol{\varepsilon}} : \widetilde{\boldsymbol{L}} : \overline{\boldsymbol{\varepsilon}} - \overline{\boldsymbol{\varepsilon}} : \sum_{k=1}^{M} \boldsymbol{a}^{(k)} \xi^{(k)} + \frac{1}{2} \sum_{k,\ell=1}^{M} (\mathcal{L}^{(k\ell)} - \mathcal{D}^{(k\ell)}) \xi^{(k)} \xi^{(\ell)},$$

where

$$\left.\begin{aligned} \widetilde{\boldsymbol{L}} = \langle \boldsymbol{A}^{\mathsf{T}} : \boldsymbol{L} : \boldsymbol{A} \rangle, \quad \boldsymbol{a}^{(k)} = \langle \boldsymbol{\mu}^{(k)} : \boldsymbol{L} : \boldsymbol{A} \rangle, \\ \mathcal{D}^{(k\ell)} = \langle \boldsymbol{\mu}^{(k)} : \boldsymbol{L} : (\boldsymbol{D} * \boldsymbol{\mu}^{(\ell)}) \rangle, \quad \mathcal{L}^{(k\ell)} = \langle \boldsymbol{\mu}^{(k)} : \boldsymbol{L} : \boldsymbol{\mu}^{(\ell)} \rangle. \end{aligned}\right\} \tag{35}$$

Alternative expressions for these coefficients are given in Appendix A. Thanks to the NTFA decomposition (22), the effective dissipation potential $\widetilde{\varphi}$ is

$$\widetilde{\varphi}(\dot{\boldsymbol{\xi}}) = \frac{1}{2} \sum_{k,\ell=1}^{M} \mathcal{L}_{\mathsf{v}}^{(k\ell)} \dot{\xi}^{(k)} \dot{\xi}^{(\ell)}, \quad \text{where} \quad \mathcal{L}_{\mathsf{v}}^{(k\ell)} = \langle \boldsymbol{\mu}^{(k)} : \boldsymbol{L}_{\mathsf{v}} : \boldsymbol{\mu}^{(\ell)} \rangle.$$

Denoting by $\mathfrak{a}^{(k)}$ the thermodynamic force associated with $\xi^{(k)}$, the two expressions of this force are

$$\left.\begin{aligned}\mathfrak{a}^{(k)} &= -\frac{\partial \widetilde{w}}{\partial \xi^{(k)}}(\overline{\boldsymbol{\varepsilon}}, \boldsymbol{\xi}) = \overline{\boldsymbol{\varepsilon}} : \boldsymbol{a}^{(k)} + \sum_{\ell=1}^{M} (\mathcal{D}^{(k\ell)} - \mathcal{L}^{(k\ell)}) \xi^{(\ell)}, \\ \mathfrak{a}^{(k)} &= \frac{\partial \widetilde{\varphi}}{\partial \dot{\xi}^{(k)}}(\dot{\boldsymbol{\xi}}) = \sum_{\ell=1}^{M} \mathcal{L}_{\mathsf{v}}^{(k\ell)} \dot{\xi}^{(\ell)}.\end{aligned}\right\}$$

Equaling these two expressions yields the following differential equation (corresponding to (27) in the general case)

$$\sum_{\ell=1}^{M} \mathcal{L}_{\mathsf{v}}^{(k\ell)} \dot{\xi}^{(\ell)} = \overline{\boldsymbol{\varepsilon}} : \boldsymbol{a}^{(k)} + \sum_{\ell=1}^{M} (\mathcal{D}^{(k\ell)} - \mathcal{L}^{(k\ell)}) \xi^{(\ell)}.$$

This ODE can be alternatively re-written as a differential equation for $\boldsymbol{\xi}$ or for $\mathfrak{a}$

$$\dot{\xi}^{(k)} = \sum_{\ell=1}^{M} \mathcal{M}_{\mathsf{v}}^{(k\ell)} \left[\overline{\boldsymbol{\varepsilon}} : \boldsymbol{a}^{(\ell)} + \sum_{m=1}^{M} (\mathcal{D}^{(\ell m)} - \mathcal{L}^{(\ell m)}) \xi^{(m)} \right], \tag{36}$$

or

$$\dot{\mathfrak{a}}^{(k)} = \dot{\overline{\boldsymbol{\varepsilon}}} : \boldsymbol{a}^{(k)} + \sum_{\ell=1}^{M} \left[(\mathcal{D}^{(k\ell)} - \mathcal{L}^{(k\ell)}) \sum_{m=1}^{M} \mathcal{M}_{\mathsf{v}}^{(\ell m)} \mathfrak{a}^{(m)} \right], \tag{37}$$

where $\mathcal{M}_{\mathsf{v}}^{(k\ell)}$ denotes the $(k\ell)$ component of the inverse of the matrix $\mathcal{L}_{\mathsf{v}}^{(k\ell)}$. Equation (37) is the ODE derived in Largenton et al. (2014).

It is important to note that the reduced differential equations (36) for $\boldsymbol{\xi}$ can be expressed only in terms of the quantities $\boldsymbol{a}^{(k)}$, $\boldsymbol{\mathcal{D}} - \boldsymbol{\mathcal{L}}, \boldsymbol{\mathcal{L}}_{\mathsf{v}}$ which can be pre-computed off-line once for all. Therefore the reduced constitutive equations can be implemented without having to compute any local fields (by contrast with the situation when φ is non quadratic).

4.5. Orientation for the rest of the paper

The situation for the *"coarse dynamics"* (in other words, the differential equations governing the evolution of the reduced variables $\boldsymbol{\xi}$) is, so far, the following one:

1. The exact coarse dynamics (27) requires to compute local fields "on-line" (each time $\langle \dfrac{\partial \varphi}{\partial \dot{\boldsymbol{\alpha}}} \left(\displaystyle\sum_{\ell=1}^{M} \dot{\xi}^{(\ell)} \boldsymbol{\mu}^{(\ell)} \right) : \boldsymbol{\mu}^{(k)} \rangle$ is called). This slows down considerably the method.
2. When the dissipation potential is quadratic, there is no need for on-line computations of local fields since all terms entering the coarse dynamics can be pre-computed once for all.

It is therefore natural to look for an approximation of the exact potential $\widetilde{\varphi}$ by a quadratic potential. This is done by looking for an appropriate approximation of the individual potentials $\varphi^{(r)}$ by quadratic potentials. The very same problem arises in homogenization of nonlinear composites when the constituents are governed by a single, non quadratic, potential. The techniques

explored in this latter context can therefore be used in the present problem. More specifically the *Tangent Second Order* (TSO) approximation of Ponte Castañeda (1996) will be explored in section 6.

However a difficulty arises when this technique is applied to the dissipation potentials $\varphi^{(r)}$. This difficulty can be summarized as follows (more details are given in Appendix C). The TSO approximation applied to $\varphi^{(r)}$ delivers an approximation of the effective dissipation potential with a leading term in the form $\frac{1}{2}\dot{\boldsymbol{\xi}}.\boldsymbol{L}_{\mathrm{v}}^{(0)}.\dot{\boldsymbol{\xi}}$, where $\boldsymbol{L}_{\mathrm{v}}^{(0)}$ depends on $\dot{\boldsymbol{\xi}}$. Unfortunately, the differential equation obtained by differentiating this term with respect to $\dot{\boldsymbol{\xi}}$ is not in the usual form $\dot{\boldsymbol{\xi}} = \mathfrak{f}(t, \boldsymbol{\xi})$, but in the form $\mathfrak{g}(\dot{\boldsymbol{\xi}}) = \mathfrak{f}(t, \boldsymbol{\xi})$ where $\mathfrak{g}$ is a nonlinear and non explicit function precisely because of the dependence of $\boldsymbol{L}_{\mathrm{v}}^{(0)}$ on $\dot{\boldsymbol{\xi}}$. The integration in time of such a doubly-nonlinear differential equation is difficult and it is preferable to arrive at a differential equation in usual form, in the above sense.

For this purpose, the relations (28) (29) can be re-written with the dual $\widetilde{\varphi}^*$ of $\widetilde{\varphi}$ as

$$\mathfrak{a} = -\frac{\partial \widetilde{w}}{\partial \boldsymbol{\xi}}(\overline{\boldsymbol{\varepsilon}}, \boldsymbol{\xi}), \quad \dot{\boldsymbol{\xi}} = \frac{\partial \widetilde{\varphi}^*}{\partial \mathfrak{a}}(\mathfrak{a}), \text{ or equivalently } \dot{\boldsymbol{\xi}} = \frac{\partial \widetilde{\varphi}^*}{\partial \mathfrak{a}}\left(-\frac{\partial \widetilde{w}}{\partial \boldsymbol{\xi}}(\overline{\boldsymbol{\varepsilon}}, \boldsymbol{\xi})\right). \tag{38}$$

The differential equation (38) for $\boldsymbol{\xi}$ is now in usual form and the above mentioned linearization techniques can be applied to $\widetilde{\varphi}^*$. However computing $\widetilde{\varphi}^*$ is a formidable task in general, since $\widetilde{\varphi}$ is not known explicitly. So the approach that will be followed in the rest of this study consists in two successive steps:

1. An accurate approximation $\widetilde{\psi}$ for $\widetilde{\varphi}^*$ will be derived in section 5 following the procedure proposed by Fritzen and Leuschner (2013). This approximation is still non quadratic and its evaluation requires computing local fields at small scale which is very costly.
2. A quadratic approximation of $\widetilde{\psi}$ is derived in section 6 which consists essentially of a Taylor expansion of $\widetilde{\psi}$ to second order (tangent second-order approximation).

4.6. Individual constituents with non-standard constitutive relations

The above model can be extended to cover the case of constituents governed by non-standard constitutive relations in the form (7). When the NTFA decomposition (22) is assumed, the extension of (31) consists of the differential equations

$$\langle \frac{\partial w}{\partial \boldsymbol{\alpha}}(\boldsymbol{\varepsilon}, \boldsymbol{\alpha}(\boldsymbol{\xi})) : \boldsymbol{\mu}^{(k)} \rangle + \langle \boldsymbol{\mathcal{G}}(\dot{\boldsymbol{\alpha}}(\dot{\boldsymbol{\xi}})) : \boldsymbol{\mu}^{(k)} \rangle = 0, \ k = 1, ..., M,$$

or equivalently

$$\frac{\partial \widetilde{w}}{\partial \xi^{(k)}}(\overline{\boldsymbol{\varepsilon}}, \boldsymbol{\xi}) + \langle \boldsymbol{\mathcal{G}}(\dot{\boldsymbol{\alpha}}(\dot{\boldsymbol{\xi}})) : \boldsymbol{\mu}^{(k)} \rangle = 0, \ k = 1, ..., M.$$

5. A hybrid formulation

For completeness, we re-derive here, in a slightly more general framework, the hybrid NTFA model of Fritzen and Leuschner (2013). It is recalled that this hybrid method will be used to derive an accurate approximation $\widetilde{\psi}$ for $\widetilde{\varphi}^*$.

5.1. Dual potential

Using the Legendre transform

$$\varphi(\dot{\boldsymbol{\alpha}}) = \operatorname*{Sup}_{\boldsymbol{\mathcal{A}}^*} \left(\dot{\boldsymbol{\alpha}} : \boldsymbol{\mathcal{A}}^* - \psi(\boldsymbol{\mathcal{A}}^*)\right),$$

in the definition of $J(\boldsymbol{\varepsilon}, \boldsymbol{\alpha})$, one gets

$$\langle J(\boldsymbol{\varepsilon}, \boldsymbol{\alpha})\rangle = \operatorname*{Sup}_{\boldsymbol{\mathcal{A}}^*} \left[\langle w(\boldsymbol{\varepsilon}, \boldsymbol{\alpha})\rangle + \Delta t \langle \boldsymbol{\mathcal{A}}^* : \frac{\boldsymbol{\alpha} - \boldsymbol{\alpha}_n}{\Delta t}\rangle - \Delta t \langle \psi(\boldsymbol{\mathcal{A}}^*)\rangle\right],$$

and

$$\operatorname*{Inf}_{\boldsymbol{\varepsilon}\in\mathcal{K}(\overline{\boldsymbol{\varepsilon}})} \operatorname*{Inf}_{\boldsymbol{\alpha}} \langle J(\boldsymbol{\varepsilon}, \boldsymbol{\alpha})\rangle = \operatorname*{Inf}_{\boldsymbol{\varepsilon}\in\mathcal{K}(\overline{\boldsymbol{\varepsilon}})} \operatorname*{Inf}_{\boldsymbol{\alpha}} \operatorname*{Sup}_{\boldsymbol{\mathcal{A}}^*} \left[\langle w(\boldsymbol{\varepsilon}, \boldsymbol{\alpha})\rangle + \Delta t \langle \boldsymbol{\mathcal{A}}^* : \frac{\boldsymbol{\alpha} - \boldsymbol{\alpha}_n}{\Delta t}\rangle - \Delta t \langle \psi(\boldsymbol{\mathcal{A}}^*)\rangle\right].$$

Taking $\boldsymbol{\alpha}$ according to the decomposition (22) yields the upper bound

$$\operatorname*{Inf}_{\boldsymbol{\xi}} \operatorname*{Sup}_{\boldsymbol{\mathcal{A}}^*} \left[\widetilde{w}(\overline{\boldsymbol{\varepsilon}}, \boldsymbol{\xi}) + \sum_{k=1}^{M} (\boldsymbol{\xi}^{(k)} - \boldsymbol{\xi}_n^{(k)}) \langle \boldsymbol{\mathcal{A}}^* : \boldsymbol{\mu}^{(k)}\rangle - \Delta t \langle \psi(\boldsymbol{\mathcal{A}}^*)\rangle\right]. \tag{39}$$

When the field $\boldsymbol{\mathcal{A}}^*$ is left completely arbitrary, the exact dual formulation (39) is, as expected, strictly equivalent to the initial primal formulation (23), with the same drawback that the resulting differential equations cannot be explicitly expressed with pre-computed quantities, but require the evaluation of local fields and nonlinear functions of them.

The duality procedure of Fritzen and Leuschner (2013) proceeds by assuming implicitly that the field $\boldsymbol{\mathcal{A}}^*(\boldsymbol{x})$ in (39) can be restricted to the form

$$\boldsymbol{\mathcal{A}}^*(\boldsymbol{x}, \overline{\boldsymbol{\varepsilon}}, \boldsymbol{\xi}^*) = -\frac{\partial w}{\partial \boldsymbol{\alpha}}(\boldsymbol{x}, \boldsymbol{\varepsilon}^*(\boldsymbol{x}), \boldsymbol{\alpha}^*(\boldsymbol{x})). \tag{40}$$

The field $\boldsymbol{\mathcal{A}}^*(\boldsymbol{x})$ in (40) is associated with the solution of the thermoelastic problem (19) in the following way: given a macroscopic strain $\overline{\boldsymbol{\varepsilon}}$ and a set $\boldsymbol{\xi}^*$ of reduced variables, $\boldsymbol{\alpha}^*$ is the field of internal variables corresponding to the reduced variables $\boldsymbol{\xi}^*$ by the NTFA decomposition (22) and $\boldsymbol{\varepsilon}^*$ is the strain field solution of the thermoelastic problem (19). Restricting the supremum in the variational problem (39) to fields $\boldsymbol{\mathcal{A}}^*$ of the form (40) yields

$$\operatorname*{Inf}_{\boldsymbol{\xi}} \operatorname*{Sup}_{\boldsymbol{\xi}^*} \left[\widetilde{w}(\overline{\boldsymbol{\varepsilon}}, \boldsymbol{\xi}) + \sum_{k=1}^{M} (\boldsymbol{\xi}^{(k)} - \boldsymbol{\xi}_n^{(k)}) \langle \boldsymbol{\mathcal{A}}^*(\overline{\boldsymbol{\varepsilon}}, \boldsymbol{\xi}^*) : \boldsymbol{\mu}^{(k)}\rangle - \Delta t \langle \psi(\boldsymbol{\mathcal{A}}^*(\overline{\boldsymbol{\varepsilon}}, \boldsymbol{\xi}^*))\rangle\right].$$

The optimality condition with respect to $\xi^{(k)}$ reads as

$$\frac{\partial \widetilde{w}}{\partial \xi^{(k)}}(\overline{\boldsymbol{\varepsilon}}, \boldsymbol{\xi}) + \langle \boldsymbol{\mathcal{A}}^* : \boldsymbol{\mu}^{(k)}\rangle = 0, \tag{41}$$

whereas the optimality condition with respect to $\xi^{*(\ell)}$ is

$$\sum_{k=1}^{M} \frac{\boldsymbol{\xi}^{(k)} - \boldsymbol{\xi}_n^{(k)}}{\Delta t} \langle \frac{\partial \boldsymbol{\mathcal{A}}}{\partial \xi^{*(\ell)}} : \boldsymbol{\mu}^{(k)}\rangle = \langle \frac{\partial \psi}{\partial \xi^{*(\ell)}}(\boldsymbol{\mathcal{A}}^*)\rangle. \tag{42}$$

From equation (41) it is found that

$$\mathfrak{a}^{(k)}(\overline{\boldsymbol{\varepsilon}}, \boldsymbol{\xi}) = -\frac{\partial \widetilde{w}}{\partial \xi^{(k)}}(\overline{\boldsymbol{\varepsilon}}, \boldsymbol{\xi}) = \langle \boldsymbol{\mathcal{A}}^* : \boldsymbol{\mu}^{(k)} \rangle = \mathfrak{a}^{(k)}(\overline{\boldsymbol{\varepsilon}}, \boldsymbol{\xi}^*). \tag{43}$$

In order to conclude that $\boldsymbol{\xi}^* = \boldsymbol{\xi}$, we need an invertibility assumption, namely:

Invertibility assumption: the relation between the generalized state variables $\boldsymbol{\xi}$ and the associated generalized forces $\mathfrak{a}$,

$$\boldsymbol{\xi} \ \rightarrow \ \mathfrak{a} = -\frac{\partial \widetilde{w}}{\partial \boldsymbol{\xi}}(\overline{\boldsymbol{\varepsilon}}, \boldsymbol{\xi}), \tag{44}$$

is one-to-one and differentiable. In other words, the effective potential $\widetilde{w}$ is a strictly convex function of $\boldsymbol{\xi}$ (it is a convex function, by convexity of the individual potentials $w^{(r)}$, but not necessarily strictly convex). The fullfilment of this invertibility condition depends on the form of the free-energy function in the phases and on the choice of the modes $\boldsymbol{\mu}^{(k)}$. It has to be checked in each different situation.

From (43) and by virtue of the invertibility assumption (44), it is concluded that $\boldsymbol{\xi}^* = \boldsymbol{\xi}$ and therefore that $\boldsymbol{\mathcal{A}}^* = \boldsymbol{\mathcal{A}}(\overline{\boldsymbol{\varepsilon}}, \boldsymbol{\xi})$ where $\boldsymbol{\mathcal{A}}(\overline{\boldsymbol{\varepsilon}}, \boldsymbol{\xi})$ denotes the expression (40). Moreover it follows from the definition of $\mathfrak{a}^{(k)}$ that

$$\frac{\partial \mathfrak{a}^{(k)}}{\partial \xi^{(\ell)}}(\overline{\boldsymbol{\varepsilon}}, \boldsymbol{\xi}) = \left\langle \frac{\partial \boldsymbol{\mathcal{A}}}{\partial \xi^{(\ell)}}(\overline{\boldsymbol{\varepsilon}}, \boldsymbol{\xi}) : \boldsymbol{\mu}^{(k)} \right\rangle.$$

Letting Δt go to 0, (42) can be written as

$$\sum_{k=1}^{M} \frac{\partial \mathfrak{a}^{(k)}}{\partial \xi^{(\ell)}}(\overline{\boldsymbol{\varepsilon}}, \boldsymbol{\xi}) \dot{\xi}^{(k)} = \left\langle \frac{\partial \psi}{\partial \xi^{(\ell)}} \left(\boldsymbol{\mathcal{A}}(\overline{\boldsymbol{\varepsilon}}, \boldsymbol{\xi}) \right) \right\rangle,$$

or equivalently

$$\dot{\xi}^{(k)} = \sum_{\ell=1}^{M} \left(\frac{\partial \mathfrak{a}}{\partial \boldsymbol{\xi}} \right)^{-1(k\ell)} \frac{\partial \widetilde{\psi}}{\partial \xi^{(\ell)}}(\overline{\boldsymbol{\varepsilon}}, \boldsymbol{\xi}), \quad \text{where} \quad \widetilde{\psi}(\overline{\boldsymbol{\varepsilon}}, \boldsymbol{\xi}) = \langle \psi(\boldsymbol{\mathcal{A}}(\overline{\boldsymbol{\varepsilon}}, \boldsymbol{\xi})) \rangle. \tag{45}$$

By the invertibility assumption, $\boldsymbol{\xi}$ can be expressed in terms of $\overline{\boldsymbol{\varepsilon}}$ and $\mathfrak{a} = (\mathfrak{a}^{(k)}|_{k=1,..,M})$, and $\widetilde{\psi}$ can be considered as a function of $(\overline{\boldsymbol{\varepsilon}}, \mathfrak{a})$,

$$\widetilde{\psi}(\overline{\boldsymbol{\varepsilon}}, \mathfrak{a}) = \widetilde{\psi}(\overline{\boldsymbol{\varepsilon}}, \boldsymbol{\xi}(\overline{\boldsymbol{\varepsilon}}, \mathfrak{a})).$$

Upon derivation of this relation, one obtains

$$\frac{\partial \widetilde{\psi}}{\partial \mathfrak{a}^{(k)}}(\overline{\boldsymbol{\varepsilon}}, \mathfrak{a}) = \sum_{\ell=1}^{M} \frac{\partial \widetilde{\psi}}{\partial \xi^{(\ell)}} \frac{\partial \xi^{(\ell)}}{\partial \mathfrak{a}^{(k)}} = \sum_{\ell=1}^{M} \left(\frac{\partial \mathfrak{a}}{\partial \boldsymbol{\xi}} \right)^{-1(k\ell)} \frac{\partial \widetilde{\psi}}{\partial \xi^{(\ell)}}(\overline{\boldsymbol{\varepsilon}}, \boldsymbol{\xi}),$$

and combining this relation with (45), the following evolution equation for $\xi^{(k)}$ is obtained

$$\dot{\xi}^{(k)} = \frac{\partial \widetilde{\psi}}{\partial \mathfrak{a}^{(k)}}(\overline{\boldsymbol{\varepsilon}}, \mathfrak{a}).$$

The final form of the evolution equation for the internal variables is

$$\mathfrak{a}^{(k)} = -\frac{\partial \widetilde{w}}{\partial \xi^{(k)}}(\overline{\boldsymbol{\varepsilon}}, \boldsymbol{\xi}), \quad \dot{\xi}^{(k)} = \frac{\partial \widetilde{\psi}}{\partial \mathfrak{a}^{(k)}}(\overline{\boldsymbol{\varepsilon}}, \mathfrak{a}). \tag{46}$$

This is the typical form of the constitutive relations in a GSM (see (2) and (4)).

Using the invertibility assumption, these evolution equations can also be formulated as differential equations for the $\mathfrak{a}^{(k)}$'s instead of the $\xi^{(k)}$'s. Indeed, upon derivation in time of the relation $\mathfrak{a}^{(k)} = \mathfrak{a}^{(k)}(\overline{\boldsymbol{\varepsilon}}, \boldsymbol{\xi})$, one gets

$$\dot{\mathfrak{a}}^{(k)} = \frac{\partial \mathfrak{a}^{(k)}}{\partial \overline{\boldsymbol{\varepsilon}}} : \dot{\overline{\boldsymbol{\varepsilon}}} + \sum_{\ell=1}^{M} \frac{\partial \mathfrak{a}^{(k)}}{\partial \xi^{(\ell)}} \dot{\xi}^{(\ell)} = \frac{\partial \mathfrak{a}^{(k)}}{\partial \overline{\boldsymbol{\varepsilon}}} : \dot{\overline{\boldsymbol{\varepsilon}}} + \frac{\partial \widetilde{\psi}}{\partial \boldsymbol{\xi}^{(k)}}(\overline{\boldsymbol{\varepsilon}}, \boldsymbol{\xi}(\overline{\boldsymbol{\varepsilon}}, \mathfrak{a})). \tag{47}$$

The two equivalent differential equations (46) and (47) can be integrated in time for a prescribed history of macroscopic strain $\overline{\boldsymbol{\varepsilon}}(t)$. This allows for the determination of the resulting history $\boldsymbol{\xi}(t)$ of the reduced variables and consequently of the history of the overall stress $\overline{\boldsymbol{\sigma}}(t)$ by means of the relation (26).

5.2. Comparison between the primal NTFA model and the hybrid model

Unfortunately, the specific choice (40) for $\mathcal{A}^*$ leads to a lower bound for the upper bound (39). In other words the bounding character of (39) is lost and the resulting variational (stationarity) problem yields only an estimate for the effective incremental potential. In other words $\widetilde{\psi}$ is not the Legendre Fenchel transform of $\widetilde{\varphi}$. Therefore the hybrid model of Fritzen and Leuschner (2013) differs, in general, from the primal NTFA model (27).

This duality gap can be illustrated by two different means. First, linearly viscoelastic materials provide a simple example where both models can be derived in closed form, evidencing a gap between the two models. Second, a numerical example will help to appreciate how this duality gap depends on the number of modes chosen to perform the analysis.

5.2.1. Linear viscoelasticity

We come back to composites with linear viscoelastic constituents discussed in section 4.4. Recall that the thermodynamic force $\boldsymbol{\mathcal{A}}$ coincides with the stress $\boldsymbol{\sigma}$ and that the force potential for the individual constituents is $\psi^{(r)}(\boldsymbol{\mathcal{A}}) = (1/2)\boldsymbol{\mathcal{A}} : \boldsymbol{M}_{\mathsf{v}}^{(r)} : \boldsymbol{\mathcal{A}}$. Thanks to the decomposition (34), the effective potential $\widetilde{\psi}$ reads as

$$\widetilde{\psi}(\overline{\boldsymbol{\varepsilon}}, \boldsymbol{\xi}) = \langle \psi(\boldsymbol{\mathcal{A}}) \rangle = \frac{1}{2}\overline{\boldsymbol{\varepsilon}} : \langle \boldsymbol{A}^T : \boldsymbol{L}^T : \boldsymbol{M}_{\mathsf{v}} : \boldsymbol{L} : \boldsymbol{A} \rangle : \overline{\boldsymbol{\varepsilon}} + \sum_{k=1}^{M} \xi^{(k)} \boldsymbol{b}^{(k)} : \overline{\boldsymbol{\varepsilon}} + \frac{1}{2} \sum_{k,\ell=1}^{M} \mathcal{R}^{(k\ell)} \xi^{(k)} \xi^{(\ell)},$$

where

$$\boldsymbol{b}^{(k)} = \langle \boldsymbol{\rho}^{(k)} : \boldsymbol{M}_{\mathsf{v}} : \boldsymbol{L} : \boldsymbol{A} \rangle, \quad \mathcal{R}^{(k\ell)} = \langle \boldsymbol{\rho}^{(k)} : \boldsymbol{M}_{\mathsf{v}} : \boldsymbol{\rho}^{(\ell)} \rangle.$$

The differential equations for $\boldsymbol{\xi}$ and $\mathfrak{a}$ in the hybrid model (corresponding to (45) and (47)) read

$$\dot{\xi}^{(k)} = \sum_{\ell=1}^{M} (\mathcal{D} - \mathcal{L})^{-1(k\ell)} \left[\overline{\boldsymbol{\varepsilon}} : \boldsymbol{b}^{(\ell)} + \sum_{m=1}^{M} \mathcal{R}^{(\ell m)} \xi^{(m)} \right], \tag{48}$$

and

$$\dot{\mathfrak{a}}^{(k)} = \dot{\overline{\boldsymbol{\varepsilon}}} : \boldsymbol{a}^{(k)} + \overline{\boldsymbol{\varepsilon}} : \boldsymbol{b}^{(k)} + \sum_{\ell,m=1}^{M} \mathcal{R}^{(k\ell)} (\mathcal{D} - \mathcal{L})^{-1(\ell m)} (\mathfrak{a}^{(m)} - \overline{\boldsymbol{\varepsilon}} : \boldsymbol{a}^{(m)}). \tag{49}$$

(48) and (49) differ from (36) and (37) respectively which shows that the primal NTFA method and the hybrid NTFA model do not coincide.

5.2.2. Nonlinear dual phase materials

We consider here a dual-phase microstructure, shown in figure 1 center, where both phases have the same volume fraction. Both phases are viscoelastic, power-law materials. The internal variable and the free-energy are identical to those of section 4.4 and the dissipation potential is given by

$$\varphi(\dot{\boldsymbol{\alpha}}) = \frac{\sigma_0 \dot{\varepsilon}_0}{m+1} \left(\frac{\dot{\alpha}_{\mathsf{eq}}}{\dot{\varepsilon}_0} \right)^{m+1} \tag{50}$$

Phase 1 is linear viscoelastic whereas phase 2 is nonlinear. The material data of the phases are

$$E^{(1)} = 100 \text{ GPa}, \quad \nu^{(1)} = 0.3, \quad \sigma_0^{(1)} = 250 \text{ MPa}, \quad \dot{\varepsilon}_0 = 10^{-5} \text{ s}^{-1}, \quad m^{(1)} = 1,$$

$$E^{(2)} = 180 \text{ GPa}, \quad \nu^{(2)} = 0.3, \quad \sigma_0^{(2)} = 50 \text{ MPa}, \quad \dot{\varepsilon}_0 = 10^{-5} \text{ s}^{-1}, \quad m^{(2)} = 0.125.$$

The composite is subjected to an in-plane shear at constant strain-rate,

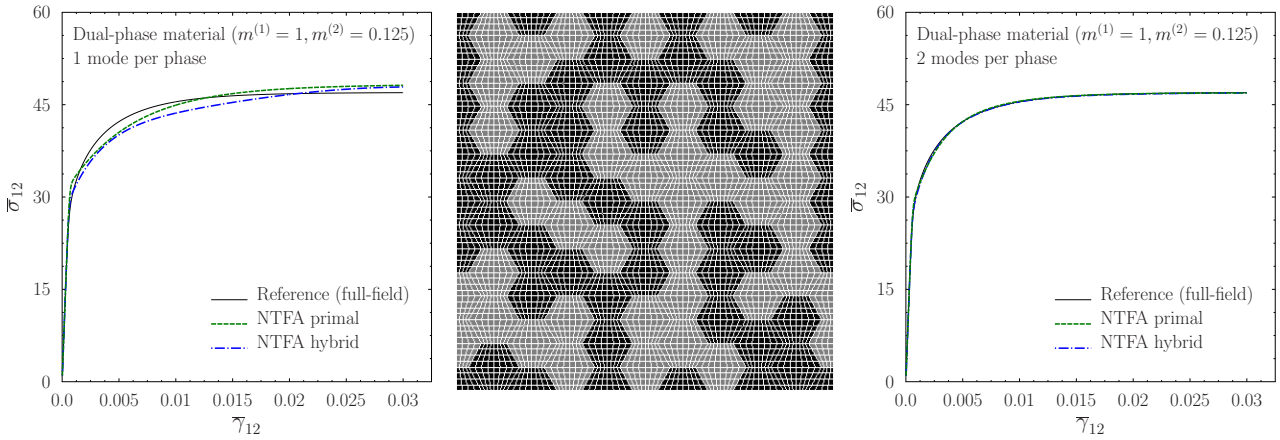

Figure 1: Dual-phase material under shear. Comparison between the primal NTFA model (27), the hybrid NTFA model (47) and full-field simulations. Left: NTFA analyses with one mode per phase. Center: Mesh of the microstructure. Each hexagon is dicretized into 64 eight-node quadratic finite elements with 2×2 Gauss points. Phase 1 in black, phase 2 in grey. Right: NTFA analyses with two modes per phase.

$$\overline{\boldsymbol{\varepsilon}}(t) = \frac{\overline{\gamma}_{12}(t)}{2}\left(\boldsymbol{e}_1 \otimes \boldsymbol{e}_2 + \boldsymbol{e}_2 \otimes \boldsymbol{e}_1\right), \quad \dot{\overline{\gamma}}_{12} = \sqrt{3}\dot{\varepsilon}_0,$$

and its exact response (up to computational errors) is analyzed with the finite-element method. Periodicity conditions are imposed on the boundary of the unit-cell and computations are performed with a constant time-step $\Delta t = (2/\sqrt{3})$s until the overall stress $\overline{\sigma}_{12}$ reaches an asymptot. Thirty snapshots of the plastic strain-field are generated along the loading and plastic modes are generated using the snapshot POD (also called Karhunen-Loève method, see Michel and Suquet, 2009, for more details). Both the primal NTFA model (27) and the hybrid model (46) have been implemented with 1, 2 or 3 modes per phase and their predictions are compared in figure 1 with full-field simulations. Two observations can be made.

1. The predictions of the two models with only one mode per phase are shown in figure 1 left and compared with full-field simulations. As expected from the theory, the two models give different predictions. The hybrid model of Fritzen and Leuschner (2013) is different from the primal NTFA model.
2. The predictions of the models with two modes per phase are shown in figure 1 right. Both models give the same predictions which are in very good agreement with the full-field simulations. The agreement is even better with 3 modes (not shown here). A good accuracy is attained with a low number of modes.

In view of this example it can be concluded that the hybrid NTFA model is different from the primal NTFA model but is close to it when enough modes are used in its implementation.

5.3. Individual constituents with non-standard constitutive relations

The above hybrid model can be extended to cover the case of constituents governed by the non-standard constitutive relations (7). The forces $\mathfrak{a}^{(k)} = -\dfrac{\partial \widetilde{w}}{\partial \xi^{(k)}}(\overline{\boldsymbol{\varepsilon}}, \boldsymbol{\xi})$ are unchanged and the differential equation (47) governing the evolution of these forces is (heuristically) modified into

$$\dot{\mathfrak{a}}^{(k)} = \frac{\partial \mathfrak{a}^{(k)}}{\partial \overline{\boldsymbol{\varepsilon}}} : \dot{\overline{\boldsymbol{\varepsilon}}} + \langle \boldsymbol{\mathcal{F}}(\boldsymbol{\mathcal{A}}) : \frac{\partial \boldsymbol{\mathcal{A}}}{\partial \xi^{(k)}} \rangle,$$

where it is understood that $\boldsymbol{\mathcal{A}}$ is the function of $\overline{\boldsymbol{\varepsilon}}$ and $\boldsymbol{\xi}$ given by (40).

5.4. Example 1: Elasto-viscoplastic constituents with linear kinematic hardening

The constitutive relations for elasto-viscoplastic phases with isotropic (possibly nonlinear) hardening and linear kinematic hardening have been presented in section 2.3. The appropriate internal variables are the viscous strain and the cumulated strain, $\boldsymbol{\alpha} = (\boldsymbol{\varepsilon}_{\mathsf{v}}, p)$, the free-energy is given by (12), the thermodynamic forces are $\boldsymbol{\mathcal{A}}_{\mathsf{v}} = \boldsymbol{\sigma} - \boldsymbol{X}$, $\mathcal{A}_{\mathsf{p}} = -R(p)$ and the force potential is (13).

According to the general NTFA scheme, all state variables should be decomposed on a set of modes, including the scalar variable p. However, since the stored energy function is a

nonquadratic function of p, the term corresponding to the stored energy in the effective free-energy cannot be expressed simply (in general) *except when the modes for the p variables are the characteristic functions of the phases*[2]. Therefore the NTFA decomposition is chosen to be

$$\varepsilon_{\mathsf{v}}(\boldsymbol{x}) = \sum_{k=1}^{M} \boldsymbol{\xi}_{\mathsf{v}}^{(k)} \boldsymbol{\mu}^{(k)}(\boldsymbol{x}), \quad p(\boldsymbol{x}) = \sum_{r=1}^{P} p^{(r)} \chi^{(r)}(\boldsymbol{x}), \tag{51}$$

where the modes $\boldsymbol{\mu}^{(k)}$ for the viscoplastic strain are assumed to be known, obtained for instance by the POD applied to a series of snapshots provided by full-field simulations (see Michel and Suquet, 2009, for more details). The reduced variables consist of the two sets of variables $\xi_{\mathsf{v}}^{(k)}|_{k=1....M}$ and $p^{(r)}|_{r=1....P}$,

$$\boldsymbol{\xi} = (\boldsymbol{\xi}_{\mathsf{v}}, \boldsymbol{p}), \quad \boldsymbol{\xi}_{\mathsf{v}} = \xi_{\mathsf{v}}^{(k)}|_{k=1....M}, \quad \boldsymbol{p} = p^{(r)}|_{r=1....P}.$$

The thermoelastic problem (19) takes the form (32). The strain field is therefore given by (33) (with $\boldsymbol{\xi}$ replaced by $\boldsymbol{\xi}_{\mathsf{v}}$). Note that the variables $p^{(r)}$ do not contribute to the strain field. The effective free-energy $\widetilde{w} = \langle w \rangle$ can be expressed in terms of quantities which can be pre-computed and reads

$$\widetilde{w}(\overline{\boldsymbol{\varepsilon}}, \boldsymbol{\xi}) = \frac{1}{2}\overline{\boldsymbol{\varepsilon}} : \widetilde{\boldsymbol{L}} : \overline{\boldsymbol{\varepsilon}} - \overline{\boldsymbol{\varepsilon}} : \sum_{k=1}^{M} \boldsymbol{a}^{(k)} \xi_{\mathsf{v}}^{(k)} + \frac{1}{2} \sum_{k,\ell=1}^{M} (\mathcal{L}^{(k\ell)} - \mathcal{D}^{(k\ell)} + \mathcal{H}^{(k\ell)}) \xi_{\mathsf{v}}^{(k)} \xi_{\mathsf{v}}^{(\ell)} + \sum_{r=1}^{P} c^{(r)} w^{(r)}(p^{(r)}).$$

$\widetilde{\boldsymbol{L}}$, $\boldsymbol{a}^{(k)}$, $\mathcal{D}$, $\mathcal{L}$ are defined in (35) (although the present constitutive relations differ from those considered in section 4.4, the effective free-energy $\widetilde{w}$ depends on the same pre-computed quantities related to the thermoelastic problem (32)) and

$$\mathcal{H}^{(k\ell)} = \langle \boldsymbol{\mu}^{(k)} : \boldsymbol{H} : \boldsymbol{\mu}^{(\ell)} \rangle.$$

The generalized forces are

$$\left.\begin{aligned} \mathfrak{a}_{\mathsf{v}}^{(k)} &= -\frac{\partial \widetilde{w}}{\partial \xi_{\mathsf{v}}^{(k)}}(\overline{\boldsymbol{\varepsilon}}, \boldsymbol{\xi}) = \boldsymbol{a}^{(k)} : \overline{\boldsymbol{\varepsilon}} + \sum_{\ell=1}^{M} (\mathcal{D}^{(k\ell)} - \mathcal{L}^{(k\ell)} - \mathcal{H}^{(k\ell)}) \xi_{\mathsf{v}}^{(\ell)}, \\ \mathfrak{a}_{\mathsf{p}}^{(r)} &= -\frac{\partial \widetilde{w}}{\partial p^{(r)}}(\overline{\boldsymbol{\varepsilon}}, \boldsymbol{\xi}) = -c^{(r)} R^{(r)}(p^{(r)}). \end{aligned}\right\} \tag{52}$$

It can be readily checked from (52) that the invertibility condition (44) is satisfied when the modes are chosen in such a way that the matrix $\mathcal{D} - \mathcal{L} - \mathcal{H}$ is invertible and when the function $R(p)$ describing isotropic hardening in each phase is monotonic.

When these conditions are satisfied, the potential $\widetilde{\psi}$ of the hybrid approach is evaluated with the thermodynamic forces resulting from the resolution of the problem (19) which takes the

[2]One can choose to decompose the field $p(\boldsymbol{x}, t)$ on a basis of modes but then the effective free-energy $\widetilde{w}$ and its gradient has to be evaluated numerically.

form (32). When the NTFA decomposition (51) is assumed, the stress field is given by (34) and the corresponding fields $\boldsymbol{\mathcal{A}}_{\mathsf{v}}$ and $\mathcal{A}_{\mathsf{p}}$ are

$$\left.\begin{array}{l} \boldsymbol{\mathcal{A}}_{\mathsf{v}}(\boldsymbol{x}) = \boldsymbol{L}(\boldsymbol{x}) : \boldsymbol{A}(\boldsymbol{x}) : \overline{\boldsymbol{\varepsilon}} + \displaystyle\sum_{k=1}^{M} \tilde{\boldsymbol{\rho}}^{(k)}(\boldsymbol{x}) \xi_{\mathsf{v}}^{(k)},\ \tilde{\boldsymbol{\rho}}^{(k)}(\boldsymbol{x}) = \boldsymbol{\rho}^{(k)}(\boldsymbol{x}) - \boldsymbol{H}(\boldsymbol{x}) : \boldsymbol{\mu}^{(k)}(\boldsymbol{x}), \\ \mathcal{A}_{\mathsf{p}}(\boldsymbol{x}) = \mathcal{A}_{\mathsf{p}}^{(r)} \chi^{(r)}(\boldsymbol{x}), \quad \mathcal{A}_{\mathsf{p}}^{(r)} = -R^{(r)}(p^{(r)}). \end{array}\right\} \tag{53}$$

The differential equation (47) for $\boldsymbol{\xi}_{\mathsf{v}}$, where $\widetilde{\psi}$ is given by (45), can be simplified by noting that only $\boldsymbol{\mathcal{A}}_{\mathsf{v}}$ depends on $\boldsymbol{\xi}_{\mathsf{v}}$. It takes the form

$$\dot{\mathfrak{a}}_{\mathsf{v}}^{(k)} = \boldsymbol{a}^{(k)} : \dot{\overline{\boldsymbol{\varepsilon}}} + \frac{\partial \widetilde{\psi}}{\partial \xi_{\mathsf{v}}^{(k)}}(\boldsymbol{\mathcal{A}}(\overline{\boldsymbol{\varepsilon}}, \boldsymbol{\xi}_{\mathsf{v}})), \tag{54}$$

where $\boldsymbol{\mathcal{A}}(\overline{\boldsymbol{\varepsilon}}, \boldsymbol{\xi}_{\mathsf{v}}) = (\boldsymbol{\mathcal{A}}_{\mathsf{v}}(\overline{\boldsymbol{\varepsilon}}, \boldsymbol{\xi}_{\mathsf{v}}), \mathcal{A}_{\mathsf{p}}(\boldsymbol{p}))$, with $\boldsymbol{\mathcal{A}}_{\mathsf{v}}(\overline{\boldsymbol{\varepsilon}}, \boldsymbol{\xi}_{\mathsf{v}})$ and $\mathcal{A}_{\mathsf{p}}(\boldsymbol{p})$ are given by (53). The differential equation (47) for the cumulated plastic strains per phase $p^{(r)}$ can also be simplified by noting that only $\mathcal{A}_{\mathsf{p}}$ depends on $\mathfrak{a}_{\mathsf{p}}$,

$$\dot{p}^{(r)} = \frac{\partial \widetilde{\psi}}{\partial \mathfrak{a}_{\mathsf{p}}^{(r)}} = \langle \frac{\partial \psi}{\partial \mathcal{A}_{\mathsf{p}}} \frac{\partial \mathcal{A}_{\mathsf{p}}}{\partial \mathfrak{a}_{\mathsf{p}}^{(r)}} \rangle = \langle \frac{\partial \psi}{\partial \mathcal{A}_{\mathsf{p}}} (\boldsymbol{\mathcal{A}}(\overline{\boldsymbol{\varepsilon}}, \boldsymbol{\xi})) \chi^{(r)} \rangle \frac{\partial \mathcal{A}_{\mathsf{p}}^{(r)}}{\partial \mathfrak{a}_{\mathsf{p}}^{(r)}} = \langle \frac{\partial \psi^{(r)}}{\partial \mathcal{A}_{\mathsf{p}}} (\boldsymbol{\mathcal{A}}(\overline{\boldsymbol{\varepsilon}}, \boldsymbol{\xi})) \rangle^{(r)}. \tag{55}$$

5.5. Example 2: Elasto-viscoplastic constituents with nonlinear kinematic hardening

The constitutive relations for elasto-viscoplastic phases with nonlinear isotropic and kinematic hardening have been given in section 2.4. The appropriate internal variables are the viscous strain, a tensor $\boldsymbol{\beta}$ accounting for kinematic hardening and the cumulated plastic or viscous strain, $\boldsymbol{\alpha} = (\boldsymbol{\varepsilon}_{\mathsf{v}}, \boldsymbol{\beta}, p)$, the free-energy and force potential are given by (15) and (17), the thermodynamics forces are $\boldsymbol{\mathcal{A}}_{\mathsf{v}} = \boldsymbol{\sigma}, \boldsymbol{\mathcal{A}}_{\beta} = -\boldsymbol{X},\ \mathcal{A}_{\mathsf{p}} = -R(p)$ (cf (16)).

According to the general NTFA scheme, all state variables are expressed on modes and for the same reason as in section 5.4, the modes for the cumulated plastic strain p are the characteristic functions of the phases,

$$\boldsymbol{\varepsilon}_{\mathsf{v}}(\boldsymbol{x}, t) = \sum_{k=1}^{M_{\mathsf{v}}} \xi_{\mathsf{v}}^{(k)}(t) \boldsymbol{\mu}_{\mathsf{v}}^{(k)}(\boldsymbol{x}),\ \boldsymbol{\beta}(\boldsymbol{x}, t) = \sum_{k=1}^{M_{\beta}} \xi_{\beta}^{(k)}(t) \boldsymbol{\mu}_{\beta}^{(k)}(\boldsymbol{x}),\ p(\boldsymbol{x}, t) = \sum_{r=1}^{P} p^{(r)}(t) \chi^{(r)}(\boldsymbol{x}), \tag{56}$$

where M_{v} and M_{β} are the number of modes for the internal variables $\boldsymbol{\varepsilon}_{\mathsf{v}}$ and $\boldsymbol{\beta}$ respectively. The local strain and stress fields are still given by (33) and (34) upon replacing $\boldsymbol{\xi}$ by $\boldsymbol{\xi}_{\mathsf{v}}$ and $\boldsymbol{\mu}^{(k)}$ by $\boldsymbol{\mu}_{\mathsf{v}}^{(k)}$. The corresponding effective free-energy is

$$\begin{aligned} \widetilde{w}(\overline{\boldsymbol{\varepsilon}}, \boldsymbol{\xi}) &= \frac{1}{2} \overline{\boldsymbol{\varepsilon}} : \widetilde{\boldsymbol{L}} : \overline{\boldsymbol{\varepsilon}} - \overline{\boldsymbol{\varepsilon}} : \sum_{k=1}^{M_{\mathsf{v}}} \xi_{\mathsf{v}}^{(k)} \boldsymbol{a}^{(k)} + \frac{1}{2} \sum_{k,\ell=1}^{M_{\mathsf{v}}} (\mathcal{L}^{(k\ell)} - \mathcal{D}^{(k\ell)}) \xi_{\mathsf{v}}^{(k)} \xi_{\mathsf{v}}^{(\ell)} \\ &+ \frac{1}{2} \sum_{k,\ell=1}^{M_{\beta}} \mathcal{H}_{\beta}^{(k\ell)} \xi_{\beta}^{(k)} \xi_{\beta}^{(\ell)} + \sum_{r=1}^{P} c^{(r)} w^{(r)}(p^{(r)}),\ \text{where } \mathcal{H}_{\beta}^{(k\ell)} = \langle \boldsymbol{\mu}_{\beta}^{(k)} : \boldsymbol{H} : \boldsymbol{\mu}_{\beta}^{(\ell)} \rangle. \end{aligned}$$

The thermodynamic forces of the reduced model are

$$\left.\begin{aligned} \mathfrak{a}_{\mathsf{v}}^{(k)} &= \boldsymbol{a}^{(k)} : \overline{\boldsymbol{\varepsilon}} + \sum_{\ell=1}^{M_{\mathsf{v}}} (\mathcal{D} - \mathcal{L})^{(k\ell)} \xi_{\mathsf{v}}^{(\ell)}, \\ \mathfrak{a}_{\beta}^{(k)} &= -\sum_{\ell=1}^{M_\beta} \mathcal{H}_\beta^{(k\ell)} \xi_\beta^{(\ell)}, \quad \mathfrak{a}_{\mathsf{p}}^{(r)} = -c^{(r)} R^{(r)}(p^{(r)}). \end{aligned}\right\}$$

The invertibility condition (44) is met as soon as the matrices $\mathcal{D} - \mathcal{L}$ and $\mathcal{H}_\beta$ are invertible and the hardening function $R(p)$ is a monotonic function of p in each phase. In the hybrid model, the effective potential $\widetilde{\psi}$ is calculated with the fields of thermodynamic forces derived from the solution of (19) (with reduces to (32) here),

$$\left.\begin{aligned} \boldsymbol{\mathcal{A}}_{\mathsf{v}}(\boldsymbol{x},t) = \boldsymbol{\sigma}(\boldsymbol{x},t) = \boldsymbol{L}(\boldsymbol{x}) : \boldsymbol{A}(\boldsymbol{x}) : \overline{\boldsymbol{\varepsilon}}(t) + \sum_{\ell=1}^{M_{\mathsf{v}}} \boldsymbol{\rho}^{(\ell)}(\boldsymbol{x}) \xi_{\mathsf{v}}^{(\ell)}(t), \\ \boldsymbol{\mathcal{A}}_\beta(\boldsymbol{x},t) = -\sum_{k=1}^{M_\beta} \boldsymbol{H}(\boldsymbol{x}) : \boldsymbol{\mu}_\beta^{(k)}(\boldsymbol{x}) \xi_\beta^{(k)}(t), \; \mathcal{A}_{\mathsf{p}}(\boldsymbol{x},t) = -\sum_{r=1}^{P} \chi^{(r)}(\boldsymbol{x}) R^{(r)}(p^{(r)}(t)). \end{aligned}\right\} \tag{57}$$

As can be seen from the constitutive equations (18) the variables $\boldsymbol{\varepsilon}_{\mathsf{v}}$ and p are standard (in the sense that their evolution derives from the force potential). The corresponding ordinary differential equations for $\boldsymbol{\xi}_{\mathsf{v}}$, or equivalenty for $\boldsymbol{\mathfrak{a}}_{\mathsf{v}}$ and $\boldsymbol{p}$, read

$$\left.\begin{aligned} \dot{\mathfrak{a}}_{\mathsf{v}}^{(k)} &= \boldsymbol{a}^{(k)} : \dot{\overline{\boldsymbol{\varepsilon}}} + \frac{\partial \widetilde{\psi}}{\partial \xi_{\mathsf{v}}^{(k)}} \left(\overline{\boldsymbol{\varepsilon}}, \boldsymbol{\xi}_{\mathsf{v}}, \boldsymbol{\xi}_\beta, \boldsymbol{p} \right), \\ \dot{p}^{(r)} &= \frac{\partial \widetilde{\psi}}{\partial \mathfrak{a}_{\mathsf{p}}^{(r)}} \left(\overline{\boldsymbol{\varepsilon}}, \boldsymbol{\xi}_{\mathsf{v}}, \boldsymbol{\xi}_\beta, \boldsymbol{p} \right). \end{aligned}\right\} \tag{58}$$

The differential equation for $\boldsymbol{\xi}_\beta$, or equivalently for $\boldsymbol{\mathfrak{a}}_\beta$, can be simplified by noting that only $\boldsymbol{\mathcal{A}}_\beta$ depends on $\boldsymbol{\xi}_\beta$,

$$\dot{\mathfrak{a}}_\beta^{(k)} = \langle \boldsymbol{\mathcal{F}}_\beta(\boldsymbol{\mathcal{A}}) : \frac{\partial \boldsymbol{\mathcal{A}}_\beta}{\partial \xi_\beta^{(k)}} \rangle = \langle \frac{\partial \psi}{\partial \boldsymbol{\mathcal{A}}_\beta}(\boldsymbol{\mathcal{A}}) : \frac{\partial \boldsymbol{\mathcal{A}}_\beta}{\partial \xi_\beta^{(k)}} \rangle + \langle \eta \frac{\partial \psi}{\partial \mathcal{A} p}(\boldsymbol{\mathcal{A}}) (\boldsymbol{H}^{-1} : \boldsymbol{\mathcal{A}}_\beta) : \frac{\partial \boldsymbol{\mathcal{A}}_\beta}{\partial \xi_\beta^{(k)}} \rangle. \tag{59}$$

The first term in (59) is $\partial \widetilde{\psi} / \partial \xi_\beta^{(k)}$, whereas the second term can be simplified by using the expression (57) for $\boldsymbol{\mathcal{A}}_\beta$, resulting in

$$\dot{\mathfrak{a}}_\beta^{(k)} = \frac{\partial \widetilde{\psi}}{\partial \xi_\beta^{(k)}} \left(\overline{\boldsymbol{\varepsilon}}, \boldsymbol{\xi}_{\mathsf{v}}, \boldsymbol{\xi}_\beta, \boldsymbol{p} \right) - \langle \eta \frac{\partial \psi}{\partial \mathcal{A} p}(\boldsymbol{\mathcal{A}}) \boldsymbol{\mathcal{A}}_\beta : \boldsymbol{\mu}_\beta^{(k)} \rangle. \tag{60}$$

A remark on the modes for the variable $\boldsymbol{\beta}$. According to the decomposition (56), modes should be generated for all the internal variables $\boldsymbol{\varepsilon}_{\mathsf{v}}, \boldsymbol{\beta}$ and p. As previously the modes for p are the characteristic functions of the phases. When the modes are localized in each individual phase,

the modes for the two tensorial variables $\boldsymbol{\varepsilon}_{\mathsf{v}}$ and $\boldsymbol{\beta}$ can be taken to be identical. Indeed the differential equation (18) can be integrated at each material point into

$$\boldsymbol{\beta}(\boldsymbol{x},t) = \mathrm{e}^{-\eta^{(r)}p^{(r)}(t)} \int_0^t \dot{\boldsymbol{\varepsilon}}_{\mathsf{v}}(\boldsymbol{x},s)\mathrm{e}^{\eta^{(r)}p^{(r)}(s)}\, ds \quad \text{in phase } r.$$

Therefore, if the decomposition (22) is assumed, and if the modes are localized in individual phases, the above relation shows that $\boldsymbol{\beta}$ can be decomposed on the same modes as $\boldsymbol{\varepsilon}_{\mathsf{v}}$.

6. Reduced differential equations: the coarse dynamics

When the dissipation potential of the phases is non quadratic, the computation of the effective potentials $\widetilde{\varphi}$ and $\widetilde{\psi}$ and of their derivatives, as required by the differential equations (27) or (47), requires the computation of local quantities such as $\varphi(\boldsymbol{x},\dot{\boldsymbol{\alpha}}(\boldsymbol{x},t))$ or $\psi(\boldsymbol{x},\boldsymbol{\mathcal{A}}(\boldsymbol{x},t))$ before taking their averages. This slows down considerably the integration of these ODE's. This observation motivates an additional reduction, namely the derivation of a differential equation for $\boldsymbol{\xi}$ where all terms can be pre-computed.

6.1. Tangent second-order linearization

It has already been noticed in section 4.4 and 5.2.1 that the effective potentials $\widetilde{\varphi}$ and $\widetilde{\psi}$ can be explicitly computed when the constituents of the composite are linear viscoelastic and the idea of the approximation is to reduce the problem to one with a quadratic potential. The very same problem arises in homogenization of composite materials comprised of nonlinear phases governed by a single potential. Replacing a non quadratic potential by a quadratic one, amounts to replacing a nonlinear composite by a linear comparison composite. This is essentially what has been explored in the last twenty years in the literature on nonlinear homogenization (Willis, 1989; Ponte Castañeda, 1991; Ponte Castañeda and Suquet, 1998; Ponte Castañeda, 1996). Two linearization techniques will be mentioned here. The first one is the variational method of Ponte Castañeda (1991), interpreted by Suquet (1995) as a secant method. The second one is the tangent second-order procedure of Ponte Castañeda (1996). The best results (except for voided materials) are obtained with the second technique, but the first one is interesting in that it allows to make contact with the original NTFA formulation of the authors (Michel and Suquet, 2003, 2009) which can be seen as a particular case of this variational technique (see Appendix B for details).

The second-order linearization technique is applied to the differential equation (47) which is recalled here,

$$\dot{\mathfrak{a}}^{(k)} = \frac{\partial \mathfrak{a}^{(k)}}{\partial \overline{\boldsymbol{\varepsilon}}} : \dot{\overline{\boldsymbol{\varepsilon}}} + \frac{\partial \widetilde{\psi}}{\partial \xi^{(k)}}(\overline{\boldsymbol{\varepsilon}},\boldsymbol{\xi}). \tag{61}$$

In each individual phase, the potential $\psi^{(r)}$ is expanded to second-order in the stress as

$$\psi^{(r)}(\boldsymbol{\mathcal{A}}) \simeq \psi^{(r)}_{TSO}(\boldsymbol{\mathcal{A}}),$$

$$\psi^{(r)}_{TSO}(\boldsymbol{\mathcal{A}}) = \psi^{(r)}(\check{\boldsymbol{\mathcal{A}}}^{(r)}) + \frac{\partial \psi^{(r)}}{\partial \boldsymbol{\mathcal{A}}}(\check{\boldsymbol{\mathcal{A}}}^{(r)}) : \left(\boldsymbol{\mathcal{A}} - \check{\boldsymbol{\mathcal{A}}}^{(r)}\right) + \frac{1}{2}\left(\boldsymbol{\mathcal{A}} - \check{\boldsymbol{\mathcal{A}}}^{(r)}\right) : \boldsymbol{M}_0^{(r)} : \left(\boldsymbol{\mathcal{A}} - \check{\boldsymbol{\mathcal{A}}}^{(r)}\right).$$

It follows from stationarity requirements (Ponte Castañeda, 1996) that the optimal choice for $\check{\boldsymbol{\mathcal{A}}}^{(r)}$ and a sensible choice for $\boldsymbol{M}_0^{(r)}$ is

$$\check{\boldsymbol{\mathcal{A}}}^{(r)} = \langle \boldsymbol{\mathcal{A}} \rangle^{(r)}, \quad \boldsymbol{M}_0^{(r)} = \frac{\partial^2 \psi^{(r)}}{\partial \boldsymbol{\mathcal{A}}^2}(\check{\boldsymbol{\mathcal{A}}}^{(r)}).$$

With these choices the effective dissipation potential is approximated by its tangent second-order expansion (TSO),

$$\left.\begin{aligned} &\widetilde{\psi}_{TSO}(\overline{\boldsymbol{\varepsilon}}, \boldsymbol{\xi}) = \sum_{r=1}^{P} c^{(r)} \left[\psi^{(r)}(\langle \boldsymbol{\mathcal{A}} \rangle^{(r)}) + \frac{1}{2} \frac{\partial^2 \psi^{(r)}}{\partial \boldsymbol{\mathcal{A}}^2}(\langle \boldsymbol{\mathcal{A}} \rangle^{(r)}) :: \boldsymbol{C}^{(r)}(\boldsymbol{\mathcal{A}}) \right], \\ &\text{where} \\ &\boldsymbol{C}^{(r)}(\boldsymbol{\mathcal{A}}) = \langle \big(\boldsymbol{\mathcal{A}} - \langle \boldsymbol{\mathcal{A}} \rangle^{(r)}\big) \otimes \big(\boldsymbol{\mathcal{A}} - \langle \boldsymbol{\mathcal{A}} \rangle^{(r)}\big) \rangle^{(r)} = \langle \boldsymbol{\mathcal{A}} \otimes \boldsymbol{\mathcal{A}} \rangle^{(r)} - \langle \boldsymbol{\mathcal{A}} \rangle^{(r)} \otimes \langle \boldsymbol{\mathcal{A}} \rangle^{(r)}. \end{aligned}\right\} \tag{62}$$

Therefore the differential equation (61) becomes

$$\begin{aligned} \dot{\mathfrak{a}}^{(k)} = \frac{\partial \mathfrak{a}^{(k)}}{\partial \overline{\boldsymbol{\varepsilon}}} : \dot{\overline{\boldsymbol{\varepsilon}}} \;\; &+ \;\; \sum_{r=1}^{P} c^{(r)} \left[\frac{\partial \psi^{(r)}}{\partial \boldsymbol{\mathcal{A}}}(\langle \boldsymbol{\mathcal{A}} \rangle^{(r)}) : \frac{\partial \langle \boldsymbol{\mathcal{A}} \rangle^{(r)}}{\partial \xi^{(k)}} + \frac{1}{2} \frac{\partial^2 \psi^{(r)}}{\partial \boldsymbol{\mathcal{A}}^2}(\langle \boldsymbol{\mathcal{A}} \rangle^{(r)}) :: \frac{\partial \boldsymbol{C}^{(r)}(\boldsymbol{\mathcal{A}})}{\partial \xi^{(k)}} \right. \\ &+ \;\; \left. \frac{1}{2} \frac{\partial^3 \psi^{(r)}}{\partial \boldsymbol{\mathcal{A}}^3}(\langle \boldsymbol{\mathcal{A}} \rangle^{(r)}) ::: \boldsymbol{C}^{(r)}(\boldsymbol{\mathcal{A}}) \otimes \frac{\partial \langle \boldsymbol{\mathcal{A}} \rangle^{(r)}}{\partial \xi^{(k)}} \right]. \end{aligned} \tag{63}$$

6.2. Example 1: Elasto-viscoplastic constituents with linear kinematic hardening

The constitutive relations for elasto-viscoplastic phases with isotropic (possibly nonlinear) hardening and linear kinematic hardening have been presented in section 2.3 and the differential equations for the hybrid model have been derived in section 5.4. Now we proceed to the derivation of the TSO approximation of the evolution equations for the reduced variables.

The TSO approximations of the differential equations (54) and (55) are

$$\dot{\mathfrak{a}}_{\mathsf{v}}^{(k)} = \boldsymbol{a}^{(k)} : \dot{\overline{\boldsymbol{\varepsilon}}} + \frac{\partial \widetilde{\psi}_{TSO}}{\partial \xi_{\mathsf{v}}^{(k)}}(\boldsymbol{\mathcal{A}}(\overline{\boldsymbol{\varepsilon}}, \boldsymbol{\xi})), \quad \dot{p}^{(r)} = \frac{\partial \widetilde{\psi}_{TSO}}{\partial \mathfrak{a}_{\mathsf{p}}^{(r)}}(\boldsymbol{\mathcal{A}}(\overline{\boldsymbol{\varepsilon}}, \boldsymbol{\xi})),$$

with

$$\left.\begin{aligned} &\frac{\partial \widetilde{\psi}_{TSO}}{\partial \xi_{\mathsf{v}}^{(k)}} = \sum_{r=1}^{P} c^{(r)} \left[\frac{\partial \psi^{(r)}}{\partial \boldsymbol{\mathcal{A}}_{\mathsf{v}}}(\langle \boldsymbol{\mathcal{A}}_{\mathsf{v}} \rangle^{(r)}, \mathcal{A}_{\mathsf{p}}^{(r)}) : \frac{\partial \langle \boldsymbol{\mathcal{A}}_{\mathsf{v}} \rangle^{(r)}}{\partial \xi_{\mathsf{v}}^{(k)}} \right. \\ &\left. + \frac{1}{2} \frac{\partial^2 \psi^{(r)}}{\partial \boldsymbol{\mathcal{A}}_{\mathsf{v}}^2}(\langle \boldsymbol{\mathcal{A}}_{\mathsf{v}} \rangle^{(r)}, \mathcal{A}_{\mathsf{p}}^{(r)}) :: \frac{\partial \boldsymbol{C}^{(r)}(\boldsymbol{\mathcal{A}}_{\mathsf{v}})}{\partial \xi_{\mathsf{v}}^{(k)}} + \frac{1}{2} \frac{\partial^3 \psi^{(r)}}{\partial \boldsymbol{\mathcal{A}}_{\mathsf{v}}^3}(\langle \boldsymbol{\mathcal{A}}_{\mathsf{v}} \rangle^{(r)}, \mathcal{A}_{\mathsf{p}}^{(r)}) ::: \boldsymbol{C}^{(r)}(\boldsymbol{\mathcal{A}}_{\mathsf{v}}) \otimes \frac{\partial \langle \boldsymbol{\mathcal{A}}_{\mathsf{v}} \rangle^{(r)}}{\partial \xi_{\mathsf{v}}^{(k)}} \right], \\ &\frac{\partial \widetilde{\psi}_{TSO}}{\partial \mathfrak{a}_{\mathsf{p}}^{(r)}} = \frac{\partial \psi^{(r)}}{\partial \mathcal{A}_{\mathsf{p}}}(\langle \boldsymbol{\mathcal{A}}_{\mathsf{v}} \rangle^{(r)}, \mathcal{A}_{\mathsf{p}}^{(r)}) + \frac{1}{2} \frac{\partial^3 \psi^{(r)}}{\partial \boldsymbol{\mathcal{A}}_{\mathsf{v}}^2 \partial \mathcal{A}_{\mathsf{p}}}(\langle \boldsymbol{\mathcal{A}}_{\mathsf{v}} \rangle^{(r)}, \mathcal{A}_{\mathsf{p}}^{(r)}) :: \boldsymbol{C}^{(r)}(\boldsymbol{\mathcal{A}}_{\mathsf{v}}). \end{aligned}\right\} \tag{64}$$

Use has been made of the fact that $\mathcal{A}_{\mathsf{p}}^{(r)} = -R^{(r)}(p^{(r)})$ has no fluctuation in phase r. Explicit expressions for the derivatives of $\psi^{(r)}$ up to third order are given in Appendix D.

It is essential to note that the different terms entering the expansion (64) and therefore the differential equations can all be expressed as functions of $(\overline{\boldsymbol{\varepsilon}}, \boldsymbol{\xi}_v, \boldsymbol{p})$ *with the help of precomputed quantities*, depending only on the average and fluctuations per phase of the fields $\boldsymbol{L} : \boldsymbol{A}$ and $\tilde{\boldsymbol{\rho}}^{(k)}$, namely

$$\left.\begin{aligned}
\langle \mathcal{A}_{\mathsf{v}} \rangle^{(r)} &= \langle \boldsymbol{L} : \boldsymbol{A} \rangle^{(r)} : \overline{\boldsymbol{\varepsilon}} + \sum_{k=1}^{M} \langle \tilde{\boldsymbol{\rho}}^{(k)} \rangle^{(r)} \xi_{\mathsf{v}}^{(k)}, \quad \frac{\partial \langle \mathcal{A}_{\mathsf{v}} \rangle^{(r)}}{\partial \xi_{\mathsf{v}}^{(k)}} = \langle \tilde{\boldsymbol{\rho}}^{(k)} \rangle^{(r)}, \\
\boldsymbol{C}^{(r)}(\mathcal{A}_{\mathsf{v}}) &= \langle \big(\mathcal{A}_{\mathsf{v}} - \langle \mathcal{A}_{\mathsf{v}} \rangle^{(r)}\big) \otimes \big(\mathcal{A}_{\mathsf{v}} - \langle \mathcal{A}_{\mathsf{v}} \rangle^{(r)}\big) \rangle^{(r)} \text{ with } \mathcal{A}_{\mathsf{v}} \text{ given by } (53), \\
&= \overline{\boldsymbol{\varepsilon}} : \langle (\boldsymbol{L} : \boldsymbol{A} - \langle \boldsymbol{L} : \boldsymbol{A} \rangle^{(r)}) \otimes (\boldsymbol{L} : \boldsymbol{A} - \langle \boldsymbol{L} : \boldsymbol{A} \rangle^{(r)}) \rangle^{(r)} : \overline{\boldsymbol{\varepsilon}} \\
&+ 2 \sum_{\ell=1}^{M} \overline{\boldsymbol{\varepsilon}} : \langle (\boldsymbol{L} : \boldsymbol{A} - \langle \boldsymbol{L} : \boldsymbol{A} \rangle^{(r)}) \otimes_s (\widetilde{\boldsymbol{\rho}}^{\ell} - \langle \widetilde{\boldsymbol{\rho}}^{\ell} \rangle^{(r)}) \rangle^{(r)} \xi_{\mathsf{v}}^{\ell} \\
&+ \sum_{k,\ell=1}^{M} \langle (\widetilde{\boldsymbol{\rho}}^{k} - \langle \widetilde{\boldsymbol{\rho}}^{k} \rangle^{(r)}) \otimes (\widetilde{\boldsymbol{\rho}}^{\ell} - \langle \widetilde{\boldsymbol{\rho}}^{\ell} \rangle^{(r)}) \rangle^{(r)} \, \xi_{\mathsf{v}}^{k} \, \xi_{\mathsf{v}}^{\ell} \\
\frac{\partial \boldsymbol{C}^{(r)}(\mathcal{A}_{\mathsf{v}})}{\partial \xi_{\mathsf{v}}^{(k)}} &= 2 \langle \big(\mathcal{A}_{\mathsf{v}} - \langle \mathcal{A}_{\mathsf{v}} \rangle^{(r)}\big) \otimes_s \big(\tilde{\boldsymbol{\rho}}^{(k)} - \langle \tilde{\boldsymbol{\rho}}^{(k)} \rangle^{(r)}\big) \rangle^{(r)} \\
&= 2 \overline{\boldsymbol{\varepsilon}} : \langle (\boldsymbol{L} : \boldsymbol{A} - \langle \boldsymbol{L} : \boldsymbol{A} \rangle^{(r)}) \otimes_s (\widetilde{\boldsymbol{\rho}}^{k} - \langle \widetilde{\boldsymbol{\rho}}^{k} \rangle^{(r)}) \rangle^{(r)} \\
&+ 2 \sum_{\ell=1}^{M} \langle (\widetilde{\boldsymbol{\rho}}^{k} - \langle \widetilde{\boldsymbol{\rho}}^{k} \rangle^{(r)}) \otimes_s (\widetilde{\boldsymbol{\rho}}^{\ell} - \langle \widetilde{\boldsymbol{\rho}}^{\ell} \rangle^{(r)}) \rangle^{(r)} \, \xi_{\mathsf{v}}^{\ell}
\end{aligned}\right\} \tag{65}$$

where $\otimes_s$ denotes the symmetric tensor product between 2 tensors,

$$\boldsymbol{a} \otimes_s \boldsymbol{b} = (1/2)(\boldsymbol{a} \otimes \boldsymbol{b} + \boldsymbol{b} \otimes \boldsymbol{a}).$$

The precomputed quantities are :

$$\left.\begin{aligned}
&\langle \boldsymbol{L} : \boldsymbol{A} \rangle^{(r)}, \ \langle \tilde{\boldsymbol{\rho}}^{(k)} \rangle^{(r)}, \ \langle (\boldsymbol{L} : \boldsymbol{A} - \langle \boldsymbol{L} : \boldsymbol{A} \rangle^{(r)}) \otimes (\boldsymbol{L} : \boldsymbol{A} - \langle \boldsymbol{L} : \boldsymbol{A} \rangle^{(r)}) \rangle^{(r)}, \\
&\langle (\boldsymbol{L} : \boldsymbol{A} - \langle \boldsymbol{L} : \boldsymbol{A} \rangle^{(r)}) \otimes_s (\widetilde{\boldsymbol{\rho}}^{\ell} - \langle \widetilde{\boldsymbol{\rho}}^{\ell} \rangle^{(r)}) \rangle^{(r)}, \ \langle (\widetilde{\boldsymbol{\rho}}^{k} - \langle \widetilde{\boldsymbol{\rho}}^{k} \rangle^{(r)}) \otimes (\widetilde{\boldsymbol{\rho}}^{\ell} - \langle \widetilde{\boldsymbol{\rho}}^{\ell} \rangle^{(r)}) \rangle^{(r)}.
\end{aligned}\right\} \tag{66}$$

6.3. Individual constituents with non-standard constitutive relations

When the individual constituents are governed by non-standard constitutive relations such as (7), the differential equation (63) is (heuristically) replaced by

$$\begin{aligned}
\dot{\mathfrak{a}}^{(k)} = \frac{\partial \mathfrak{a}^{(k)}}{\partial \overline{\boldsymbol{\varepsilon}}} : \dot{\overline{\boldsymbol{\varepsilon}}} \ &+ \ \sum_{r=1}^{P} c^{(r)} \left[\boldsymbol{\mathcal{F}}^{(r)}(\langle \mathcal{A} \rangle^{(r)}) : \frac{\partial \langle \mathcal{A} \rangle^{(r)}}{\partial \xi^{(k)}} + \frac{1}{2} \frac{\partial \boldsymbol{\mathcal{F}}^{(r)}}{\partial \mathcal{A}} (\langle \mathcal{A} \rangle^{(r)}) :: \frac{\partial \boldsymbol{C}^{(r)}(\mathcal{A})}{\partial \xi^{(k)}} \right. \\
&+ \ \left. \frac{1}{2} \frac{\partial^2 \boldsymbol{\mathcal{F}}^{(r)}}{\partial \mathcal{A}^2} (\langle \mathcal{A} \rangle^{(r)}) ::: \boldsymbol{C}^{(r)}(\mathcal{A}) \otimes \frac{\partial \langle \mathcal{A} \rangle^{(r)}}{\partial \xi^{(k)}} \right],
\end{aligned}$$

or alternatively

$$\begin{aligned}\dot{\xi}^{(k)} &= \sum_{r=1}^{P} c^{(r)} \left[\boldsymbol{\mathcal{F}}^{(r)}(\langle \boldsymbol{\mathcal{A}} \rangle^{(r)}) : \frac{\partial \langle \boldsymbol{\mathcal{A}} \rangle^{(r)}}{\partial \mathfrak{a}^{(k)}} + \frac{1}{2} \frac{\partial \boldsymbol{\mathcal{F}}^{(r)}}{\partial \boldsymbol{\mathcal{A}}} (\langle \boldsymbol{\mathcal{A}} \rangle^{(r)}) :: \frac{\partial \boldsymbol{C}^{(r)}(\boldsymbol{\mathcal{A}})}{\partial \mathfrak{a}^{(k)}} \right. \\ &+ \left. \frac{1}{2} \frac{\partial^2 \boldsymbol{\mathcal{F}}^{(r)}}{\partial \boldsymbol{\mathcal{A}}^2} (\langle \boldsymbol{\mathcal{A}} \rangle^{(r)}) ::: \boldsymbol{C}^{(r)}(\boldsymbol{\mathcal{A}}) \otimes \frac{\partial \langle \boldsymbol{\mathcal{A}} \rangle^{(r)}}{\partial \mathfrak{a}^{(k)}} \right].\end{aligned}$$

Remark 2: When the more general class of constitutive relations (8) is considered, the same linearization technique can be applied, at the expense of expanding $\boldsymbol{\mathcal{F}}^{(r)}$ to second order, not only with respect to $\boldsymbol{\mathcal{A}}$ but also with respect to $\dot{\boldsymbol{\varepsilon}}$ and $\boldsymbol{\alpha}$. This more general formulation is left for future work.

6.4. Example 2: Elasto-viscoplastic constituents with nonlinear kinematic hardening

The constitutive relations for elasto-viscoplastic phases with nonlinear isotropic and kinematic hardening have been given in section 2.4 and the differential equations for the hybrid model have been derived in section 5.5. The TSO approximation of (58) is obtained upon replacement of $\widetilde{\psi}$ with

$$\begin{aligned}\widetilde{\psi}_{TSO}(\overline{\boldsymbol{\varepsilon}}, \boldsymbol{\xi}) &= \sum_{r=1}^{P} c^{(r)} \left[\psi^{(r)}(\langle \boldsymbol{\mathcal{A}} \rangle^{(r)}) + \frac{1}{2} \frac{\partial^2 \psi^{(r)}}{\partial \boldsymbol{\mathcal{A}}_{\mathsf{v}}^2} (\langle \boldsymbol{\mathcal{A}} \rangle^{(r)}) :: \boldsymbol{C}^{(r)}(\boldsymbol{\mathcal{A}}_{\mathsf{v}}) \right. \\ &+ \left. \frac{1}{2} \frac{\partial^2 \psi^{(r)}}{\partial \boldsymbol{\mathcal{A}}_{\beta}^2} (\langle \boldsymbol{\mathcal{A}} \rangle^{(r)}) :: \boldsymbol{C}^{(r)}(\boldsymbol{\mathcal{A}}_{\beta}) + \frac{\partial^2 \psi^{(r)}}{\partial \boldsymbol{\mathcal{A}}_{\mathsf{v}} \partial \boldsymbol{\mathcal{A}}_{\beta}} (\langle \boldsymbol{\mathcal{A}} \rangle^{(r)}) :: \boldsymbol{C}^{(r)}(\boldsymbol{\mathcal{A}}_{\mathsf{v}}, \boldsymbol{\mathcal{A}}_{\beta}) \right],\end{aligned}$$

where

$$\boldsymbol{C}^{(r)}(\boldsymbol{\mathcal{A}}_{\mathsf{v}}, \boldsymbol{\mathcal{A}}_{\beta}) = \langle \left(\boldsymbol{\mathcal{A}}_{\mathsf{v}} - \langle \boldsymbol{\mathcal{A}}_{\mathsf{v}} \rangle^{(r)} \right) \otimes_s \left(\boldsymbol{\mathcal{A}}_{\beta} - \langle \boldsymbol{\mathcal{A}}_{\beta} \rangle^{(r)} \right) \rangle^{(r)}.$$

The same potential $\widetilde{\psi}_{TSO}$ is used to approximate the first term in the right-hand side of (60). Detailed expressions for the different derivatives of $\widetilde{\psi}_{TSO}$ are given in Appendix D. It remains to specify the TSO approximation of the term $\langle \eta \frac{\partial \psi}{\partial \mathcal{A}p}(\boldsymbol{\mathcal{A}}) \boldsymbol{\mathcal{A}}_{\beta} : \boldsymbol{\mu}_{\beta}^{(k)} \rangle$ in (60). The term to be approximated to second order in the fluctuations reads as

$$\sum_{r=1}^{P} c^{(r)} \eta^{(r)} \langle \frac{\partial \psi^{(r)}}{\partial \mathcal{A}p}(\boldsymbol{\mathcal{A}}) \boldsymbol{\mathcal{A}}_{\beta} : \boldsymbol{\mu}_{\beta}^{(k)} \rangle^{(r)},$$

and the technical details of this approximation are again given in Appendix D. Simplifications occur in the specific case of the constitutive relations (18) since $\boldsymbol{\mathcal{A}}_{\mathsf{v}}$ and $\boldsymbol{\mathcal{A}}_{\beta}$ play identical roles in the expression of the potential $\psi^{(r)}$ (note however that the fluctuations of $\boldsymbol{\mathcal{A}}_{\mathsf{v}}$ and $\boldsymbol{\mathcal{A}}_{\beta}$ might be different). The final form of the ordinary differential equations are

$$\begin{aligned}\dot{\mathfrak{a}}_{\mathsf{v}}^{(k)} &= \boldsymbol{a}^{(k)} : \dot{\overline{\boldsymbol{\varepsilon}}} + \sum_{r=1}^{P} c^{(r)} \left[\frac{\partial \psi^{(r)}}{\partial \boldsymbol{\mathcal{A}}_{\mathsf{v}}} (\langle \boldsymbol{\mathcal{A}} \rangle^{(r)}) : \frac{\partial \langle \boldsymbol{\mathcal{A}}_{\mathsf{v}} + \boldsymbol{\mathcal{A}}_{\beta} \rangle^{(r)}}{\partial \xi_{\mathsf{v}}^{(k)}} \right. \\ &+ \frac{1}{2} \frac{\partial^2 \psi^{(r)}}{\partial \boldsymbol{\mathcal{A}}_{\mathsf{v}}^2} (\langle \boldsymbol{\mathcal{A}} \rangle^{(r)}) :: \frac{\partial \boldsymbol{C}^{(r)}(\boldsymbol{\mathcal{A}}_{\mathsf{v}} + \boldsymbol{\mathcal{A}}_{\beta})}{\partial \xi_{\mathsf{v}}^{(k)}} \\ &+ \left. \frac{1}{2} \frac{\partial^3 \psi^{(r)}}{\partial \boldsymbol{\mathcal{A}}_{\mathsf{v}}^3} (\langle \boldsymbol{\mathcal{A}} \rangle^{(r)}) ::: \boldsymbol{C}^{(r)}(\boldsymbol{\mathcal{A}}_{\mathsf{v}} + \boldsymbol{\mathcal{A}}_{\beta}) \otimes \frac{\partial \langle \boldsymbol{\mathcal{A}}_{\mathsf{v}} + \boldsymbol{\mathcal{A}}_{\beta} \rangle^{(r)}}{\partial \xi_{\mathsf{v}}^{(k)}} \right],\end{aligned} \tag{67}$$

$$\dot{\mathfrak{a}}_\beta^{(k)} = \sum_{r=1}^{P} c^{(r)} \left\{ \frac{\partial \psi^{(r)}}{\partial \boldsymbol{\mathcal{A}}_{\mathsf{v}}}(\langle \boldsymbol{\mathcal{A}} \rangle^{(r)}) : \frac{\partial \langle \boldsymbol{\mathcal{A}}_{\mathsf{v}} + \boldsymbol{\mathcal{A}}_\beta \rangle^{(r)}}{\partial \xi_\beta^{(k)}} + \frac{1}{2} \frac{\partial^2 \psi^{(r)}}{\partial \boldsymbol{\mathcal{A}}_{\mathsf{v}}^2}(\langle \boldsymbol{\mathcal{A}} \rangle^{(r)}) :: \frac{\partial \boldsymbol{C}^{(r)}(\boldsymbol{\mathcal{A}}_{\mathsf{v}} + \boldsymbol{\mathcal{A}}_\beta)}{\partial \xi_\beta^{(k)}} \right.$$
$$+ \frac{1}{2} \frac{\partial^3 \psi^{(r)}}{\partial \boldsymbol{\mathcal{A}}_{\mathsf{v}}^3}(\langle \boldsymbol{\mathcal{A}} \rangle^{(r)}) ::: \boldsymbol{C}^{(r)}(\boldsymbol{\mathcal{A}}_{\mathsf{v}} + \boldsymbol{\mathcal{A}}_\beta) \otimes \frac{\partial \langle \boldsymbol{\mathcal{A}}_{\mathsf{v}} + \boldsymbol{\mathcal{A}}_\beta \rangle^{(r)}}{\partial \xi_\beta^{(k)}}$$
$$\left. - \eta^{(r)} \left[\dot{p}^{(r)} \langle \boldsymbol{\mathcal{A}}_\beta : \boldsymbol{\mu}_\beta^{(k)} \rangle^{(r)} + \frac{\partial^2 \psi^{(r)}}{\partial \boldsymbol{\mathcal{A}}_{\mathsf{v}} \partial \boldsymbol{\mathcal{A}}_{\mathsf{p}}}(\langle \boldsymbol{\mathcal{A}} \rangle^{(r)}) : \langle (\boldsymbol{\mathcal{A}}_{\mathsf{v}} + \boldsymbol{\mathcal{A}}_\beta - \langle \boldsymbol{\mathcal{A}}_{\mathsf{v}} + \boldsymbol{\mathcal{A}}_\beta \rangle^{(r)}) \boldsymbol{\mathcal{A}}_\beta : \boldsymbol{\mu}_\beta^{(k)} \rangle^{(r)} \right] \right\}, \tag{68}$$

$$\dot{p}^{(r)} = \frac{\partial \widetilde{\psi}_{TSO}}{\partial \mathfrak{a}_{\mathsf{p}}^{(r)}} = \frac{\partial \psi^{(r)}}{\partial \boldsymbol{\mathcal{A}}_{\mathsf{p}}}(\langle \boldsymbol{\mathcal{A}} \rangle^{(r)}) + \frac{1}{2} \frac{\partial^3 \psi^{(r)}}{\partial \boldsymbol{\mathcal{A}}_{\mathsf{v}}^2 \partial \boldsymbol{\mathcal{A}}_{\mathsf{p}}}(\langle \boldsymbol{\mathcal{A}} \rangle^{(r)}) :: \boldsymbol{C}^{(r)}(\boldsymbol{\mathcal{A}}_{\mathsf{v}} + \boldsymbol{\mathcal{A}}_\beta) \tag{69}$$

Once again, the right-hand sides of (67), (68), (69) are functions of the unknowns $\mathfrak{a}_{\mathsf{v}}$, $\mathfrak{a}_\beta$ *and* $\boldsymbol{p}$ *and of other pre-computed quantities depending only on the average per phase and fluctuations of the fields* $\boldsymbol{L} : \boldsymbol{A}$, $\boldsymbol{\rho}^{(k)}$ *and* $\boldsymbol{H} : \boldsymbol{\mu}_\beta^{(k)}$ *through relations similar to (66).* It will be seen in section 7 that the resolution of these reduced ODEs is considerably faster than the integration of the ODEs (58) and (60).

7. Examples

Metal-matrix composites consisting of an elasto-viscoplastic matrix reinforced by short fibers will provide a good test example for the method. These discontinuous fiber composites (typically Al/Al2O3) are, among other applications, being considered in the automotive industry as potential candidates for local reinforcements of engine components subjected to severe thermomechanical loadings (Berini et al., 2005). They are composed of an aluminum matrix reinforced by discontinuous fibers of Alumina. The short fibers are parallel to a given plane $(1, 2)$ but with a random orientation in this plane. Their volume fraction is $c^{(2)} = 10\%$, their average aspect ratio w (defined as the ratio between the fiber length to the fiber diameter) is $w = 15$. A typical artificial microstructure used in the full-field simulations is shown in figure 2. The elastic properties of the two constituents are taken (from the literature) as

$$\text{Matrix: } E^{(1)} = 55 \text{ GPa}, \quad \nu^{(1)} = 0.33, \quad \text{Fibers: } E^{(2)} = 300 \text{ GPa}, \quad \nu^{(2)} = 0.25. \tag{70}$$

For the purpose of identification in the operating conditions, both the matrix and the composite are submitted to a low cycle fatigue experiment (a few cycles) at 300°C, consisting in a uniaxial tension-compression test, where the strain varies linearly between two extreme values at a constant-strain-rate with alternative sign. More precisely, for the matrix,

$$\boldsymbol{\sigma} = \sigma(t)\, \boldsymbol{e}_1 \otimes \boldsymbol{e}_1, \quad \dot{\varepsilon}_{11} = \pm 10^{-3} \text{s}^{-1}, \quad -2.5\, 10^{-3} \leq \varepsilon_{11} \leq 2.5\, 10^{-3},$$

and for the composite,

$$\overline{\boldsymbol{\sigma}} = \overline{\sigma}(t)\, \boldsymbol{e}_1 \otimes \boldsymbol{e}_1, \quad \dot{\overline{\varepsilon}}_{11} = \pm 1.4\, 10^{-3} \text{s}^{-1}, \quad -3.48441\, 10^{-3} \leq \overline{\varepsilon}_{11} \leq 3.58454\, 10^{-3}.$$

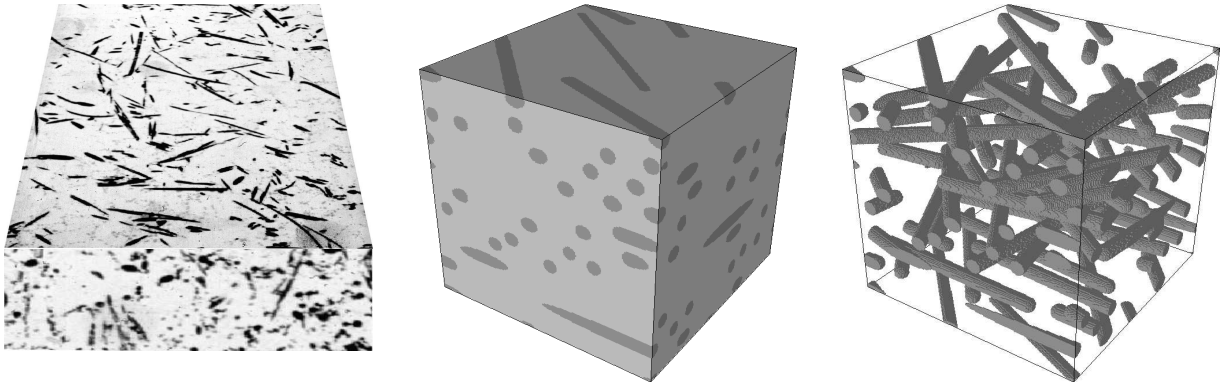

(a) (b) (c)

Figure 2: Short-fiber composite. Fiber volume-fraction $c^{(2)} = 0.1$. (a) Micrograph. (b) Typical realization of the unit-cell. (c) Same as in (b) but with the fibers alone.

7.1. Matrix

At 300°C, the Aluminum matrix is viscoplastic. The two constitutive relations (11) and (18), with linear hardening on one hand and with nonlinear hardening on the other hand, can be used to reproduce the experimental results. Two sets of material data have been identified with the two models.

1. A good fit for the model (11) with linear kinematic hardening was obtained with no isotropic hardening ($R(p) = \text{constant}$)

$$\left.\begin{aligned} \sigma_0 \dot{\varepsilon}_0^{-\frac{1}{n}} &= 130 \text{ MPa.s}^{\frac{1}{n}}, \quad n = 3.6, \\ R(p) = \sigma_y &= 25 \text{ MPa}, \quad H = 1800 \text{ MPa}, \end{aligned}\right\} \tag{71}$$

   where the fourth-order tensor $\boldsymbol{H}$ in (11) is related to the hardening modulus H by $\boldsymbol{H} = (2/3)H\boldsymbol{K}$.

2. A good fit for the model (18) with nonlinear kinematic hardening was obtained again with no isotropic hardening and

$$\left.\begin{aligned} \sigma_0 \dot{\varepsilon}_0^{-\frac{1}{n}} &= 150 \text{ MPa.s}^{\frac{1}{n}}, \quad n = 3.6, \\ R(p) = \sigma_y &= 15 \text{ MPa}, \quad H = 10000 \text{ MPa}, \quad \eta = 900 \text{ MPa}. \end{aligned}\right\} \tag{72}$$

The experimental tests were simulated numerically. Three cycles were performed to reach the stabilized cycle. The comparison between the predictions of the models and the experimental results is shown in figure 3 left. A few discrepancies are observed, which can be explained as follows:

- The experimental results show an asymmetry between tension and compression, probably due to the presence of residual stresses which were not completely suppressed by the thermal treatment. The extremal stresses are 45 MPa in tension and -40 MPa in compression,

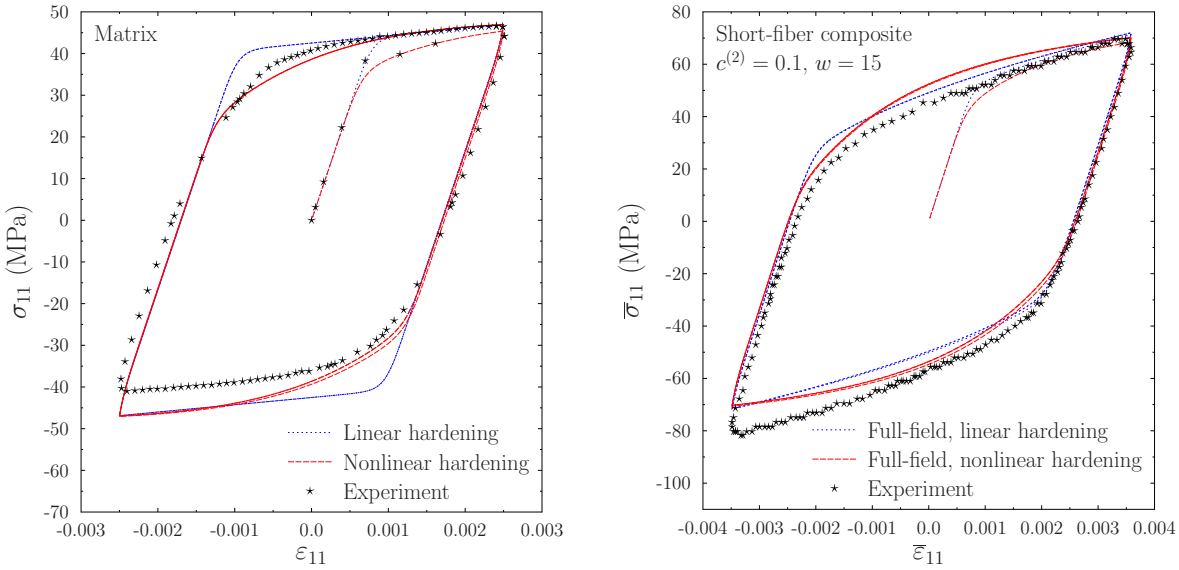

Figure 3: Cyclic uniaxial tension-compression test. Experimental results (symbols), constitutive model with linear kinematic hardening (dotted line), nonlinear kinematic hardening (dashed line). Left: matrix alone. Right: composite.

approximately. No attempt was made here to adjust the initial value of the back-stress to account for this asymmetry (this is one possibility among others) mostly because the residual stresses in the composite are likely to be completely different from those in the matrix alone. The identification has been performed to match the results in the tensile regime, where the agreement is good at least with the nonlinear model. This explains why the agreement is less satisfactory in compression.

- The difference between the two models with linear and the nonlinear kinematic hardening is seen in their prediction of the Bauschinger effect (level of stress at which deviation from linearity occurs upon unloading or reloading) where the stress strain curve is rounded. The Bauschinger effect is better captured by the nonlinear model, as is well established in the literature. An even better fit would be obtained by introducing several back-stresses. This was not done here to keep the complexity of the model reasonable.

7.2. Composites. Full-field simulations

We first proceed with the full-field simulations. The computational method used for this purpose is based on fast Fourier transforms which is a convenient alternative to Finite Elements for volume elements subjected to periodic boundary conditions (Michel et al., 1999). In this approach each volume element is discretized into N^3 voxels of equal size. Different realizations with 40 cylindrical short fibers randomly arranged parallel to the $(1, 2)$ plane were generated (a typical realization is shown in figure 2 center and right).

Discretization. First a parametric study of the spatial discretization (number of voxels) required to approach convergence with respect to the discretization. Simulations were performed with

three different discretizations of the same unit-cell into 75^3, 147^3 and 243^3 voxels, with no significant differences between the results of the two finest discretizations. Therefore all simulations were performed with a unit-cell discretized into 147^3 voxels.

Representativity. Then it was observed that different realizations gave slightly different results and therefore that the stationarity of the results with respect to the size of the volume element could not be ensured with 40 fibers in the volume element. However, the question of the size of the representative volume element *is not* the question which is addressed here. The aim of this study is to show that predictions of the NTFA model are very close to the results of the full-field simulations *on the same configuration*, with a dramatic reduction in cost. Therefore it is legitimate to perform this comparison on a single configuration. The configuration used for comparison is shown in figure 2 center and right.

The two constitutive models for the matrix material, with linear and with nonlinear hardening, were used in the simulations. All simulations were performed with constant time-steps, 200 time-steps in the initial loading branch and 800 time-steps by cycle. Three cycles were simulated to reach a stabilized cycle.

The comparison of the full-field simulations with experimental results is shown in figure 3 right. A reasonable agreement can be observed, with the same discrepancy as for the matrix alone: the asymmetry of the experimental results which is not observed in the simulations is due to residual stresses which are not modeled in the full-field simulations. Again, it should be emphasized that our objective here *is not* to validate the material parameters of the matrix or the full-field simulations by comparison with experiments, but to validate the NTFA model by comparison with full-field simulations on a realistic example. Therefore in the remainder of this study only comparisons between full-field simulations and the NTFA models will be shown.

7.3. Composites. NTFA models

7.3.1. Modes

The plastic modes were generated by the snapshot POD (or Karhunen-Loève) method based on 100 snapshots $\boldsymbol{\theta}^{(k)}(x)$ stored during the full-field simulations. More specifically 20 snapshots of the plastic strain fields are stored during the initial loading phase every 10 time steps and 80 snapshots are stored during the subsequent first cycle, again every 10 time steps. These snapshots $\boldsymbol{\theta}^{(k)}$ are tensorial fields (as the plastic strain field). Then, following the classical POD procedure, the correlation matrix of these snapshots is formed

$$g^{(k\ell)} = \langle \boldsymbol{\theta}^{(k)}(x) : \boldsymbol{\theta}^{(\ell)}(x) \rangle,$$

and its eigenvalues $\lambda^{(k)}$ and eigenvectors $\boldsymbol{v}^{(k)}$ are computed. The actual modes are expressed as a combination of the eigenvectors as

$$\boldsymbol{\mu}^{(k)}(x) = \sum_{\ell=1}^{N} v_\ell^{(k)} \boldsymbol{\theta}^{(\ell)}(x),$$

where N denotes the number of snapshots (here $N = 100$). Note that the modes, as the eigenvectors of the symmetric matrix $\boldsymbol{g}$, are orthogonal to each other. Another well-known feature

of the K-L transform is that the quantity of relevant information (its correlation with the set of snapshots) contained in an eigenvector $\boldsymbol{v}^{(k)}$ is expressed by the magnitude of the corresponding eigenvalue $\lambda^{(k)}$. This property can be used to truncate the set of modes, retaining the most relevant ones. Ordering the eigenvalues in decreasing order, the M modes corresponding to the largest eigenvalues can be selected by applying a threshold criterion

$$\sum_{k=1}^{M} \lambda^{(k)} / \left(\sum_{k=1}^{N} \lambda^{(k)} \right) \geq \alpha. \tag{73}$$

In the present study $\alpha = 0.9999 = 1 - 10^{-4}$. It was found that 6 modes are required to meet the criterion (73) for the model with linear kinematic hardening and only 5 for the model with nonlinear kinematic hardening.

Typical examples of modes are shown in figure 4. As can be seen the modes of higher number incorporate more and more details on the local viscoplastic strains (which are concentrated around the fibers in this example).

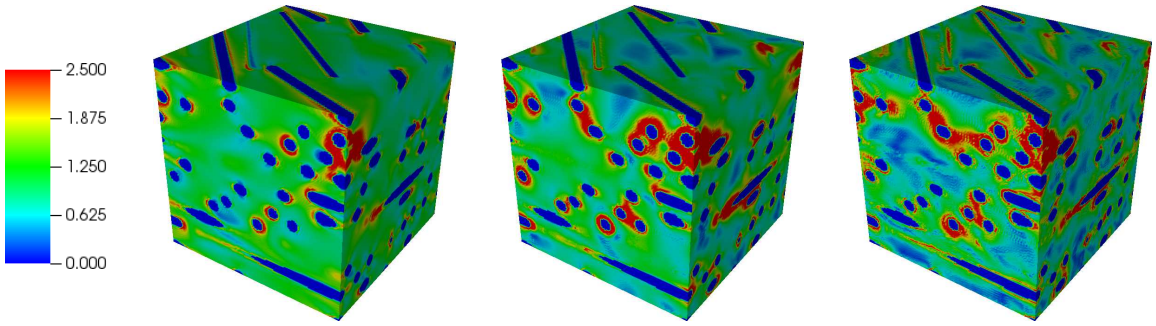

(a) (b) (c)

Figure 4: Matrix with nonlinear kinematic hardening. Snapshot of the modes (the equivalent strain μ_{eq} is shown). (a) Mode 1. (b) Mode 2. (c) Mode 3.

7.3.2. Effective response

The predictions of the two NTFA approaches, NTFA hybrid and NTFA-TSO (fine and coarse dynamics respectively), for the overall response of the composite are compared in figure 5. In the plot on the left, where the matrix is assumed with linear kinematic hardening, the hybrid NTFA model is in better agreement with the full-field simulations. However, the situation is reversed in the figure on the right, where the matrix is assumed to exhibit a nonlinear kinematic hardening. In both cases, it can be concluded that both NTFA approaches are in excellent agreement with the full-field simulations. If the two NTFA models are compared it is observed that there is no loss in accuracy by choosing the coarse dynamics instead of the fine dynamics (in other words the NTFA-TSO model is a good approximation of the hybrid NTFA model).

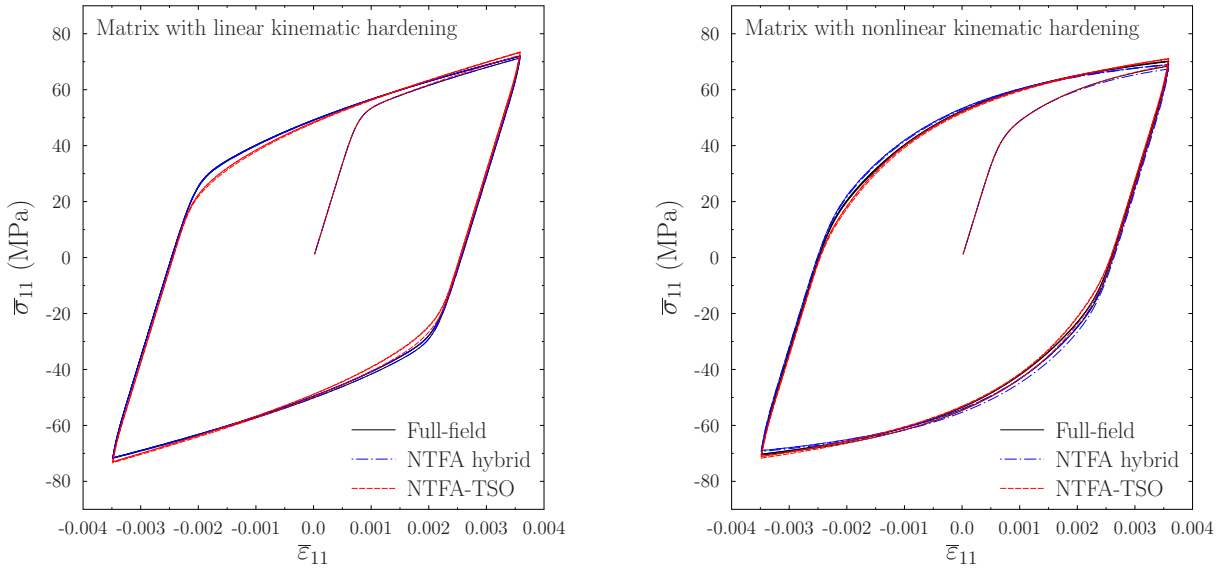

Figure 5: Overall response of the short-fiber composite under cyclic uniaxial tension-compression test. Comparison between the full-field simulations (solid line), the hybrid NTFA model (dot-dashed line) and the NTFA-TSO model (dashed line). Left: matrix with linear kinematic hardening. Right: matrix with nonlinear kinematic hardening.

7.3.3. Gain in computational time

The CPU times for the different methods (Full-field simulations, hybrid NTFA model, NTFA-TSO) are compared in Table 1 (Intel Xeon X5687 @ 3.6 GHz). The different acceleration ratios, measured by the CPU ratios shown in Table 1, can be commented as follows:

- In the hybrid version of the NTFA, the acceleration is entirely due to the reduction in the number of unknowns. Typically if 6 modes are used for the matrix with linear kinematic hardening, the number of unknowns drops from 6×147^3 to 6. However the evolution equations for the viscoplastic strain fields are not reduced. Their time integration remains very costly since at each time-step the microscopic (or local) stress field and the associated microscopic viscoplastic strain-rate have to be computed. The acceleration factor due to the hybrid model is 4 in this specific example.

- The acceleration observed in the NTFA-TSO simulations has two origins, the reduction in the number of variables describing the plastic strain field, and the reduction in the "coarse dynamics". As can be seen the resulting acceleration is spectacular, by a factor of 10^4 to $7.\ 10^4$ (compared to the full-field simulations) depending on the constitutive relations of the phases. The acceleration due to the TSO linearization over the hybrid model is by a factor of 10^3 to 10^4.

7.4. Composite. Local fields

Another significant advantage of the NTFA method, already emphasized in Michel and Suquet (2003, 2004, 2009) is that the local fields can be easily reconstructed from the knowledge

Hardening type	Full-field (FFT) Reference	NTFA hybrid (CPU ratio= FFT/ hybrid)	NTFA-TSO (CPU ratio= FFT/TSO)
Linear hardening	189 175 s.	48 259 s. (CPU ratio = 3.92)	2.66 s. (CPU ratio = 71 118)
Nonlinear hardening	189 800 s.	72 159 s. (CPU ratio = 2.63)	15.96 s. (CPU ratio = 11 892)

Table 1: Comparison of CPU times for the different simulations. Processor Intel Xeon X5687 @ 3.6 GHz.

of the reduced state variables $(\overline{\boldsymbol{\varepsilon}}, \boldsymbol{\xi})$ and from pre-computed fields. This *localization rule* is often linear. This is in particular true in the two examples considered in this study:

1. The local fields of state variables are, by construction of the NTFA, reconstructed by means of the decomposition (51) or (56).
2. The local fields of thermodynamic forces (stress, back-stress) are reconstructed by means of the relation (53) or (57).

The localization procedure itself does not depend on the type of dynamics (fine or coarse) used to determine the reduced state variables $(\overline{\boldsymbol{\varepsilon}}, \boldsymbol{\xi})$, but the results may differ, since the state variables predicted by the two NTFA models are different.

The local stress fields at the end of the 3rd cycle reconstructed by means of the relations (34) predicted by the hybrid NTFA model and by the NTFA-TSO model are compared in figure 6 with those obtained by full-field simulations. The local norm of $\boldsymbol{\sigma}$ at point $\boldsymbol{x}$ is defined as

$$||\boldsymbol{\sigma}(\boldsymbol{x})|| = \left(\sum_{i,j=1}^{3} \sigma_{ij}(\boldsymbol{x}) \sigma_{ij}(\boldsymbol{x}) \right)^{1/2} . \tag{74}$$

The NTFA predictions and the full-field simulations can hardly been distinguished by eye. A more convenient way of comparison is to compare the statistics of the fields, rather than their local values. The statistical informations which will be used for the purpose of comparison are the average per phase of the fields, their fluctuations and their probability density functions. Attention will be focused in the sequel on the comparison of these statistical information fields in the matrix.

Average stress. The predictions of the different model for the averaged stress in the matrix along the direction of the loading are compared with that observed the full-field simulations in figure 7 . Both NTFA models match quite well the full-field simulations. When the matrix has a linear kinematic hardening, the predictions of the hybrid NTFA model cannot be distinguished from the full-field results. A slight discrepancy can be observed with the NTFA-TSO model. The situation is reversed when the matrix hardening is nonlinear: the NTFA-TSO predictions are almost on top of the full-field results, whereas a small discrepancy exists with the hybrid NTFA model. The average stress in the fibers shows the same trends and is not shown here.

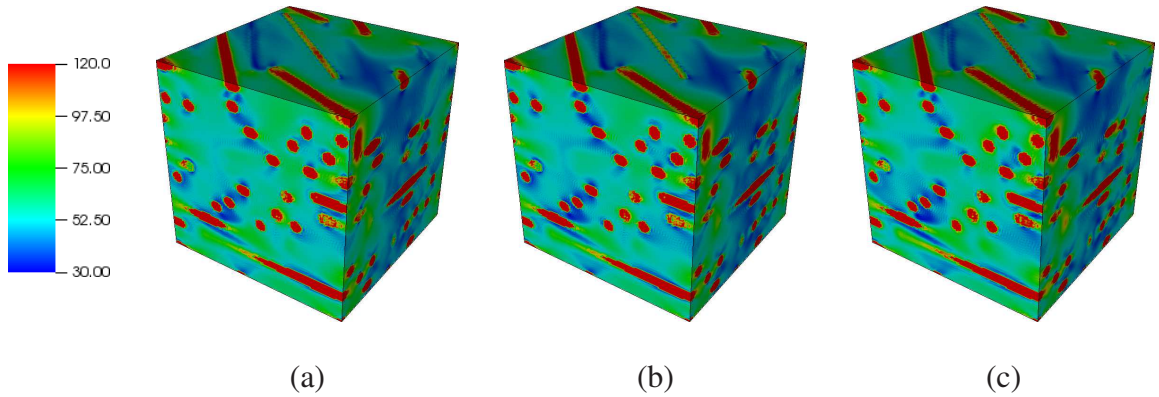

Figure 6: Matrix with nonlinear kinematic hardening. Norm of the local stress field at the end of the 3rd cycle (units: MPa). (a) Full-field. (b) NTFA hybrid. (c) NTFA-TSO.

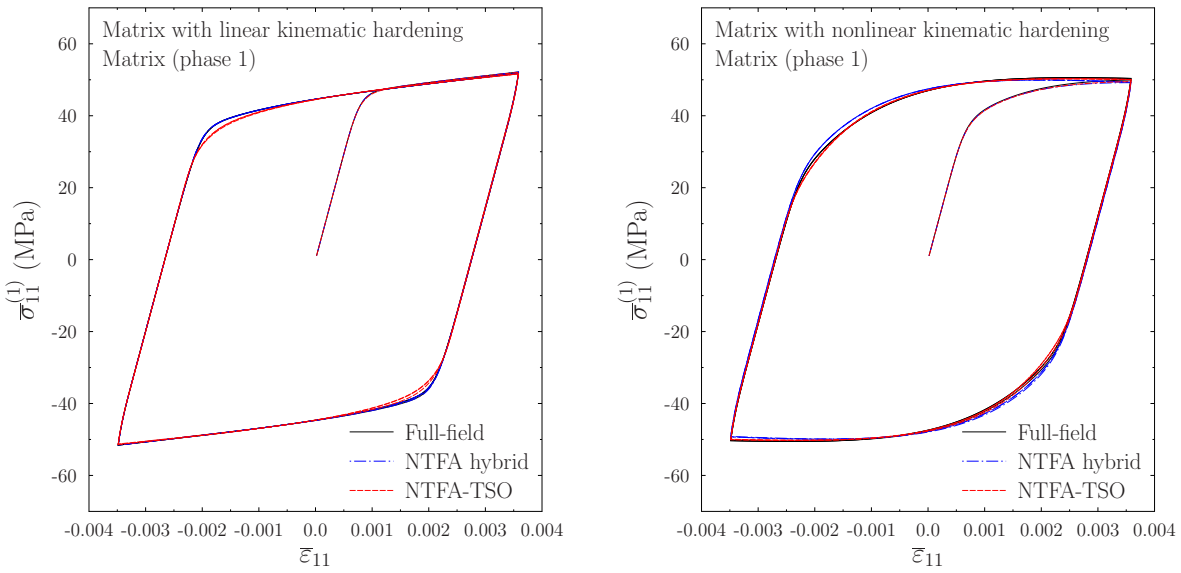

Figure 7: Average stress in the matrix. Comparison between full-field simulations (solid line), the hybrid NTFA model (dot-dashed line) and the NTFA-TSO model (dashed line). Left: matrix with linear hardening. Right: matrix with nonlinear hardening.

Stress fluctuations. The fluctuations of the stress field in the matrix are compared in figure 8 with that found with the full-field simulations. The fluctuations are measured by $\sqrt{\boldsymbol{C}^{(1)}(\boldsymbol{\sigma}) :: \boldsymbol{K}}$, where $\boldsymbol{C}^{(1)}$ is the fourth-order tensor of fluctuations in the matrix (as defined in (62)) and $\boldsymbol{K}$ is the projector on deviatoric symmetric tensors.

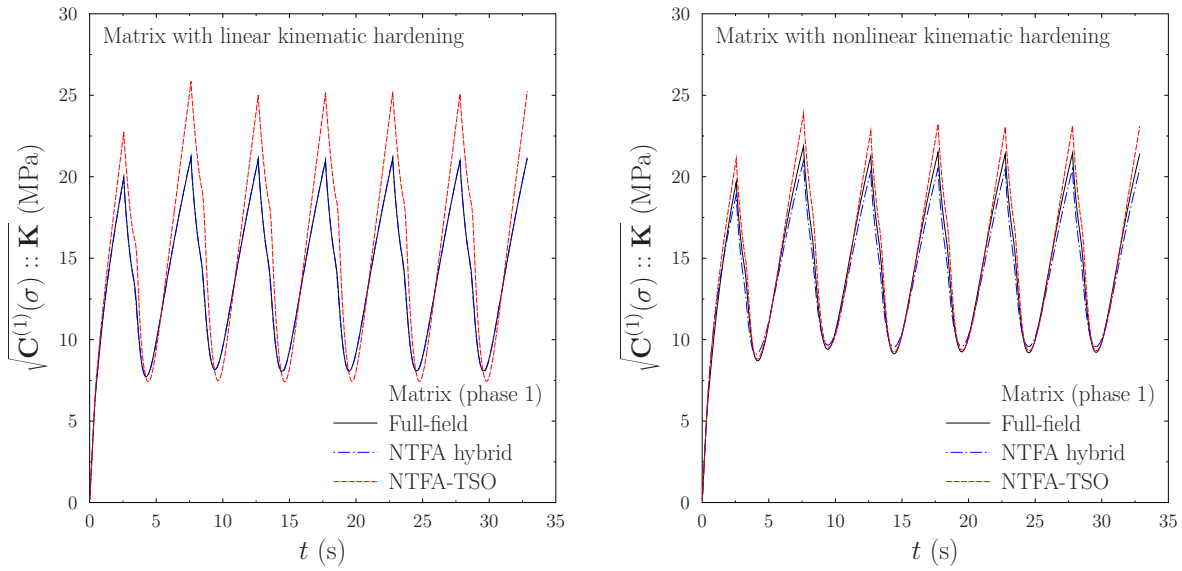

Figure 8: Stress fluctuations in the matrix. Comparison between full-field simulations (solid line), the hybrid NTFA model (dot-dashed line) and the NTFA-TSO model (dashed line). Left: matrix with linear kinematic hardening. Right: matrix with nonlinear kinematic hardening.

The hybrid NTFA model matches quite well the full-field simulations, whereas the NTFA-TSO model overestimates the peak of the stress fluctuations when the matrix hardening is linear. When the matrix hardening is nonlinear both NTFA models are in good agreement with the full-field simulations.

Probability distribution of the local stress fields. Finally the probability density function of the norm of the stress fields in the matrix are compared in figure 9. The norm (74) of the stress $\boldsymbol{\sigma}$ at point $\boldsymbol{x}$ is used for this comparison. Again, when the matrix hardening is linear, the hybrid NTFA model matches quite well the full-field simulations, whereas the distribution predicted by the NTFA-TSO model is slightly shifted, but remains in good agreement with the reference results. When the matrix hardening is nonlinear both NTFA models are in good agreement with the full-field simulations.

7.5. Discussion

The above two examples give us indications, which are in fact generic trends according to our experience, about the relative figure of merits of the two different reduction steps, reduction of the unknowns (through the POD) and reduction of the evolution equations (through the TSO linearization).

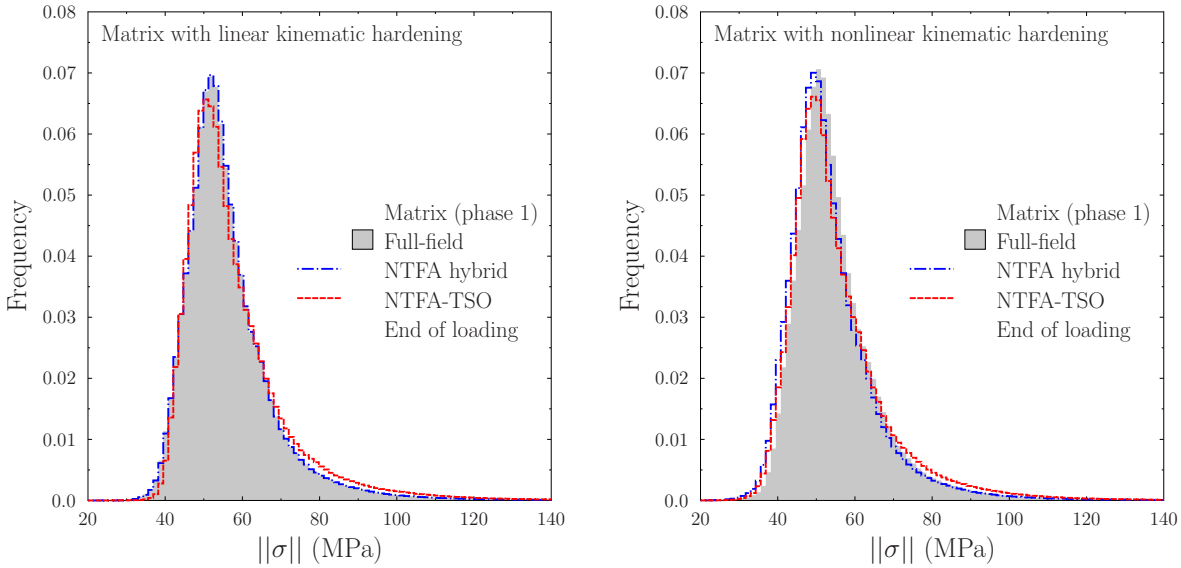

Figure 9: Probability distribution of the norm of the stress field in the matrix at the end of 3rd cycle. Comparison between full-field simulations (full bars), the hybrid NTFA model (dot-dashed line) and the NTFA-TSO model (dashed line). Left: matrix with linear kinematic hardening. Right: matrix with nonlinear kinematic hardening.

The acceleration due to the reduction in the number of unknowns obviously depends on the reduced basis which has been chosen. In the above examples the snapshot POD was used and the reduced basis was formed with eigenvectors containing 99.99% of the information. It should also be emphasized that, by contrast with most usual model reduction methods, the POD is applied here to the internal variables and not to the displacement fields. With these data, and without further reduction in the dynamics, the resulting acceleration over the full-field simulations was by factor of 4 (hybrid NTFA model). The local fields were found to be very accurately reproduced by the reduced model and the method can be considered as a high-fidelity reduction method.

When in addition to the reduction of unknowns, the dynamics is reduced according to the TSO procedure another acceleration by factor of the order of 10^3 is obtained. The local fields are still in agreement with the full-field simulations, although the agreement is slightly less perfect than with the hybrid method but still very acceptable. The main advantage of the NTFA-TSO model is that it does require any on-line computations but makes only use of quantities which can be precomputed off-line. In addition, the acceleration due to the reduction in the dynamics is by far more spectacular than the acceleration due to the sole reduction in the number of unknowns.

A more general question pertaining to these comparisons between the NTFA predictions and full-field simulations is how good are the predictions of the reduced model for loading paths which are *not* the paths used for the identification of the modes (the comparisons performed here are along the paths used for generating the modes). It is therefore important to make a distinction between the *learning loading paths*, which are used to generate the snapshots from which the modes are extracted, and *validation loading paths* which should be different from the learning

paths to show that the method has a much wider range of applicability than the learning paths. In Largenton *et al* (2014), where the constituents are linear viscoelastic, the learning paths were uniaxial, but the validation paths were multi-axial and the predictions of the reduced-order model based on modes determined from uniaxial paths were in very good agreement with full-field simulations. In their earlier work, the authors (Michel and Suquet, 2003, 2004) arrived at the same conclusion for two-phase composites with the earlier version of the NTFA and since the present version NTFA-TSO of the model is more accurate than the earlier version of the NTFA, it is expected that the new model with modes generated from uniaxial tests will give accurate predictions for multi-axial loadings for moderate nonlinearities. However, it should be clearly recognized that a reduced-order model based on a finite (and hopefully small) number of tests cannot be expected to be accurate for *any* loading path. The learning paths, their direction and their amplitude, should contain enough information and should not be too different from the validation paths, or the paths used in the application of the model. How to design properly the learning paths is an open question and so far, this choice is left to the user.

8. Conclusion

The present study extends in different directions and improves on the previous Nonuniform Transformation Field Analysis of Michel and Suquet (2003), based on a decomposition of the local fields of internal variables on a reduced basis of modes.

1. When the constitutive relations of the constituents derive from two potentials, it is shown that this structure is preserved by the primal NTFA model.
2. Another structure-preserving model, the hybrid NTFA model of Fritzen and Leuschner (2013), has been analyzed. It is found to differ (slightly) from the primal NTFA model (it does not exhibit the same variational upper bound character), but is close to it when the modes are rich enough. However, and more importantly, it requires "on-line" computations of local fields and does not meet the objective of the original NTFA approach to fully decouple the computations at the scale of the unit-cell and at the scale of structure.
3. New reduced evolution equations (or coarse dynamics) for the reduced variables have been proposed, based on an expansion to second order (TSO) of the potential of the hybrid model, a linearization technique which has proven its usefulness in nonlinear homogenization. The coarse dynamics can then be entirely expressed in terms of quantities which can be pre-computed once for all (off-line). Roughly speaking, these pre-computed quantities depend on the average and fluctuations per phase of the modes and of the associated stress fields.
4. By contrast with the evolution equations of the original NTFA model, the derivation of the new coarse dynamics is now more general and more systematic.
5. The accuracy of the new NTFA-TSO model is assessed by comparison with full-field simulations. The acceleration provided by the new coarse dynamics over the full-field computations (and over the hybrid model) is then spectacular and found to be much larger than the acceleration due to to the reduction in the number of variables.

6. Although the derivation of the "coarse dynamics" is the main contribution of the present study, it is worth noting that the notion of global modes proposed in Largenton et al. (2014) for linearly viscoelastic phases, is generalized here to nonlinear constituents.

Acknowledments: The authors acknowledge the support of the Labex MEC and of A*Midex through grants ANR-11-LABX-0092 and ANR-11-IDEX-0001-02.

References:

Amiable, S., Chapuliot, S., Constantinescu, A., Fissolo, A., 2006. A comparison of lifetime prediction methods for a thermal fatigue experiment. Int. J. Fatigue **28**, 692–706.

Armstrong, P., Frederick, C., 1966. A mathematical representation of the multiaxial Bauschinger effect. Central Electricity Generating Board and Berkeley Nuclear Laboratories, Research & Development Department Report RD/B/N731, reprinted in *Mat. High Temp.* **24** (2007), pp 11–26.

Berini, B., Bourgeois, M., Boussaa, D., Suquet, P., Thomas, J.-J., 2005. Multiscale modeling of the thermomechanical viscoplastic behavior of metal matrix composites. In: 8th Conference on Computational Plasticity. Barcelona (Spain), pp. 210–213, http://congress.cimne.com/complas05/admin/Files/FilePaper/p210.pdf.

Berkooz, G., Holmes, P., Lumley, J.L., 1993. The Proper Orthogonal Decomposition in the analysis of turbulent flows. Annu. Rev. Fluid Mech. **25**, 539-575.

Besson, J., Cailletaud, G., Chaboche, J.-L., Forest, S., Blétry, M., 2010. Nonlinear Mechanics of Materials. Solids Mechanics and Applications. Springer, Dordrecht.

Chaboche, J.-L., 2008. A review of some plasticity and viscoplasticity constitutive theories. Int. J. Plasticity **24**, 1642–1693.

Chatterjee, A., 2000. An introduction to the proper orthogonal decomposition. Current Science, **78**, 808–817.

Chinesta, F., Cueto, E., 2014. PGD-Based Modeling of Materials, Structures and Processes. Springer, Heidelberg.

Dvorak, G., 1992. Transformation field analysis of inelastic composite materials. Proc. R. Soc. Lond. A **437**, 311–327.

Dvorak, G., Bahei-El-Din, Y., Wafa, A., 1994. The modeling of inelastic composite materials with the transformation field analysis. Modelling Simul. Mater. Sci. Eng **2**, 571–586.

Feyel, F., Chaboche, J.-L., 2000. FE2 multiscale approach for modelling the elastoviscoplastic behaviour of long fibre SiC/Ti composite materials. Comput. Methods Appl. Mech. Eng. **183**, 309–330.

Fish, J., Shek, K., Pandheeradi, M., Shepard, M., 1997. Computational plasticity for composite structures based on mathematical homogenization: Theory and practice. Comput. Methods Appl. Mech. Engrg. **148**, 53–73.

Fish, J., Yu, Q., 2002. Computational Mechanics of Fatigue and Life Predictions for Composite Materials and Structures. Comput. Methods Appl. Mech. Engrg. **191**, 4827–4849.

Fritzen, F., Böhlke, T., 2010. Three-dimensional finite element implementation of the nonuniform transformation field analysis. International Journal for Numerical Methods in Engineering **84**, 803–829.

Fritzen, F., Leuschner, M., 2013. Reduced basis hybrid computational homogenization based on a mixed incremental formulation. Comput. Methods Appl. Mech. Engrg. 260, 143–154.

Germain, P., Nguyen, Q.S., Suquet, P., 1983. Continuum Thermodynamics. J. Appl. Mech. **50**, 1010–1020.

Halphen, B., Nguyen, Q.S., 1975. Sur les matériaux standard généralisés. J. Mécanique **14**, 39–63.

Holmes, P., Lumley, J., Berkooz, G., 1996. Structures, Dynamical Systems and Symmetry. Cambridge University Press, Cambridge.

Idiart, M., Moulinec, H., Ponte Castañeda, P., Suquet, P., 2006. Macroscopic behavior and field fluctuations in viscoplastic composites: second-order estimates versus full-field simulations. J. Mech. Phys. Solids **54** , 1029–1063, doi:10.1016/j.jmps.2005.11.004.

Kattan, P., Voyiadjis, G., 1993. Overall damage and elastoplastic deformation in fibrous metal matrix composites. Int. J. Plasticity **9**, 931–949.

Lahellec, N., Suquet, P., 2007a. Effective behavior of linear vicoelastic composites: a time-integration approach. Int. J. Sol. Struct. **44**, 507–529, doi:10.1016/j.ijsolstr.2006.04.038.

Lahellec, N., Suquet, P., 2007b. On the effective behavior of nonlinear inelastic composites: I. Incremental variational principles. J. Mech. Phys. Solids **55** , 1932–1963, doi:10.1016/j/jmps.2007.02.003.

Lall, S., Krysl, P., Marsden, J., 2003. Structure-preserving model reduction for mechanical systems. Physica D **184**, 304–318.

Largenton, R., Michel, J.-C., Suquet, P., 2014. Extension of the nonuniform transformation field analysis to linear viscoelastic composites in the presence of aging and swelling. *Mechanics of Materials* **73**, 76–100, http://dx.doi.org/10.1016/j.mechmat.2014.02.004.

Latourte, F., Salez, A., Guery, A., Mahé, M., 2014. Deformation studies from in situ SEM experiments of a reactor pressure vessel steel at room and low temperatures. J. Nuclear Materials **454**, 373–380.

Lucia, D., Beran, P., Silva, W., 2004. Reduced-order modeling: new approaches for computational physics. Progress in Aerospace Sciences 40, 51–117.

Mandel, J., 1972. Plasticité classique et Viscoplasticité. Vol. **97** of CISM Lecture Notes. Springer-Verlag, Wien.

Mialon, P., 1986. Eléments d'analyse et de résolution numérique des relations de l'élastoplasticité. Tech. rep., EDF. Bulletin de la Direction des Etudes et recherches. Série C. Mathématiques, Informatique.

Michel, J.-C., Galvanetto, U., Suquet, P., 2000. Constitutive relations involving internal variables based on a micromechanical analysis. In: Maugin, G., Drouot, R., Sidoroff, F. (Eds.), Continuum Thermomechanics: The Art and Science of Modelling Material Behaviour. Klüwer Acad. Pub., Dordrecht, pp. 301–312.

Michel, J.-C., Moulinec, H., Suquet, P., 1999. Effective properties of composite materials with periodic microstructure: a computational approach. Comp. Meth. Appl. Mech. Engng. **172**, 109–143.

Michel, J.-C., Suquet, P., 2003. Nonuniform Transformation Field Analysis. Int. J. Solids Structures **40**, 6937–6955, doi:10.1016/S0020-7683(03)00346-9.

Michel, J.-C., Suquet, P., 2004. Computational analysis of nonlinear composite structures using the Nonuniform Transformation Field Analysis. Comp. Meth. Appl. Mech. Engrg. **193**, 5477–5502.

Michel, J.-C., Suquet, P., 2009. Nonuniform Transformation Field Analysis: a reduced model for multiscale nonlinear problems in Solid Mechanics. In: Aliabadi, F., Galvanetto, U. (Eds.), Multiscale Modelling in Solid Mechanics – Computational Approaches. Imperial College Press, London, pp. 159–206, chapter 4.

Miehe, C., 2002. Strain-driven homogenization of inelastic micro-structures and composites based on an incremental variational formulation. Int. J. Numer. Meth. Engng **55**, 1285–1322.

Miehe, C., Schotte, J., Lambrecht, M., 2002. Homogenization of inelastic materials at finite strains based on incremental variational principles. Application to the texture analysis of polycrystals. J. Mech. Phys. Solids **50**, 2123–2167.

Milton, G., 2002. The Theory of Composites. Cambridge University Press, Cambridge.

Ortiz, M., Stainier, L., 1999. The variational formulation of viscoplastic constitutive updates. Comput. Methods Appl. Mech. Engrg **171**, 419–444.

Ponte Castañeda, P., 1991. The effective mechanical properties of nonlinear isotropic composites. J. Mech. Phys. Solids **39**, 45–71.

Ponte Castañeda, P., 1996. Exact second-order estimates for the effective mechanical properties of nonlinear composite materials. J. Mech. Phys. Solids **44**, 827–862.

Ponte Castañeda, P., Suquet, P., 1998. Nonlinear composites. In: der Giessen, E. V., Wu, T. (Eds.), Advances in Applied Mechanics. Vol. **34**. Academic Press, New York, pp. 171–302.

Radermacher, A., Reese, S., 2014. Model reduction in elastoplasticity: proper orthogonal decomposition combined with adaptive sub-structuring. Comput. Mech. **54**, 677–687.

Rice, J., 1970. On the structure of stress-strain relations for time-dependent plastic deformation in metals. J. Appl. Mech. **37**, 728–737.

Ryckelynck, D., Benziane, D., 2010. Multi-level a priori Hyper-reduction of mechanical models involving internal variables. Comput Methods Appl. Mech. Eng **199**, 1134–1142.

Samrout, H., El Abdi, R., Chaboche, J.-L., 1997. Model for 28CrMoV5-8 steel undergoing thermomechanical cyclic loadings. Int. J. Solids Structures **34**, 4547–4556.

Sirovich, L., 1987. Turbulence and the dynamics of coherent structures. Quarterly of Applied Mathematics **45**, 561–590.

Suquet, P., 1985. Local and global aspects in the mathematical theory of plasticity. In: Sawczuk, A., Bianchi, G. (Eds.), Plasticity Today: Modelling, Methods and Applications. Elsevier, London, pp. 279–310.

Suquet, P., 1987. Elements of Homogenization for Inelastic Solid Mechanics. In: Sanchez-Palencia, E., Zaoui, A. (Eds.), Homogenization Techniques for Composite Media. Vol. **272** of Lecture Notes in Physics. Springer Verlag, New York, pp. 193–278.

Suquet, P., 1995. Overall properties of nonlinear composites : a modified secant moduli theory and its link with Ponte Castañeda's nonlinear variational procedure. C.R. Acad. Sc. Paris **320**, Série IIb, 563–571.

Terada, K., Kikuchi, N., 2001. A class of general algorithms for multi-scale analyses of heterogeneous media. Comp. Meth. Appl. Mech. Engng **190**, 5427–5464.

Willis, J., 1989. The structure of overall constitutive relations for a class of nonlinear composites. IMA J. Appl. Math. **43**, 231–242.

Appendix A. Symmetry of $\boldsymbol{D}$ and alternative expressions

By definition (cf (35)),

$$\mathcal{D}^{(k\ell)} = \langle \boldsymbol{\mu}^{(k)} : \boldsymbol{L} : (\boldsymbol{D} * \boldsymbol{\mu}^{(\ell)}) \rangle.$$

Since $\boldsymbol{L} : (\boldsymbol{D} * \boldsymbol{\mu}^{(k)} - \boldsymbol{\mu}^{(k)})$ is an equilibrated stress field, and $\boldsymbol{D} * \boldsymbol{\mu}^{(\ell)}$ is compatible strain field with zero average, one has (Hill's lemma),

$$\langle (\boldsymbol{\mu}^{(k)} - \boldsymbol{D} * \boldsymbol{\mu}^{(k)}) : \boldsymbol{L} : (\boldsymbol{D} * \boldsymbol{\mu}^{(\ell)}) \rangle = 0.$$

Therefore

$$\langle \boldsymbol{\mu}^{(k)} : \boldsymbol{L} : (\boldsymbol{D} * \boldsymbol{\mu}^{(\ell)}) \rangle = \langle (\boldsymbol{D} * \boldsymbol{\mu}^{(k)}) : \boldsymbol{L} : (\boldsymbol{D} * \boldsymbol{\mu}^{(\ell)}) \rangle,$$

which proves the symmetry of $\boldsymbol{D}$. For the same reason (Hill's lemma),

$$\langle (\boldsymbol{\mu}^{(k)} - \boldsymbol{D} * \boldsymbol{\mu}^{(k)}) : \boldsymbol{L} : (\boldsymbol{\mu}^{(\ell)} - \boldsymbol{D} * \boldsymbol{\mu}^{(\ell)}) \rangle = \langle \boldsymbol{\mu}^{(k)} : \boldsymbol{L} : (\boldsymbol{\mu}^{(\ell)} - \boldsymbol{D} * \boldsymbol{\mu}^{(\ell)}) \rangle = \mathcal{L}^{(k\ell)} - \mathcal{D}^{(k\ell)}.$$

Therefore the matrix $\mathcal{L} - \mathcal{D}$ is symmetric and positive. Denoting

$$\boldsymbol{\rho}^{(\ell)}(\boldsymbol{x}) = \boldsymbol{L}(\boldsymbol{x}) : (\boldsymbol{D} * \boldsymbol{\mu}^{(\ell)}(\boldsymbol{x}) - \boldsymbol{\mu}^{(\ell)}(\boldsymbol{x})),$$

one gets

$$\mathcal{L}^{(k\ell)} - \mathcal{D}^{(k\ell)} = \langle \boldsymbol{\rho}^{(k)} : \boldsymbol{M} : \boldsymbol{\rho}^{(\ell)} \rangle, \quad \boldsymbol{M} = \boldsymbol{L}^{-1}.$$

It can be readily checked that $\mathcal{L} - \mathcal{D}$ is positive definite provided that $\boldsymbol{M}$ is positive definite and that the fields $\boldsymbol{\rho}^{(k)}$ are linearly independent.

Alternate expressions for the different quantities in (35) can be derived using Hill's lemma

$$\left.\begin{aligned} \widetilde{\boldsymbol{L}} &= \langle \boldsymbol{A}^{\mathsf{T}} : \boldsymbol{L} : \boldsymbol{A} \rangle = \langle \boldsymbol{L} : \boldsymbol{A} \rangle, \\ \boldsymbol{a}^{(k)} &= \langle (\boldsymbol{\mu}^{(k)} - \boldsymbol{D} * \boldsymbol{\mu}^{(k)}) : \boldsymbol{L} : \boldsymbol{A} \rangle = \langle \boldsymbol{\mu}^{(k)} : \boldsymbol{L} : \boldsymbol{A} \rangle = -\langle\, \boldsymbol{L} : (\boldsymbol{D} * \boldsymbol{\mu}^{(k)} - \boldsymbol{\mu}^{(k)}) \rangle. \end{aligned}\right\}$$

Appendix B. Coarse dynamics by the variational or modified secant method

Appendix B.1. A rigorous variational upper bound for the primal NTFA

For simplicity it is assumed that the only internal variable is the viscoplastic strain and that the dissipation potential $\varphi^{(r)}$ of phase r can be written, for all phases, as a function of the equivalent viscoplastic strain-rate,

$$\boldsymbol{\alpha} = \boldsymbol{\varepsilon}_{\mathsf{v}}, \quad \varphi^{(r)}(\dot{\boldsymbol{\alpha}}) = f^{(r)}(\dot{\alpha}^2_{\mathsf{eq}}), \quad \dot{\alpha}^2_{\mathsf{eq}} = \frac{2}{3}\dot{\boldsymbol{\alpha}} : \dot{\boldsymbol{\alpha}},$$

where $f^{(r)}$ is a *concave* scalar function. Then by concavity of $f^{(r)}$,

$$\langle f^{(r)}(\dot{\alpha}^2_{\mathsf{eq}}) \rangle^{(r)} \leq f^{(r)} \left(\langle \dot{\alpha}^2_{\mathsf{eq}} \rangle^{(r)} \right),$$

and it follows that

$$\langle\varphi(\dot{\boldsymbol{\alpha}})\rangle = \sum_{r=1}^{P} c^{(r)}\varphi^{(r)}(\dot{\boldsymbol{\alpha}}) = \sum_{r=1}^{P} c^{(r)}\langle f^{(r)}(\dot{\alpha}^2_{\mathsf{eq}})\rangle^{(r)} \leq \sum_{r=1}^{P} c^{(r)} f^{(r)}\left(\langle\dot{\alpha}^2_{\mathsf{eq}}\rangle^{(r)}\right).$$

According to the decomposition (22)

$$\langle\dot{\alpha}^2_{\mathsf{eq}}\rangle^{(r)} = \sum_{k,\ell=1}^{M} M_r^{(k\ell)}\dot{\xi}^{(k)}\dot{\xi}^{(\ell)}, \quad M_r^{(k\ell)} = \frac{2}{3}\langle\boldsymbol{\mu}^{(k)}.\boldsymbol{\mu}^{(\ell)}\rangle^{(r)}.$$

Finally the overall dissipation potential $\widetilde{\varphi}(\dot{\boldsymbol{\xi}})$ is bounded from above by

$$\widetilde{\varphi}(\dot{\boldsymbol{\xi}}) \leq \sum_{r=1}^{P} c^{(r)} f^{(r)}\left(\sum_{k,\ell=1}^{N} M_r^{(k\ell)}\dot{\xi}^{(k)}\dot{\xi}^{(\ell)}\right) = \sum_{r=1}^{P} c^{(r)}\Phi^{(r)}\left(\left|\left|\dot{\boldsymbol{\xi}}\right|\right|^{(r)}\right), \tag{B.1}$$

where

$$\left|\left|\dot{\boldsymbol{\xi}}\right|\right|^{(r)} = \left(\sum_{k,\ell=1}^{M} M_r^{(k\ell)}\dot{\xi}^{(k)}\dot{\xi}^{(\ell)})\right)^{1/2}, \quad \Phi^{(r)}(x) = f^{(r)}(x^2).$$

Using the right-hand-side of (B.1) as the effective dissipation potential yields

$$\mathfrak{a}^{(k)} = \frac{\partial\widetilde{\varphi}}{\partial\dot{\xi}^{(k)}}(\dot{\boldsymbol{\xi}}) = \sum_{\ell=1}^{M}\left(\sum_{r=1}^{P} c^{(r)}\frac{\Phi'^{(r)}\left(\left|\left|\dot{\boldsymbol{\xi}}\right|\right|^{(r)}\right)}{\left|\left|\dot{\boldsymbol{\xi}}\right|\right|^{(r)}} M_r^{(k\ell)}\right)\dot{\xi}^{(\ell)}. \tag{B.2}$$

This equation, together with the second equation in (28) gives a nonlinear differential equation for the $\xi^{(k)}$'s or alternatively for the $\mathfrak{a}^{(k)}$'s.

Appendix B.2. Connection with the original NTFA model of Michel and Suquet (2003)

The equation (B.2) can be further simplified by introducing

$$e_r^{(k)} = c^{(r)}\langle\boldsymbol{\mu}^{(k)} : \boldsymbol{\alpha}\rangle^{(r)} = \frac{3}{2}\sum_{\ell=1}^{M} M_r^{(k\ell)}\xi^{(\ell)}. \tag{B.3}$$

Define

$$\boldsymbol{N}_r = \boldsymbol{M}_r^{-1} \quad \text{and} \quad ||\dot{\boldsymbol{e}}_r||^{(r)} = \left(\sum_{k,\ell=1}^{M} N_r^{(k\ell)}\dot{e}_r^{(k)}\dot{e}_r^{(\ell)})\right)^{1/2}$$

and note that $||\dot{\boldsymbol{e}}_r||^{(r)} = \frac{1}{c^{(r)}}\left|\left|\dot{\boldsymbol{\xi}}\right|\right|^{(r)}$. Then (B.2) takes the simpler form

$$\mathfrak{a}^{(k)} = \sum_{r=1}^{P} c^{(r)}\Phi'^{(r)}\left(\frac{2}{3c^{(r)}}\,||\dot{\boldsymbol{e}}_r||^{(r)}\right)\frac{\dot{e}_r^{(k)}}{||\dot{\boldsymbol{e}}_r||^{(r)}} \tag{B.4}$$

If we further assume as in Michel and Suquet (2003) that each mode has its support in a single phase and that the modes are orthogonal and normalized such that

$$\langle (\mu_{\mathsf{eq}}^{(k)})^2 \rangle = \frac{1}{c^{(r)}}, \tag{B.5}$$

then $M_r^{(k\ell)} = 1/(c^{(r)})^2$, and

$$\left|\left|\dot{\boldsymbol{\xi}}\right|\right|^{(r)} = \frac{1}{c^{(r)}} \left|\dot{\boldsymbol{\xi}}\right|, \ \left|\dot{\boldsymbol{\xi}}\right| = \left(\sum_{\ell=1}^{M^{(r)}} (\dot{\xi}^{(\ell)})^2 \right)^{1/2}, \ ||\dot{\boldsymbol{e}}_r||^{(r)} = c^{(r)} \left|\dot{\boldsymbol{e}}\right|, \ \left|\dot{\boldsymbol{e}}\right| = \left(\sum_{\ell=1}^{M^{(r)}} (\dot{e}^{(\ell)})^2 \right)^{1/2},$$

where the subscript r has been dropped in the last equality since $\boldsymbol{e}$ refers only to the modes having their support in phase r. The evolution equation for the modes with support in phase r reads as

$$\mathfrak{a}^{(k)} = \Phi'^{(r)} \left(\frac{2}{3} \left|\dot{\boldsymbol{e}}\right| \right) \frac{\dot{e}^{(k)}}{\left|\dot{\boldsymbol{e}}\right|},$$

and this relation can be inverted into

$$\dot{e}^{(k)} = \frac{3}{2} \frac{\Psi'^{(r)} \left(|\mathfrak{a}| \right)}{|\mathfrak{a}|} \mathfrak{a}^{(k)}, \quad \text{with } |\mathfrak{a}| = \left(\sum_{\ell=1}^{M^{(r)}} (\mathfrak{a}^{(\ell)})^2 \right)^{1/2}, \tag{B.6}$$

where $\Psi^{(r)}$ is the dual convex of $\Phi^{(r)}$. (B.6) is recognized (after some algebra) to be the evolution equation (52) in the coupled model of Michel and Suquet (2003). As is well known, the predictions of the variational linearization are too stiff and this excessive stiffness can be corrected by a proper normalization of the modes as done in Michel and Suquet (2003).

Appendix C. TSO expansion for the primal NTFA model

The tangent second-order linearization for the primal NTFA approach consists in substituting $\varphi^{(r)}$ with $\varphi_{TSO}^{(r)}$, its expansion to second order in $\dot{\boldsymbol{\alpha}}$,

$$\varphi_{TSO}^{(r)}(\dot{\boldsymbol{\alpha}}) = \varphi^{(r)}(\check{\boldsymbol{\alpha}}^{(r)}) + \frac{\partial \varphi^{(r)}}{\partial \dot{\boldsymbol{\alpha}}}(\check{\boldsymbol{\alpha}}^{(r)}) : \left(\dot{\boldsymbol{\alpha}} - \check{\boldsymbol{\alpha}}^{(r)}\right) + \frac{1}{2} \left(\dot{\boldsymbol{\alpha}} - \check{\boldsymbol{\alpha}}^{(r)}\right) : \boldsymbol{L}_0^{(r)} : \left(\dot{\boldsymbol{\alpha}} - \check{\boldsymbol{\alpha}}^{(r)}\right).$$

It follows from stationarity requirements (Ponte Castañeda, 1996) that the optimal choice for $\check{\boldsymbol{\alpha}}^{(r)}$ and a reasonable choice for $\boldsymbol{L}_0^{(r)}$ are

$$\check{\boldsymbol{\alpha}}^{(r)} = \langle \boldsymbol{\alpha} \rangle^{(r)} = \sum_{k=1}^{M} \dot{\xi}^{(k)} \langle \boldsymbol{\mu}^{(k)} \rangle^{(r)}, \quad \boldsymbol{L}_0^{(r)} = \frac{\partial^2 \varphi^{(r)}}{\partial \dot{\boldsymbol{\alpha}}^2}(\check{\boldsymbol{\alpha}}^{(r)}).$$

Then the effective dissipation potential is approximated by

$$\widetilde{\varphi}(\dot{\boldsymbol{\xi}}) = \sum_{r=1}^{P} c^{(r)} \left[\varphi^{(r)}(\langle \dot{\boldsymbol{\alpha}} \rangle^{(r)}) + \frac{1}{2} \frac{\partial^2 \varphi^{(r)}}{\partial \dot{\boldsymbol{\alpha}}^2}(\langle \dot{\boldsymbol{\alpha}} \rangle^{(r)}) :: \boldsymbol{C}^{(r)}(\dot{\boldsymbol{\alpha}}) \right],$$

where

$$\boldsymbol{C}^{(r)}(\dot{\boldsymbol{\alpha}}) = \langle \big(\dot{\boldsymbol{\alpha}} - \langle\dot{\boldsymbol{\alpha}}\rangle^{(r)}\big) \otimes \big(\dot{\boldsymbol{\alpha}} - \langle\dot{\boldsymbol{\alpha}}\rangle^{(r)}\big)\rangle^{(r)} = \langle\dot{\boldsymbol{\alpha}} \otimes \dot{\boldsymbol{\alpha}}\rangle^{(r)} - \langle\dot{\boldsymbol{\alpha}}\rangle^{(r)} \otimes \langle\dot{\boldsymbol{\alpha}}\rangle^{(r)}$$

$$= \sum_{k,\ell} \dot{\xi}^{(k)}\dot{\xi}^{(\ell)}\boldsymbol{C}_r^{(k\ell)}(\boldsymbol{\mu}), \quad \boldsymbol{C}_r^{(k\ell)}(\boldsymbol{\mu}) = \langle\boldsymbol{\mu}^{(k)} \otimes \boldsymbol{\mu}^{(\ell)}\rangle^{(r)} - \langle\boldsymbol{\mu}^{(k)}\rangle^{(r)} \otimes \langle\boldsymbol{\mu}^{(\ell)}\rangle^{(r)}.$$

Therefore the approximate $\widetilde{\varphi}(\dot{\boldsymbol{\xi}})$ reads as

$$\sum_{r=1}^{P} c^{(r)} \left[\varphi^{(r)}\left(\sum_{k=1}^{M} \xi^{(k)}\langle\boldsymbol{\mu}^{(k)}\rangle^{(r)}\right) + \frac{1}{2}\frac{\partial^2\varphi^{(r)}}{\partial\dot{\boldsymbol{\alpha}}^2}\left(\sum_{k=1}^{M} \xi^{(k)}\langle\boldsymbol{\mu}^{(k)}\rangle^{(r)}\right) :: \left(\sum_{k,\ell=1}^{M} \dot{\xi}^{(k)}\dot{\xi}^{(\ell)}\boldsymbol{C}_r^{(k\ell)}(\boldsymbol{\mu})\right)\right],$$

and

$$\begin{aligned}\frac{\partial\widetilde{\varphi}}{\partial\dot{\xi}^{(k)}} &= \sum_{r=1}^{P} c^{(r)} \left[\frac{\partial\varphi^{(r)}}{\partial\dot{\boldsymbol{\alpha}}}(\langle\dot{\boldsymbol{\alpha}}\rangle^{(r)}) : \langle\boldsymbol{\mu}^{(k)}\rangle^{(r)} + \frac{\partial^2\varphi^{(r)}}{\partial\dot{\boldsymbol{\alpha}}^2}(\langle\dot{\boldsymbol{\alpha}}\rangle^{(r)}) :: \left(\sum_{\ell=1}^{M} \dot{\xi}^{(\ell)}\boldsymbol{C}_r^{(k\ell)}(\boldsymbol{\mu})\right)\right. \\ &+ \left.\frac{1}{2}\frac{\partial^3\varphi^{(r)}}{\partial\dot{\boldsymbol{\alpha}}^3}(\langle\dot{\boldsymbol{\alpha}}\rangle^{(r)}) ::: \left(\sum_{k,\ell=1}^{M} \dot{\xi}^{(k)}\dot{\xi}^{(\ell)}\boldsymbol{C}_r^{(k\ell)}(\boldsymbol{\mu}) \otimes \langle\boldsymbol{\mu}^{(k)}\rangle^{(r)}\right)\right].\end{aligned} \tag{C.1}$$

Finally a differential equation for $\boldsymbol{\xi}$ is obtained by re-writing (28) with the help of (C.1)

$$\begin{aligned}-\frac{\partial\widetilde{w}}{\partial\xi^{(k)}}(\overline{\boldsymbol{\varepsilon}}, \boldsymbol{\xi}) &= \sum_{r=1}^{P} c^{(r)} \left[\frac{\partial\varphi^{(r)}}{\partial\dot{\boldsymbol{\alpha}}}(\langle\dot{\boldsymbol{\alpha}}\rangle^{(r)}) : \langle\boldsymbol{\mu}^{(k)}\rangle^{(r)} + \frac{\partial^2\varphi^{(r)}}{\partial\dot{\boldsymbol{\alpha}}^2}(\langle\dot{\boldsymbol{\alpha}}\rangle^{(r)}) :: \left(\sum_{\ell=1}^{M} \dot{\xi}^{(\ell)}\boldsymbol{C}_r^{(k\ell)}(\boldsymbol{\mu})\right)\right. \\ &+ \left.\frac{1}{2}\frac{\partial^3\varphi^{(r)}}{\partial\dot{\boldsymbol{\alpha}}^3}(\langle\dot{\boldsymbol{\alpha}}\rangle^{(r)}) ::: \left(\sum_{k,\ell=1}^{M} \dot{\xi}^{(k)}\dot{\xi}^{(\ell)}\boldsymbol{C}_r^{(k\ell)}(\boldsymbol{\mu}) \otimes \langle\boldsymbol{\mu}^{(k)}\rangle^{(r)}\right)\right].\end{aligned}$$

This is a nonlinear differential equation in the form $g(\dot{\boldsymbol{\xi}}) = f(\boldsymbol{\xi}, t)$.

Appendix D. Expansion of potentials

Appendix D.1. Linear kinematic hardening with nonlinear isotropic hardening

The expansion to second order of the effective potential $\widetilde{\psi}$ for the composites considered in section 5.5 is

$$\widetilde{\psi}_{TSO} = \sum_{r=1}^{P} c^{(r)} \left[\psi^{(r)}(\langle\boldsymbol{\mathcal{A}}\rangle^{(r)}) + \frac{1}{2}\frac{\partial^2\psi^{(r)}}{\partial\boldsymbol{\mathcal{A}}_{\mathsf{v}}^2}(\langle\boldsymbol{\mathcal{A}}\rangle^{(r)}) :: \boldsymbol{C}^{(r)}(\boldsymbol{\mathcal{A}}_{\mathsf{v}})\right],$$

with

$$
\left.
\begin{aligned}
\psi^{(r)}(\boldsymbol{\mathcal{A}}_{\mathsf{v}},\mathcal{A}_{\mathsf{p}}) &= \frac{\dot{\varepsilon}_0\sigma_0}{n+1}\left[\frac{f(\boldsymbol{\mathcal{A}})}{\sigma_0}\right]^{n+1}, \quad f(\boldsymbol{\mathcal{A}}) = \left[(\mathcal{A}_{\mathsf{v}})_{\mathsf{eq}}+\mathcal{A}_{\mathsf{p}}\right]^{+},\\
\frac{\partial\psi^{(r)}}{\partial\boldsymbol{\mathcal{A}}_{\mathsf{v}}}(\boldsymbol{\mathcal{A}}_{\mathsf{v}},\mathcal{A}_{\mathsf{p}}) &= \dot{\varepsilon}_0\left[\frac{f(\boldsymbol{\mathcal{A}})}{\sigma_0}\right]^{n}\boldsymbol{N}_{\mathsf{v}}, \quad \boldsymbol{N}_{\mathsf{v}} = \frac{3}{2}\frac{\boldsymbol{\mathcal{A}}_{\mathsf{v}}^{\mathsf{dev}}}{(\mathcal{A}_{\mathsf{v}})_{\mathsf{eq}}},\\
\frac{\partial\psi^{(r)}}{\partial\mathcal{A}_{\mathsf{p}}}(\boldsymbol{\mathcal{A}}_{\mathsf{v}},\mathcal{A}_{\mathsf{p}}) &= \dot{\varepsilon}_0\left[\frac{f(\boldsymbol{\mathcal{A}})}{\sigma_0}\right]^{n}, \quad \frac{\partial^2\psi^{(r)}}{\partial\mathcal{A}_{\mathsf{p}}^2}(\boldsymbol{\mathcal{A}}_{\mathsf{v}},\mathcal{A}_{\mathsf{p}}) = n\frac{\dot{\varepsilon}_0}{\sigma_0}\left[\frac{f(\boldsymbol{\mathcal{A}})}{\sigma_0}\right]^{n-1},\\
\frac{\partial^2\psi^{(r)}}{\partial\boldsymbol{\mathcal{A}}_{\mathsf{v}}^2}(\boldsymbol{\mathcal{A}}_{\mathsf{v}},\mathcal{A}_{\mathsf{p}}) &= \frac{\dot{\varepsilon}_0}{\sigma_0}\left[\frac{f(\boldsymbol{\mathcal{A}})}{\sigma_0}\right]^{n-1}\left[\left(n-\frac{f(\boldsymbol{\mathcal{A}})}{(\mathcal{A}_{\mathsf{v}})_{\mathsf{eq}}}\right)\boldsymbol{N}_{\mathsf{v}}\otimes\boldsymbol{N}_{\mathsf{v}}+\frac{3}{2}\frac{f(\boldsymbol{\mathcal{A}})}{(\mathcal{A}_{\mathsf{v}})_{\mathsf{eq}}}\boldsymbol{K}\right],\\
\frac{\partial^2\psi^{(r)}}{\partial\boldsymbol{\mathcal{A}}_{\mathsf{v}}\partial\mathcal{A}_{\mathsf{p}}}(\boldsymbol{\mathcal{A}}_{\mathsf{v}},\mathcal{A}_{\mathsf{p}}) &= n\frac{\dot{\varepsilon}_0}{\sigma_0}\left[\frac{f(\boldsymbol{\mathcal{A}})}{\sigma_0}\right]^{n-1}\boldsymbol{N}_{\mathsf{v}},\\
\frac{\partial^3\psi^{(r)}}{\partial\boldsymbol{\mathcal{A}}_{\mathsf{v}}\partial\mathcal{A}_{\mathsf{p}}^2}(\boldsymbol{\mathcal{A}}) &= n(n-1)\frac{\dot{\varepsilon}_0}{\sigma_0^2}\left[\frac{f(\boldsymbol{\mathcal{A}})}{\sigma_0}\right]^{n-2}\boldsymbol{N}_{\mathsf{v}},\\
\frac{\partial^3\psi^{(r)}}{\partial\boldsymbol{\mathcal{A}}_{\mathsf{v}}^2\partial\mathcal{A}_{\mathsf{p}}}(\boldsymbol{\mathcal{A}}) &= n\frac{\dot{\varepsilon}_0}{\sigma_0^2}\left[\frac{f(\boldsymbol{\mathcal{A}})}{\sigma_0}\right]^{n-2}\left[\left((n-1)-\frac{f(\boldsymbol{\mathcal{A}})}{(\mathcal{A}_{\mathsf{v}})_{\mathsf{eq}}}\right)\boldsymbol{N}_{\mathsf{v}}\otimes\boldsymbol{N}_{\mathsf{v}}+\frac{3}{2}\frac{f(\boldsymbol{\mathcal{A}})}{(\mathcal{A}_{\mathsf{v}})_{\mathsf{eq}}}\boldsymbol{K}\right],\\
\frac{\partial^3\psi^{(r)}}{\partial\boldsymbol{\mathcal{A}}_{\mathsf{v}}^3}(\boldsymbol{\mathcal{A}}) &= \frac{\dot{\varepsilon}_0}{\sigma_0^2}\left[\frac{f(\boldsymbol{\mathcal{A}})}{\sigma_0}\right]^{n-2}\left[\alpha\boldsymbol{N}_{\mathsf{v}}\otimes\boldsymbol{N}_{\mathsf{v}}\otimes\boldsymbol{N}_{\mathsf{v}}+\beta\boldsymbol{K}\hat{\otimes}\boldsymbol{N}_{\mathsf{v}}\right],\\
\alpha &= \left(n-\frac{f(\boldsymbol{\mathcal{A}})}{(\mathcal{A}_{\mathsf{v}})_{\mathsf{eq}}}\right)\left(n-1-2\frac{f(\boldsymbol{\mathcal{A}})}{(\mathcal{A}_{\mathsf{v}})_{\mathsf{eq}}}\right)-\frac{f(\boldsymbol{\mathcal{A}})}{(\mathcal{A}_{\mathsf{v}})_{\mathsf{eq}}}\left(1-\frac{f(\boldsymbol{\mathcal{A}})}{(\mathcal{A}_{\mathsf{v}})_{\mathsf{eq}}}\right),\\
\beta &= \frac{3}{2}\frac{f(\boldsymbol{\mathcal{A}})}{(\mathcal{A}_{\mathsf{v}})_{\mathsf{eq}}}\left(n-\frac{f(\boldsymbol{\mathcal{A}})}{(\mathcal{A}_{\mathsf{v}})_{\mathsf{eq}}}\right),
\end{aligned}
\right\}
$$

where $\boldsymbol{K}$ is the fourth-order projector on symmetric deviatoric tensors and

$$(\boldsymbol{K}\hat{\otimes}\boldsymbol{a})_{ijkh\ell m} = K_{ijkh}a_{\ell m}+K_{ij\ell m}a_{kh}+K_{kh\ell m}a_{ij}.$$

Appendix D.2. Nonlinear kinematic hardening with nonlinear isotropic hardening

The expansion to second order of the effective potential $\widetilde{\psi}$ for the composites considered in section 5.5 is

$$
\begin{aligned}
\widetilde{\psi}_{TSO} &= \sum_{r=1}^{P} c^{(r)}\left[\psi^{(r)}(\langle\boldsymbol{\mathcal{A}}\rangle^{(r)})+\frac{1}{2}\frac{\partial^2\psi^{(r)}}{\partial\boldsymbol{\mathcal{A}}_{\mathsf{v}}^2}(\langle\boldsymbol{\mathcal{A}}\rangle^{(r)})::\boldsymbol{C}^{(r)}(\boldsymbol{\mathcal{A}}_{\mathsf{v}})\right.\\
&+ \left.\frac{1}{2}\frac{\partial^2\psi^{(r)}}{\partial\boldsymbol{\mathcal{A}}_{\beta}^2}(\langle\boldsymbol{\mathcal{A}}\rangle^{(r)})::\boldsymbol{C}^{(r)}(\boldsymbol{\mathcal{A}}_{\beta})+\frac{\partial^2\psi^{(r)}}{\partial\boldsymbol{\mathcal{A}}_{\mathsf{v}}\partial\boldsymbol{\mathcal{A}}_{\beta}}(\langle\boldsymbol{\mathcal{A}}\rangle^{(r)})::\boldsymbol{C}^{(r)}(\boldsymbol{\mathcal{A}}_{\mathsf{v}},\boldsymbol{\mathcal{A}}_{\beta})\right].
\end{aligned}
$$

Use has been made of the fact that there is no fluctuation in $\mathcal{A}_{\mathsf{p}}$. Then

$$\begin{aligned}\frac{\partial\widetilde{\psi}_{TSO}}{\partial\xi_{\mathsf{v}}^{(k)}} &= \sum_{r=1}^{P} c^{(r)}\left[\frac{\partial\psi^{(r)}}{\partial\boldsymbol{\mathcal{A}}_{\mathsf{v}}}(\langle\boldsymbol{\mathcal{A}}\rangle^{(r)}) : \frac{\partial\langle\boldsymbol{\mathcal{A}}_{\mathsf{v}}\rangle^{(r)}}{\partial\xi_{\mathsf{v}}^{(k)}}\right.\\ &+ \frac{1}{2}\frac{\partial^2\psi^{(r)}}{\partial\boldsymbol{\mathcal{A}}_{\mathsf{v}}^2}(\langle\boldsymbol{\mathcal{A}}\rangle^{(r)}) :: \frac{\partial\boldsymbol{C}^{(r)}(\boldsymbol{\mathcal{A}}_{\mathsf{v}})}{\partial\xi_{\mathsf{v}}^{(k)}} + \frac{\partial^2\psi^{(r)}}{\partial\boldsymbol{\mathcal{A}}_{\mathsf{v}}\partial\boldsymbol{\mathcal{A}}_{\beta}}(\langle\boldsymbol{\mathcal{A}}\rangle^{(r)}) :: \frac{\partial\boldsymbol{C}^{(r)}(\boldsymbol{\mathcal{A}}_{\mathsf{v}},\boldsymbol{\mathcal{A}}_{\beta})}{\partial\xi_{\mathsf{v}}^{(k)}}\\ &+ \frac{1}{2}\frac{\partial^3\psi^{(r)}}{\partial\boldsymbol{\mathcal{A}}_{\mathsf{v}}^3}(\langle\boldsymbol{\mathcal{A}}\rangle^{(r)}) ::: \boldsymbol{C}^{(r)}(\boldsymbol{\mathcal{A}}_{\mathsf{v}}) \otimes \frac{\partial\langle\boldsymbol{\mathcal{A}}_{\mathsf{v}}\rangle^{(r)}}{\partial\xi_{\mathsf{v}}^{(k)}} + \frac{1}{2}\frac{\partial^3\psi^{(r)}}{\partial\boldsymbol{\mathcal{A}}_{\beta}^2\partial\boldsymbol{\mathcal{A}}_{\mathsf{v}}}(\langle\boldsymbol{\mathcal{A}}\rangle^{(r)}) ::: \boldsymbol{C}^{(r)}(\boldsymbol{\mathcal{A}}_{\beta}) \otimes \frac{\partial\langle\boldsymbol{\mathcal{A}}_{\mathsf{v}}\rangle^{(r)}}{\partial\xi_{\mathsf{v}}^{(k)}}\\ &+ \left.\frac{\partial^3\psi^{(r)}}{\partial\boldsymbol{\mathcal{A}}_{\mathsf{v}}^2\partial\boldsymbol{\mathcal{A}}_{\beta}}(\langle\boldsymbol{\mathcal{A}}\rangle^{(r)}) ::: \boldsymbol{C}^{(r)}(\boldsymbol{\mathcal{A}}_{\mathsf{v}},\boldsymbol{\mathcal{A}}_{\beta}) \otimes \frac{\partial\langle\boldsymbol{\mathcal{A}}_{\mathsf{v}}\rangle^{(r)}}{\partial\xi_{\mathsf{v}}^{(k)}}\right],\end{aligned}$$

where

$$\frac{\partial\langle\boldsymbol{\mathcal{A}}_{\mathsf{v}}\rangle^{(r)}}{\partial\xi_{\mathsf{v}}^{(k)}} = \langle\boldsymbol{\rho}^{(k)}\rangle^{(r)}, \quad \frac{\partial\boldsymbol{C}^{(r)}(\boldsymbol{\mathcal{A}}_{\mathsf{v}})}{\partial\xi_{\mathsf{v}}^{(k)}} = 2\langle\left(\boldsymbol{\rho}^{(k)} - \langle\boldsymbol{\rho}^{(k)}\rangle^{(r)}\right)\otimes_s\left(\boldsymbol{\mathcal{A}}_{\mathsf{v}} - \langle\boldsymbol{\mathcal{A}}_{\mathsf{v}}\rangle^{(r)}\right)\rangle^{(r)},$$
$$\frac{\partial\boldsymbol{C}^{(r)}(\boldsymbol{\mathcal{A}}_{\mathsf{v}},\boldsymbol{\mathcal{A}}_{\beta})}{\partial\xi_{\mathsf{v}}^{(k)}} = \langle\left(\boldsymbol{\rho}^{(k)} - \langle\boldsymbol{\rho}^{(k)}\rangle^{(r)}\right)\otimes_s\left(\boldsymbol{\mathcal{A}}_{\beta} - \langle\boldsymbol{\mathcal{A}}_{\beta}\rangle^{(r)}\right)\rangle^{(r)}.$$

The derivative of $\widetilde{\psi}_{TSO}$ with respect to $\xi_{\beta}^{(k)}$ has exactly the same form, except that all derivatives with respected to $\xi_{\mathsf{v}}^{(k)}$ must be replaced by derivatives with respect to $\xi_{\beta}^{(k)}$ and with the following relations

$$\frac{\partial\langle\boldsymbol{\mathcal{A}}_{\beta}\rangle^{(r)}}{\partial\xi_{\beta}^{(k)}} = -\boldsymbol{H}^{(r)} : \langle\boldsymbol{\mu}_{\beta}^{(k)}\rangle^{(r)}, \quad \frac{\partial\boldsymbol{C}^{(r)}(\boldsymbol{\mathcal{A}}_{\beta})}{\partial\xi_{\beta}^{(k)}} = -2\langle\boldsymbol{H}^{(r)} : \left(\boldsymbol{\mu}_{\beta}^{(k)} - \langle\boldsymbol{\mu}_{\beta}^{(k)}\rangle^{(r)}\right)\otimes_s\left(\boldsymbol{\mathcal{A}}_{\beta} - \langle\boldsymbol{\mathcal{A}}_{\beta}\rangle^{(r)}\right)\rangle^{(r)},$$
$$\frac{\partial\boldsymbol{C}^{(r)}(\boldsymbol{\mathcal{A}}_{\beta},\boldsymbol{\mathcal{A}}_{\mathsf{v}})}{\partial\xi_{\beta}^{(k)}} = -\langle\boldsymbol{H}^{(r)} : \left(\boldsymbol{\mu}_{\beta}^{(k)} - \langle\boldsymbol{\mu}_{\beta}^{(k)}\rangle^{(r)}\right)\otimes_s\left(\boldsymbol{\mathcal{A}}_{\mathsf{v}} - \langle\boldsymbol{\mathcal{A}}_{\mathsf{v}}\rangle^{(r)}\right)\rangle^{(r)}.$$

Similarly,

$$\begin{aligned}\frac{\partial\widetilde{\psi}_{TSO}}{\partial\mathfrak{a}_{\mathsf{p}}^{(r)}} &= \langle\frac{\partial\psi_{TSO}}{\partial\mathcal{A}_{\mathsf{p}}}\rangle^{(r)} = \frac{\partial\psi^{(r)}}{\partial\mathcal{A}_{\mathsf{p}}}(\langle\boldsymbol{\mathcal{A}}\rangle^{(r)}) + \frac{1}{2}\frac{\partial^3\psi^{(r)}}{\partial\boldsymbol{\mathcal{A}}_{\mathsf{v}}^2\partial\mathcal{A}_{\mathsf{p}}}(\langle\boldsymbol{\mathcal{A}}\rangle^{(r)}) :: \boldsymbol{C}^{(r)}(\boldsymbol{\mathcal{A}}_{\mathsf{v}})\\ &+\frac{1}{2}\frac{\partial^3\psi^{(r)}}{\partial\boldsymbol{\mathcal{A}}_{\beta}^2\partial\mathcal{A}_{\mathsf{p}}}(\langle\boldsymbol{\mathcal{A}}\rangle^{(r)}) :: \boldsymbol{C}^{(r)}(\boldsymbol{\mathcal{A}}_{\beta}) + \frac{\partial^3\psi^{(r)}}{\partial\boldsymbol{\mathcal{A}}_{\mathsf{v}}\partial\boldsymbol{\mathcal{A}}_{\beta}\partial\mathcal{A}_{\mathsf{p}}}(\langle\boldsymbol{\mathcal{A}}\rangle^{(r)}) :: \boldsymbol{C}^{(r)}(\boldsymbol{\mathcal{A}}_{\mathsf{v}},\boldsymbol{\mathcal{A}}_{\beta}).\end{aligned}$$

The TSO approximation of the non-standard term in (60) is

$$
\begin{aligned}
& \langle \frac{\partial \psi^{(r)}_{TSO}}{\partial \mathcal{A}_{\mathsf{p}}}(\boldsymbol{\mathcal{A}})\boldsymbol{\mathcal{A}}_\beta : \boldsymbol{\mu}^{(k)}_\beta \rangle^{(r)} = \frac{\partial \psi^{(r)}}{\partial \mathcal{A}_{\mathsf{p}}}(\langle \boldsymbol{\mathcal{A}} \rangle^{(r)}) \langle \boldsymbol{\mathcal{A}}_\beta : \boldsymbol{\mu}^{(k)}_\beta \rangle^{(r)} \\
+ \quad & \frac{\partial^2 \psi^{(r)}}{\partial \boldsymbol{\mathcal{A}}_{\mathsf{v}} \partial \mathcal{A}_{\mathsf{p}}}(\langle \boldsymbol{\mathcal{A}} \rangle^{(r)}) : \langle (\boldsymbol{\mathcal{A}}_{\mathsf{v}} - \langle \boldsymbol{\mathcal{A}}_{\mathsf{v}} \rangle^{(r)}) \boldsymbol{\mathcal{A}}_\beta : \boldsymbol{\mu}^{(k)}_\beta \rangle^{(r)} \\
+ \quad & \frac{\partial^2 \psi^{(r)}}{\partial \boldsymbol{\mathcal{A}}_{\beta} \partial \mathcal{A}_{\mathsf{p}}}(\langle \boldsymbol{\mathcal{A}} \rangle^{(r)}) : \langle (\boldsymbol{\mathcal{A}}_{\beta} - \langle \boldsymbol{\mathcal{A}}_{\beta} \rangle^{(r)}) \boldsymbol{\mathcal{A}}_\beta : \boldsymbol{\mu}^{(k)}_\beta \rangle^{(r)} \\
+ \quad & \frac{1}{2} \frac{\partial^3 \psi^{(r)}}{\partial \boldsymbol{\mathcal{A}}^2_{\mathsf{v}} \partial \mathcal{A}_{\mathsf{p}}}(\langle \boldsymbol{\mathcal{A}} \rangle^{(r)}) :: \langle \big(\boldsymbol{\mathcal{A}}_{\mathsf{v}} - \langle \boldsymbol{\mathcal{A}}_{\mathsf{v}} \rangle^{(r)}\big) \otimes \big(\boldsymbol{\mathcal{A}}_{\mathsf{v}} - \langle \boldsymbol{\mathcal{A}}_{\mathsf{v}} \rangle^{(r)}\big) \rangle^{(r)} \langle \boldsymbol{\mathcal{A}}_\beta : \boldsymbol{\mu}^{(k)}_\beta \rangle^{(r)} \\
+ \quad & \frac{1}{2} \frac{\partial^3 \psi^{(r)}}{\partial \boldsymbol{\mathcal{A}}^2_{\beta} \partial \mathcal{A}_{\mathsf{p}}}(\langle \boldsymbol{\mathcal{A}} \rangle^{(r)}) :: \langle \big(\boldsymbol{\mathcal{A}}_{\beta} - \langle \boldsymbol{\mathcal{A}}_{\beta} \rangle^{(r)}\big) \otimes \big(\boldsymbol{\mathcal{A}}_{\beta} - \langle \boldsymbol{\mathcal{A}}_{\beta} \rangle^{(r)}\big) \rangle^{(r)} \langle \boldsymbol{\mathcal{A}}_\beta : \boldsymbol{\mu}^{(k)}_\beta \rangle^{(r)} \\
+ \quad & \frac{\partial^3 \psi^{(r)}}{\partial \boldsymbol{\mathcal{A}}_{\mathsf{v}} \partial \boldsymbol{\mathcal{A}}_{\beta} \partial \mathcal{A}_{\mathsf{p}}}(\langle \boldsymbol{\mathcal{A}} \rangle^{(r)}) :: \langle \big(\boldsymbol{\mathcal{A}}_{\beta} - \langle \boldsymbol{\mathcal{A}}_{\beta} \rangle^{(r)}\big) \otimes_s \big(\boldsymbol{\mathcal{A}}_{\mathsf{v}} - \langle \boldsymbol{\mathcal{A}}_{\mathsf{v}} \rangle^{(r)}\big) \rangle^{(r)} \langle \boldsymbol{\mathcal{A}}_\beta : \boldsymbol{\mu}^{(k)}_\beta \rangle^{(r)},
\end{aligned}
$$

$$
\begin{aligned}
\text{with}\quad \psi^{(r)}(\boldsymbol{\mathcal{A}}) &= \frac{\sigma_0\dot{\varepsilon}_0}{n+1}\left[\frac{f(\boldsymbol{\mathcal{A}})}{\sigma_0}\right]^{n+1}, \quad f(\boldsymbol{\mathcal{A}}) = \left[(\mathcal{A}_{\mathsf{v}}+\mathcal{A}_\beta)_{\mathsf{eq}}+\mathcal{A}_{\mathsf{p}}\right]^+,\\
\frac{\partial\psi^{(r)}}{\partial\boldsymbol{\mathcal{A}}_{\mathsf{v}}}(\boldsymbol{\mathcal{A}}) &= \frac{\partial\psi^{(r)}}{\partial\boldsymbol{\mathcal{A}}_\beta}(\boldsymbol{\mathcal{A}}) = \dot{\varepsilon}_0\left[\frac{f(\boldsymbol{\mathcal{A}})}{\sigma_0}\right]^n \boldsymbol{N}, \quad \boldsymbol{N} = \frac{3}{2}\frac{(\boldsymbol{\mathcal{A}}_{\mathsf{v}}+\boldsymbol{\mathcal{A}}_\beta)^{\mathsf{dev}}}{(\mathcal{A}_{\mathsf{v}}+\mathcal{A}_\beta)_{\mathsf{eq}}},\\
\frac{\partial\psi^{(r)}}{\partial\mathcal{A}_{\mathsf{p}}}(\boldsymbol{\mathcal{A}}) &= \dot{\varepsilon}_0\left[\frac{f(\boldsymbol{\mathcal{A}})}{\sigma_0}\right]^n, \quad \frac{\partial^2\psi^{(r)}}{\partial\mathcal{A}_{\mathsf{p}}^2}(\boldsymbol{\mathcal{A}}_{\mathsf{v}},\mathcal{A}_{\mathsf{p}}) = n\frac{\dot{\varepsilon}_0}{\sigma_0}\left[\frac{f(\boldsymbol{\mathcal{A}})}{\sigma_0}\right]^{n-1},\\
\frac{\partial^2\psi^{(r)}}{\partial\boldsymbol{\mathcal{A}}_{\mathsf{v}}^2}(\boldsymbol{\mathcal{A}}) &= \frac{\dot{\varepsilon}_0}{\sigma_0}\left[\frac{f(\boldsymbol{\mathcal{A}})}{\sigma_0}\right]^{n-1}\left[\left(n-\frac{f(\boldsymbol{\mathcal{A}})}{(\mathcal{A}_{\mathsf{v}})_{\mathsf{eq}}}\right)\boldsymbol{N}\otimes\boldsymbol{N}+\frac{3}{2}\frac{f(\boldsymbol{\mathcal{A}})}{(\mathcal{A}_{\mathsf{v}})_{\mathsf{eq}}}\boldsymbol{K}\right],\\
\frac{\partial^2\psi^{(r)}}{\partial\boldsymbol{\mathcal{A}}_\beta^2}(\boldsymbol{\mathcal{A}}) &= \frac{\partial^2\psi^{(r)}}{\partial\boldsymbol{\mathcal{A}}_{\mathsf{v}}\partial\boldsymbol{\mathcal{A}}_\beta}(\boldsymbol{\mathcal{A}}) = \frac{\partial^2\psi^{(r)}}{\partial\boldsymbol{\mathcal{A}}_{\mathsf{v}}^2}(\boldsymbol{\mathcal{A}}),\\
\frac{\partial^2\psi^{(r)}}{\partial\boldsymbol{\mathcal{A}}_{\mathsf{v}}\partial\mathcal{A}_{\mathsf{p}}}(\boldsymbol{\mathcal{A}}) &= \frac{\partial^2\psi^{(r)}}{\partial\boldsymbol{\mathcal{A}}_\beta\partial\mathcal{A}_{\mathsf{p}}}(\boldsymbol{\mathcal{A}}) = n\frac{\dot{\varepsilon}_0}{\sigma_0}\left[\frac{f(\boldsymbol{\mathcal{A}})}{\sigma_0}\right]^{n-1}\boldsymbol{N},\\
\frac{\partial^3\psi^{(r)}}{\partial\boldsymbol{\mathcal{A}}_{\mathsf{v}}\partial\mathcal{A}_{\mathsf{p}}^2}(\boldsymbol{\mathcal{A}}) &= \frac{\partial^3\psi^{(r)}}{\partial\boldsymbol{\mathcal{A}}_\beta\partial\mathcal{A}_{\mathsf{p}}^2}(\boldsymbol{\mathcal{A}}) = n(n-1)\frac{\dot{\varepsilon}_0}{\sigma_0^2}\left[\frac{f(\boldsymbol{\mathcal{A}})}{\sigma_0}\right]^{n-2}\boldsymbol{N},\\
\frac{\partial^3\psi^{(r)}}{\partial\boldsymbol{\mathcal{A}}_{\mathsf{v}}^2\partial\mathcal{A}_{\mathsf{p}}}(\boldsymbol{\mathcal{A}}) &= n\frac{\dot{\varepsilon}_0}{\sigma_0^2}\left[\frac{f(\boldsymbol{\mathcal{A}})}{\sigma_0}\right]^{n-2}\left[\left((n-1)-\frac{f(\boldsymbol{\mathcal{A}})}{(\mathcal{A}_{\mathsf{v}})_{\mathsf{eq}}}\right)\boldsymbol{N}\otimes\boldsymbol{N}+\frac{3}{2}\frac{f(\boldsymbol{\mathcal{A}})}{(\mathcal{A}_{\mathsf{v}})_{\mathsf{eq}}}\boldsymbol{K}\right],\\
\frac{\partial^3\psi^{(r)}}{\partial\boldsymbol{\mathcal{A}}_{\mathsf{v}}\partial\boldsymbol{\mathcal{A}}_\beta\partial\mathcal{A}_{\mathsf{p}}}(\boldsymbol{\mathcal{A}}) &= \frac{\partial^3\psi^{(r)}}{\partial\boldsymbol{\mathcal{A}}_\beta^2\partial\mathcal{A}_{\mathsf{p}}}(\boldsymbol{\mathcal{A}}) = \frac{\partial^3\psi^{(r)}}{\partial\boldsymbol{\mathcal{A}}_{\mathsf{v}}^2\partial\mathcal{A}_{\mathsf{p}}}(\boldsymbol{\mathcal{A}}),\\
\frac{\partial^3\psi^{(r)}}{\partial\boldsymbol{\mathcal{A}}_{\mathsf{v}}^3}(\boldsymbol{\mathcal{A}}) &= \frac{\dot{\varepsilon}_0}{\sigma_0^2}\left[\frac{f(\boldsymbol{\mathcal{A}})}{\sigma_0}\right]^{n-2}\left[\alpha\boldsymbol{N}\otimes\boldsymbol{N}\otimes\boldsymbol{N}+\beta\boldsymbol{K}\hat{\otimes}\boldsymbol{N}\right],\\
\alpha &= \left(n-\frac{f(\boldsymbol{\mathcal{A}})}{(\mathcal{A}_{\mathsf{v}})_{\mathsf{eq}}}\right)\left(n-1-2\frac{f(\boldsymbol{\mathcal{A}})}{(\mathcal{A}_{\mathsf{v}})_{\mathsf{eq}}}\right)-\frac{f(\boldsymbol{\mathcal{A}})}{(\mathcal{A}_{\mathsf{v}})_{\mathsf{eq}}}\left(1-\frac{f(\boldsymbol{\mathcal{A}})}{(\mathcal{A}_{\mathsf{v}})_{\mathsf{eq}}}\right),\\
\beta &= \frac{3}{2}\frac{f(\boldsymbol{\mathcal{A}})}{(\mathcal{A}_{\mathsf{v}})_{\mathsf{eq}}}\left(n-\frac{f(\boldsymbol{\mathcal{A}})}{(\mathcal{A}_{\mathsf{v}})_{\mathsf{eq}}}\right),\\
\frac{\partial^3\psi^{(r)}}{\partial\boldsymbol{\mathcal{A}}_\beta^3}(\boldsymbol{\mathcal{A}}) &= \frac{\partial^3\psi^{(r)}}{\partial\boldsymbol{\mathcal{A}}_{\mathsf{v}}^2\partial\boldsymbol{\mathcal{A}}_\beta}(\boldsymbol{\mathcal{A}}) = \frac{\partial^3\psi^{(r)}}{\partial\boldsymbol{\mathcal{A}}_{\mathsf{v}}\partial\boldsymbol{\mathcal{A}}_\beta^2}(\boldsymbol{\mathcal{A}}) = \frac{\partial^3\psi^{(r)}}{\partial\boldsymbol{\mathcal{A}}_{\mathsf{v}}^3}(\boldsymbol{\mathcal{A}}).
\end{aligned}
$$